AN INVESTIGATION OF PHOSPHO-REGULATION AND THE ROLE CTP:PHOSPHOCHOLINE CYTIDYLYLTRANSFERASE α IN PROMOTING RAS-INDUCED MALIGNANT TRANSFORMATION OF INTESTINAL EPITHELIAL CELLS

by

Michael J. McPhee

Submitted in partial fulfilment of the requirements
for the degree of Master of Science

at

Dalhousie University
Halifax, Nova Scotia
August 2018

DEDICATION PAGE

I want to dedicate this thesis to my mother Beverly, my sister Rachel, and to my brother Chris for all their love and encouragement over the years. I cannot imagine completing this work without their support. I also want to dedicate this thesis to my loved ones who have suffered from cancer: my amazing grandmother Myrna McPhee, Roy Fletcher, Everett Lavender, and to my late father, Clyde, who passed away from melanoma in July of 2014.

This work is also dedicated to my many talented friends who have created a wonderful community here in Halifax and Dartmouth for artists and musicians.

TABLE OF CONTENTS

LIST OF FIGURES

Abstract

CTP:phosphocholine cytidylyltransferase alpha (CCTα) catalyzes the rate-limiting step of PC synthesis via the CDP-choline pathway. This study investigated CCTα regulation by phosphorylation using phospho-specific antibodies raised against p-S315/S319 and p-Y359/S362. Both antibodies detected endogenous CCTα and CCTβ in human cells, but Y359/S362 did not detect overexpressed CCTα or CCTβ. Oleate/BSA treatments induced dephosphorylation of CCTα at S315/S319 but not Y359/S362 in multiple human and rat cell lines. This correlated with translocation of CCTα to the inner nuclear membrane (INM) and decreased nuclear p-S315/S319 signal. Choline depletion of H-ras-transformed rat intestinal epithelial cells (IEC-ras) also induced dephosphorylation of S315/S319. This study is the first to use phospho-specific antibodies for CCTα to monitor dephosphorylation in response to enzyme activation. The mechanism of CCTα promoting IEC-ras survival was also investigated, suggesting that autophagy, PERK-eIF2α-ATF4-CHOP, and Keap1-Nrf2 pathways are not induced by inhibiting PC synthesis in IEC-ras. How CCTα promotes malignancy remains unknown.

LIST OF ABBREVIATIONS USED

4E-BP	Eukaryotic translation initiation factor 4E-binding protein 1
AA	Arachidonic acid
ABCA1	ATP-binding cassette transporter member 1
ADP	Adenosine 5'-diphosphate
AI	Autoinhibitory
AMP	Adenosine 5'-monophosphate
AMPK	AMP kinase
Ap1	Activator protein 1
Atg	Autophagy-related protein
ATF	Activating transcription factor
ATP	Adenosine 5'-triphosphate
BSA	Bovine serum albumin
CPT/CEPT	Choline/choline-ethanolamine phosphotransferase
CCT	CTP:phosphocholine cytidylyltransferase
Cdc	Cell-division cycyle
CDP	Cytidine 5'-diphosphosphate
CE	Cholesterol ester
CF-DMEM	Choline-free DMEM
CHO	Chinese hamster ovary
CHT	High-affinity choline transporter
CLT	Choline transporter-like protein
DAG	Diacylglycerol
DAGK	DAG kinase
DEPTOR	DEP domain-containing mTOR-interacting protein
DMEM	Dulbecco's modified Eagle's medium
ECM	Extracellular matrix
EGF	Epidermal growth factor
eIF2α	Eukaryotic initiation factor 2 α
ER	Endoplasmic reticulum
ERK	Extracellular signal-regulated kinase
ER-MAM	ER-mitochondria-associated membrane
FBS	Fetal bovine serume
FRB	FKBP-rapamycin-binding
GABARAP	Gamma-aminobutyric acid receptor-associated protein
GATE16	Golgi-associated ATPase enhancer 16 kDa
GRP78	Glucose-regulated protein 78
HDL	High-density lipoprotein
HEK	Human embryonic kidney
HIF1α	Hypoxia-inducible factor 1 α
JNK	c-Jun N-terminal kinase
IEC	Intestinal epithelial cell
IEC-MEM	IEC-modified Eagle's medium
IFNγ	Interferon γ

IL-3	Interleukin 3
INM	Inner nuclear membrane
IRE1α	Inositol-requiring element 1 α
Keap1	Kelch-like ECH associated protein 1
LC3b	Microtubule-associated proteins 1A/1B light chain 3B
LD	Lipid droplet
LPA	Lyso-phosphatidic acid
LPC	Lyso-phosphatidylcholine
LPS	Lipopolysaccharide
MAPK	Mitogen-activated protein kinase
MEK	MAP/ERK kinase
mRNA	Messenger ribonucleic acid
mTOR	Mechanistic target of rapamycin
mTORC1	mTOR complex 1
NE	Nuclear envelope
NLS	Nuclear-localization signal
Nrf2	Nuclear factor erythroid 2-related factor 2
NT	Non-target
OCT	Organic cation transporter
OCTN	Organic cation/carnitine transporter
PA	Phosphatidic acid
PAE	Porcrine aortic endothelial cells
PAF	Platelet-activating factor
PAGE	Polyacrylamide gel electrophoresis
PARP	Poly (ADP-ribose) polymerase
PBS	Phosphate-buffered saline
PC	Phosphatidylcholine
PDGF	Platelet-derived growth factor
PDI	Protein-disulfide isomerase
PE	Phosphatidylethanolamine
PEI	Polyethylenimine
PEMT	Phosphatidylethanolamine N-methyltransferase
PERK	Protein kinase RNA-like endoplasmic reticulum kinase
PG	Prostaglandin
PI3K	PI3P kinase
PI3P	Phosphatidylinositol 3’-phosphate
PI3,5P	Phosphatidylinositol 3,5’-phosphate
PI4K	PI4P kinase
PI4P	Phosphatidylinositol 4’-phosphate
PI5K	PI5P kinase
PI5P	Phosphatidylinositol 5’-phosphate
PKA	Protein kinase A
PKC	Protein kinase C
PLA_2	Phospholipase A_2
PLC	Phospholipase C
PLD	Phospholipase D

PS	Phosphatidylserine
PSD	PS decarboxylase
PSS1	PS synthase 1
SDS	Sodium dodecyl sulfate
SEM	Standard error of the mean
S6K1	Ribosomal protein S6 kinase beta-1
Sp1	Specificity protein 1
SREBP	Sterol regulatory element-binding protein
TAG	Triacylglycerol
TBS	Tris-buffered saline
TEF-4	Transcriptional enhancer factor 4
TNFα	Tumor necrosis factor α
TPA	Tissue plasminogen activator
TXA2	Thromboxane
tRNA	Transfer RNA
ULK1	Unc-51 like autophagy activating kinase
UPR	Unfolded protein response
VLDL	Very low-density lipoprotein
Vps34	PI3K Class III
WIPI	WD-repeat protein interacting with phosphoinositides
Xbp1	X-box binding protein 1

ACKNOWLEDGEMENTS

This thesis and the work described herein would not have been possible without the help of a good many people. I would like to thank Dr. Roy Duncan and Dr. Aarnoud C. van der Spoel for being members of my supervisory committee and providing helpful feedback and support throughout my project. I also wish to acknowledge Robert Douglas for providing cells each week and his excellent work in managing the lab. Many thanks are in order to Mark Charman, Jason Foster, Dr. Kexin Zhao, Kyle Lee, Dr. Antonietta Pietrangelo, and Abdul Zetrini for providing an abundance of technical assistance and for making the Ridgway Lab an enjoyable place to do research. I would also like to acknowledge the rest of the Atlantic Research Centre for their kindness, cooperation, and assistance during my time here. In particular, I would like to thank Byong Hoon Yoo for technical assistance when working with the IEC-18 and IEC-ras cell lines.

Funding for this research was provided in part by an operating grant from the Canadian Institute for Health Research (CIHR). Additional funding was generously provided by the QEII Health Sciences Centre Foundation and the CIBC Graduate Scholarship in Medical Research, which I was awarded through the Beatrice Hunter Cancer Research Institute as part of their wonderful Cancer Research Training Program. Many thanks to all involved with the BHCRI, both administrators and researchers. I would also like to thank the Faculty of Graduate Studies for providing a travel grant that allowed me to present my research at the 2018 Canadian Lipoprotein Conference in Toronto, ON.

The administrative staff of the Department of Biochemistry & Molecular Biology also deserve many thanks for their assistance on many occasions. I would have been lost without their help.

And finally, I would like to thank my supervisor Dr. Neale D. Ridgway. In addition to providing me with an excellent research project, he also was incredibly supportive and patient during my two years as his student. I am both lucky and grateful to him that I had the opportunity to be trainee in the Ridgway Lab and for all the encouragement and research experience that I have received.

Chapter 1: Introduction

1.1 Project overview

This study consisted of two primary investigations: 1) using phospho-specific antibodies to study CTP:phosphocholine cytidylyltransferase alpha (CCTα) regulation by phosphorylation, and 2) investigating the role of CCTα in promoting survival of H-ras-transformed rat intestinal epithelial cells (IEC-ras). For the first investigation, I used two phospho-specific antibodies to monitor changes in phosphorylation of CCTα when activated by oleate or choline depletion in multiple mammalian cell lines. After validating these antibodies, I used them to determine that dephosphorylation of Ser315/Ser319 was correlated with CCTα activation while Tyr359/Ser362 was not. For the second investigation, I used choline depletion and shRNA knockdown of CCTα to determine the mechanism by which inhibition of phosphatidylcholine (PC) biosynthesis might trigger cell death in IEC-ras. I monitored protein markers for three cellular stress pathways: A) autophagy, B) the unfolded protein response (UPR) and C) the Keap1-Nrf2 pathway. Ultimately, I did not find any significant effect of either choline depletion or CCTα knockdown on any of these pathways.

This thesis will begin by reviewing PC biosynthesis and the enzymes of the CDP-choline pathway, focusing primarily on CCTα and its regulation by phosphorylation to establish the rationale for investigation 1. For investigation 2, I will provide background on the three cellular stress pathways that we hypothesized could be activated in IEC-ras following choline depletion or CCTα knockdown that could promote cell death.

1.2 Phosphatidylcholine

1.2.1 Overview of phosphatidylcholine structural properties and biosynthesis

PC is a glycerophospholipid that compromises 30 to 60% of mammalian cellular membranes.[1–3] The structure of PC confers biophysical properties that promote the formation of organelle membranes and is necessary for the formation and secretion of lipoproteins and lung surfactant.[4] PC is an amphipathic molecule with a hydrophilic phosphocholine headgroup esterified at the *sn-3* position of a glycerol moiety with two hydrophobic fatty acyl chains esterified at the *sn-1* and *sn-2* positions (**Figure 1.1a**). Typically, the *sn-1* position acyl-chain is saturated while the *sn-2* position acyl-chain is unsaturated. On account of its polar head group and acyl chain composition, PC has a cylindrical structure and forms relatively planar lipid bilayers.[5] PC promotes membrane fluidity in physiological conditions and reduces the lateral packing stress of non-bilayer lipids like diacylglyercol (DAG) and phosphatidylethanolamine (PE) (**Figure 1.1b**).[2,6]

The primary route for *de novo* PC biosynthesis is the CDP-choline pathway, which occurs in all mammalian tissues and uses choline as a substrate (**Figure 1.2**).[7] Choline is taken up into the cytoplasm by choline transporters and is subsequently phosphorylated by choline kinase (CK) using ATP to produce phosphocholine.[8–10] In the nucleus, CCTα catalyzes the rate-limiting cytidylation of phosphocholine to produce CDP-choline.[11] Finally, endoplasmic reticulum (ER)-localized choline/choline-ethanolamine phosphotransferases (CPT/CEPT) catalyze the transfer of phosphorylated choline from CDP-choline to DAG to produce PC at the ER membrane.[12] The CDP-choline pathway is complemented by the phosphatidylethanolamine methyltransferase (PEMT) pathway,

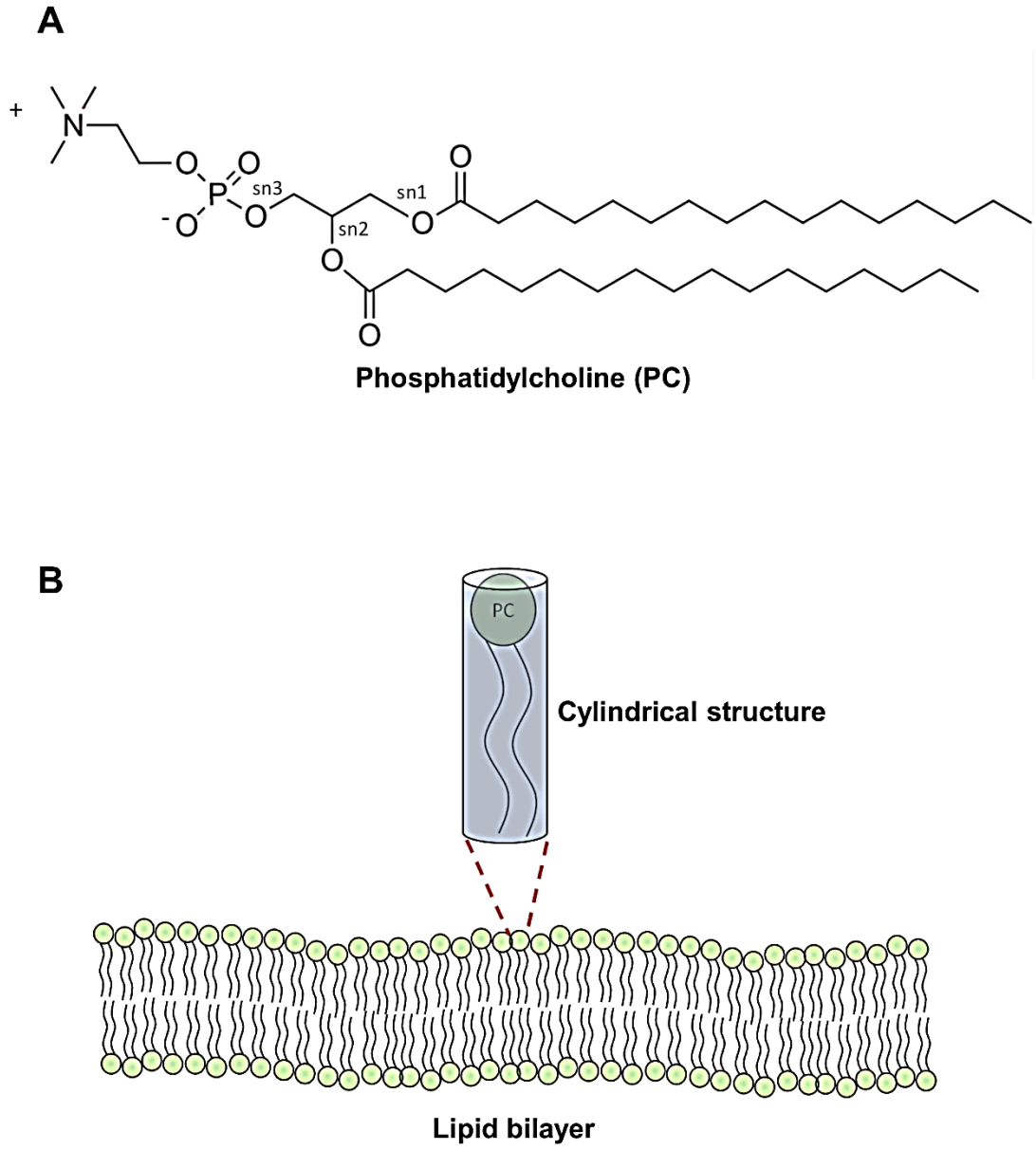

Figure 1.1. PC structure and placement in lipid bilayers. A) PC is a glycerophospholipid with two fatty acyl chains attached via ester linkages at the *sn-1* and *2* positions of a glycerol moiety. A phosphodiester linkage connects the choline headgroup to the *sn-3* position. B) Due to the relative size of the choline headgroup and its fatty acyl chains, PC is cylindrical and forms planar lipid bilayer membranes.

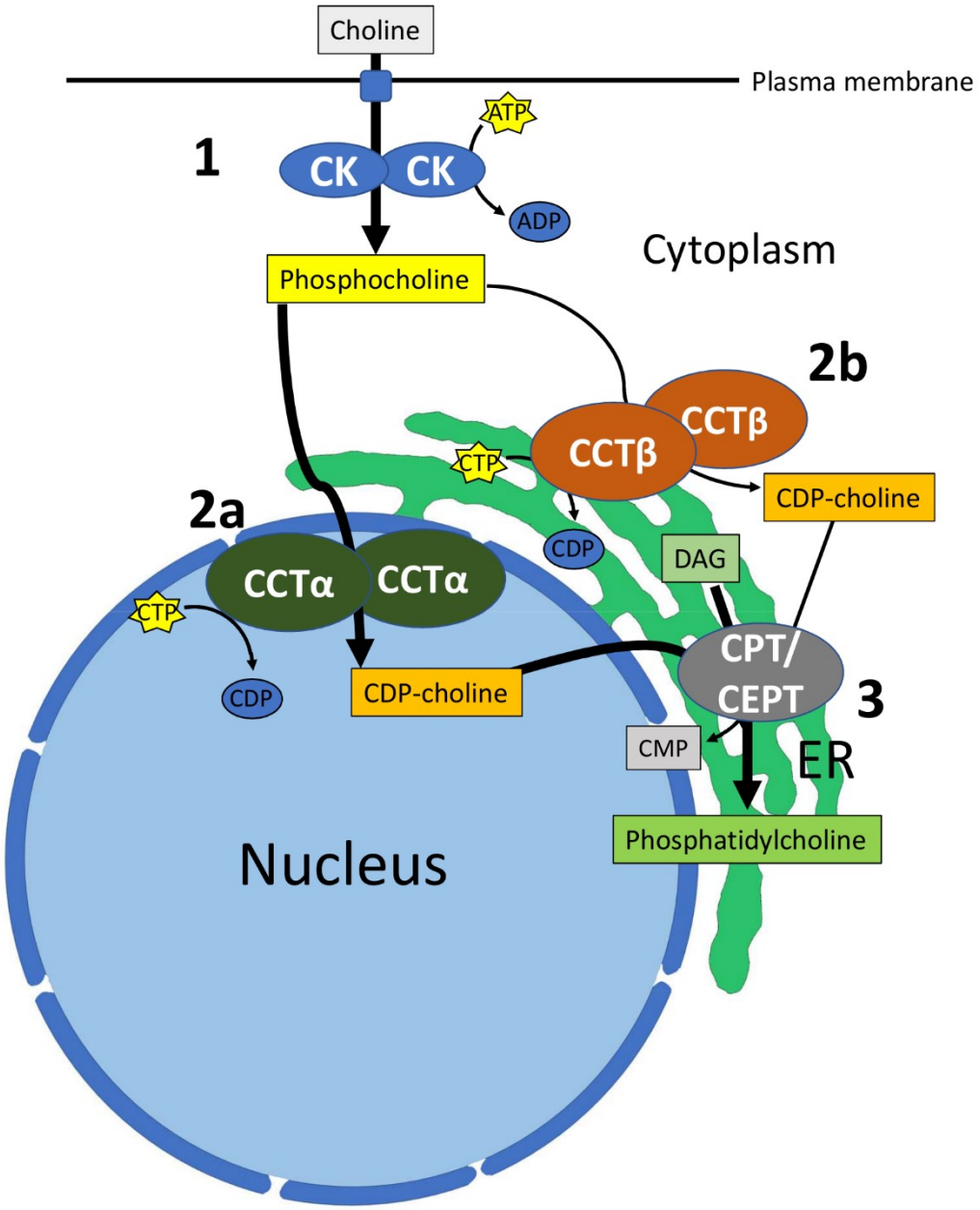

Figure 1.2. The CDP-choline pathway. 1) Choline is taken up by facilitated transport and is phosphorylated by choline kinase (CK) in the cytoplasm to produce phosphocholine. 2) Phosphocholine is then cytidylated by a) CTP:phosphocholine cytidylyltransferase alpha (CCTα) in the nucleus or also b) CCTβ in the cytoplasm to produce CDP-choline. 3) The phosphocholine headgroup is then transferred to diacylglycerol (DAG) by choline/choline-ethanolamine phosphotransferase (CPT/CEPT) in the ER membrane to produce phosphatidylcholine (PC).

which catalyzes three successive methylations of PE to produce PC in the liver.[13]

1.2.2 Phosphatidylcholine function in membrane biogenesis

The ER is comprised of about 60% PC and is the primary site of PC biosynthesis.[2,12,14] Depletion of PC from the ER membrane through choline depletion or inhibition of CDP-choline pathway enzymes triggers an ER stress response in addition to impairing protein trafficking to the Golgi.[15–17] Depending on the cell type, the outer leaflet of the plasma membrane is comprised of 15 to 40% PC. PC also serves as a substrate for the synthesis of other glycerophospholipids. Phosphatidylserine (PS) is synthesized from PC by PS synthase 1 (PSS1) at ER-mitochondrial-associated membrane sites (ER-MAM) through an exchange of choline with serine headgroups.[18,19] PS is transported to the inner mitochondrial membrane where PS decarboxylase (PSD) converts PS to phosphatidylethanolamine (PE).[20] Sphingomyelin, a prominent sphingolipid in the plasma membrane that is associated with the formation of cholesterol-rich 'lipid rafts', is derived from PC by the activity of sphingomyelin synthase, which transfers the phosphocholine head group of PC to ceramide.[21–23] Given the extent of PC and PC-derived lipids in mammalian cell membranes, inhibition of PC synthesis has the potential to dysfunction at the cellular and physiological level.

Lipid droplet (LD) and lipoprotein monolayers are comprised of up to 50% PC, and PC biosynthesis is required for the formation and stabilization of these neutral lipid-containing structures.[24,25] LDs sequester triacylglycerides (TAG) and cholesterol esters (CE) from the hydrophilic cytosol and store them until they are required for energy production or membrane biogenesis.[26] LDs are dynamic organelles and their size and

number are significantly affected by PC availability in the cell. For example, CCTα knockdown in bone marrow-derived macrophages and knockdown of the CCTα homologue CCT1 in *Drosophila* larvae and S2 cells increased lipid droplet size and TAG mass.[25] In differentiated 3T3-L1 cells and rat intestinal epithelial cells (IEC-18), lentiviral knockdown of CCTα also promoted the formation of fewer and larger LDs.[27] The presence of PC in LD monolayers acts as a surfactant to stabilize LDs, thus PC-deficient LD monolayers promote coalescence as a means of increasing the LD surface-to-volume ratio to accommodate increased TAG storage.[25]

Lipoproteins are an integral part of lipid transport in the circulation between the liver, intestine, and other organs and tissues, and are important for maintaining cholesterol homeostasis.[28] Previous reports have found that altering PC synthesis by PEMT or CCTα knockout impaired hepatic secretion of lipoproteins. In a liver-specific Cre-mediated CCTα knockout mouse model, secretion of apoB100-associated very low-density lipoprotein (VLDL) and apoAI-associated high-density lipoprotein (HDL) from the liver was reduced by approximately 50%.[29] Expression of PEMT and CCTβ2 was increased in liver-specific CCTα knockout mice but was not sufficient to compensate for the loss of CCTα. Liver-specific CCTα knockout in mice caused a reduction in cholesterol and PC efflux to apoAI due to a 50% decrease in ABCA1 CCTα-knockout hepatocytes.[30] When CCTα expression was restored using adenoviral delivery *in vivo*, ABCA1 expression in addition to VLDL and HDL secretion were restored. In humans, different biallelic loss-of-function mutations in *Pcyt1a*, the gene that encodes CCTα, were identified in two unrelated patients.[31] These mutations were associated with significantly reduced PC synthesis, resulting in decreased plasma HDL, lipid dystrophy, skeletal defects, insulin

resistance, and hepatic steatosis. Taken together, these reports indicate that PC biosynthesis regulates lipoprotein secretion and plays an important physiological role in lipid homeostasis.

1.2.3 Phosphatidylcholine as a substrate for lipid second messengers and inflammatory mediators

PC serves as a substrate for phospholipases that generate lipid second messengers in signal transduction pathways (**Figure 1.3**).[32] PC-specific phospholipase C (PC-PLC) cleaves the *sn-3* position phosphodiester linkage to produce DAG and phosphocholine. Early events in several signal transduction pathways involve PLC cleavage of phosphatidylinositol 4,5-bisphosphate (PI 4,5-P_2) to produce a pool of DAG that activates protein kinase C (PKC).[32–34] However, PC is also a significant source of DAG generation in several signal transduction pathways. For instance, lipopolysaccharide (LPS) treatment of alveolar macrophages induced the production of PC-derived DAG and ceramide that activated PKCζ and downstream mitogen-activated protein kinases (MAPK), highlighting the contribution of PC-derived PLC cleavage products to LPS signal transduction.[35] A similar observation was made in peritoneal macrophages that were stimulated with platelet-activating factor (PAF), which is also a PC-derived metabolite and chemoattractant.[36] Quantification of DAG in macrophages stimulated with PAF revealed that early generation (~30 s) of DAG was primarily derived from PI, but sustained DAG generation (>2 min) was significantly derived from PC (15-30%).[37] This percentage was even greater when cells were treated with 12-*O*-tetradecanoylphorbol-13-acetate (TPA) and ionomycin to stimulate PKC

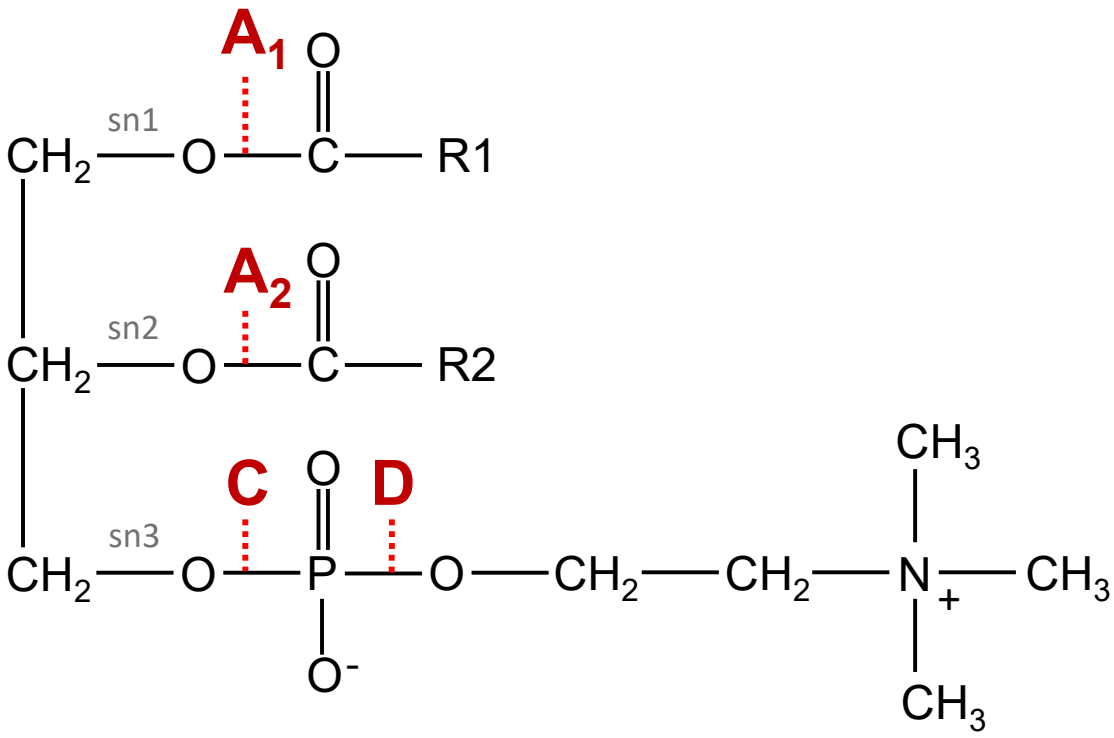

Figure 1.3. Phospholipase cleavage sites on PC. Phospholipase A_1 and A_2 cleave the ester linkage at the *sn-1* and *sn-2* position, respectively, to release a free fatty acid and lyso-PC. Phospholipase C cleaves the phosphodiester linkage at the *sn3* position to produce phosphocholine and DAG, while phospholipase D cleaves the phosphodiester linkage to produce choline and PA.

activity, with PC-derived DAG comprising up to ~50%. Similar PC-PLC pathways involving PKC-independent signalling have also been described in response to cytokine stimulation (TNFα, IFNγ, and IL-3) of receptor tyrosine kinases and carbachol stimulation of muscarinic acetylcholine receptors.[38–41]

PC-PLC acts downstream of mitogen-stimulated Ras signaling. Co-transfection of NIH-3T3 cells with PC-PLC and H-ras with an inhibitory Asn17 mutation demonstrated that PC-PLC was itself capable of stimulating cell proliferation.[42] Furthermore, mutant H-ras was also shown to inhibit PC-PLC-mediated PC hydrolysis following treatment with serum and epidermal growth factor. Exogenous PC-PLC treatment of NIH-3T3 cells was found to induce Raf signaling comparable with EGF, and inhibition of PC-PLC with tricyclodecan-9-yl prevented EGF, TPA, and serum-induced Raf activation.[43] Another study demonstrated that similar inhibition of endogenous PC-PLC inhibited platelet-derived growth factor (PDGF) activation of MAPK in macrophages, although this had no significant effect on EGF-induced signaling.[44] In Rat-1 fibroblasts, this phenotype was also observed along with evidence that EGF did not significantly activate PC-PLC.[45]

Phospholipase D (PC-PLD) cleaves the phosphodiester linkage between phosphate and choline to produce free choline and phosphatidic acid (PA). Like DAG, PA is an important lipid second messenger that is involved in various mitogenic signal transduction pathways that promotes Ca^{2+} mobilization, cytoskeletal organization, and interacts with an array of signal transduction proteins, including the mechanistic target of rapamycin (mTOR) complex.[46–48] The mTOR complex 1 (mTORC1) acts as a mitogen and nutrient sensor at the cytoplasmic surface of the lysosomal membrane and promotes cell growth and proliferation.[49–51] PA stimulated mTOR activity in HEK293 cells and activation was

prevented following pre-treatment with rapamycin, as both rapamycin and PA interact with the mTOR FK506-binding protein (FKBP12) rapamycin-binding (FRB) domain.[47] Knockdown of PLD1 with siRNA in HEK293 and COS-7 cells reduced mTOR-directed phosphorylation of both S6 kinase 1 (S6K1) and eukaryotic translation initiation factor 4E binding protein (4E-BP), causing a reduction in cell size and proliferation.[52] This same report also identified that cell division control protein 42 (Cdc42), which contributes to regulation of the cell cycle through interactions with proteins including S6K1 and 4E-BP, required PLD1 to stimulate S6K1 independent of mTOR.

PA generation from PC is stimulated through nutrient sensing pathways involving activation of PLD1. Class III phosphatidylinositol 3-phosphate-kinase (PI3K or Vps34) generation of phosphatidylinositol 3'-phosphate (PI3P) was required for activation of PLD1 in HEK293 cells, which then translocated to the lysosome.[53] Interestingly, knockdown using PLD1 and Vps34-specific shRNA eliminated amino acid sensing capabilities of mTORC1. A similar report also found that PLD1 and Vps34 activity were necessary for mTORC1 amino acid and glucose sensing in cancer cell lines including MDA-MB-231 cells.[54] Leucyl-tRNA synthetase was identified as an amino acid sensor by binding free leucine and subsequently stimulating Vps34 complex activity at the lysosome, activating PLD1 and promoting its translocation.[55,56] This directly established a link between intracellular amino acid content and generation of mTORC1-stabilizing PA by PLD1.

While a significant pool of PA is generated by phosphorylation of DAG by DAG kinases, there is additional evidence to support a specific role for PLD-generated PA from PC in mTORC1 activation.[57] Porcine aortic endothelial (PAE) cells, COS-7 and Rat1 cells

transfected with either PLD1b or PLD2a generated the same species of PA following stimulation, consisting mostly of PA containing mono- and di-saturated fatty acids.[58] In HEK293 cells, PA containing unsaturated fatty acids displaced the mTOR inhibitor DEPTOR upon mitogen stimulation, whereas PA with palmitic acid did not.[59] These data suggest that the FRB domain of mTOR can recognize specific molecular species of PA that stimulate activation. These results indicate that PLD1 and PLD2 isoforms primarily utilized the same pools of PC as a substrate for generation PA, and that differences in the fatty acid content of DAG produced by PC-PLC could prevent functional interconversion between pools of PA produced by DAGK and PLD. Taken together, PLD production of PA from PC contributes significantly to mTOR nutrient sensing in mammalian cells.

In addition to intracellular lipid second messengers, PC also serves as an important substrate for production of extracellular signals and inflammatory mediators that can act either locally or distally in the tissues in response to injury or infection. Cytosolic phospholipase A_2 ($cPLA_2$) cleaves the *sn-2* position ester linkage of PC to produce lyso-PC and a free fatty acid. Arachidonic acid (AA) produced by $cPLA_2$ activity is a important precursor for eicosanoid mediators of inflammation.[60] Cyclooxgenase 1/2 act on AA to produce prostaglandin (PG) H2, a precursor of active prostaglandins (PGD2, PGE2, PGF2α), prostacyclin (PGI2), and thromboxane (TXA2).[61] Lipooxygenases also act on AA to produce precursors of the leukotrienes.[62]

As discussed previously, PAF is a PC-derived inflammatory mediator that is responsible for multiple effects depending on the target cell, including platelet aggregation, contraction of smooth muscle cells, cytokine production, priming, and chemotaxis.[63] PC remodeling to LPC is the most common route of PAF synthesis *in vivo*, where $PLA2_2$

cleaves AA at *sn-2* to produce LPC that is subsequently replaced with an acetyl group. PAF receptors interact weakly with PAF containing an acyl chain at the *sn-1* position, so PAF almost exclusively contains a *sn-1* alkyl-ether linkage instead of the typical ester linkage.

Finally, LPC serves as a major substrate for lyso-PA (LPA) synthesis by autotaxin, an enzyme with phospholipase activity.[64] LPA is secreted into circulation and potentially signals 5 G protein-coupled receptors (GPCRs)(LPA_{1-5}) and can have a wide range of effects on different cell types. For example, LPA appears to have a protective role against myocardial infarction as demonstrated, but it also contributes to atherosclerosis through increased smooth muscle cell migration, monocyte infiltration, inflammatory cytokine release, and LDL uptake into arterial plaquess[65]

In summary, PC-derived metabolites generated by phospholipases contribute significantly to both cellular and physiological functions in mammals. The conversion of PC by PLD and PLC to produce PA and DAG has been implicated in signal transduction pathways that promote cancer cell malignancy.[66–68] Like PLD and PLC, the enzymes of the CDP-choline pathway are found to be upregulated in some cancers and contribute to cancer cell proliferation and maligancy.[69] In the next section, I will elaborate on the enzymes of CDP-choline pathway.

1.3 The CDP-choline pathway for PC biosynthesis

1.3.1 Choline transporters

Choline is a water-soluble nutrient that is transported across the plasma membrane of cells by four different families of choline transporters. High-affinity choline transporters (CHTs) like CHT1 were first identified in neurons of *C. elegans* and rats.[9] CHT1 uptake of choline is Na^+-dependent and serves as the rate-limiting step in acetylcholine biosynthesis. Despite its involvement in acetylcholine biosynthesis, CHT1 shares little sequence homology with the neurotransmitter transporter family and closely resembles Na^+-dependent glucose transporters.[9,70,71] Choline transporter-like proteins (CTLs) have an intermediate affinity for choline and are Na^+-independent.[72] Up to five homologues of CTL have been identified in the human genome, and there is occurrence of alternative splicing for several of these genes.[73] CTL1 is expressed in all human tissues and aberrant upregulation of CTL1 expression in skeletal muscle is associated with myopathy.[74] Finally, organic cation transporters (OCTs) and organic cation/carnitine transporters (OCTNs) are responsible for uptake of a variety of cation substrates and have low affinity for choline.[75] There are three members of each family of transporter that are collectively distributed throughout epithelial cells in the liver (OCT1 and OCT3), the intestine (OCTN1, OCTN2, and OCT3), the kidneys (OCTN1, OCTN2, OCT2, and OCT3), the placenta (OCTN2 and OCT3), and the lungs (OCT1, OCT2, OCT3, OCTN1, and OCTN2). Together, these transporters take up choline into the cytoplasm where it is utilized by the CDP-choline pathway.

1.3.2 Choline kinase

In the cytoplasm, choline kinase (CK) catalyzes the ATP-dependent phosphorylation of choline to produce phosphocholine, committing choline to the CDP-choline pathway.[76] Two isoforms CKα and CKβ share approximately 57-59% of their amino acid sequence.[77–79] CKα also has two isoforms corresponding to spliced variants from the *Chka* gene, whereas CKβ is the only isoform encoded by *Chkb*.[79,80] CKα and CKβ are ubiquitously expressed in human, rat and mouse tissues.[81] CKα and CKβ form heterodimers that comprise up to of 80% of active enzyme in murine tissues. Interestingly, CK heterodimers have a similar affinity for both choline and ethanolamine, while CK homodimers have higher affinity for ethanolamine.[69]

While CKα and CKβ are present in all tissues, their expression varies and is tissue specific. As a result, dysfunction or knockout in mice of either enzyme produces different phenotypes. Homozygous *Chka*$^{-/-}$ knockout in mice was embryonic-lethal while heterozygous *Chka*$^{+/-}$ knockout had no significant effect on PC levels.[82] No compensatory increase in other enzymes of the CDP-choline pathway were observed in *Chka*$^{+/-}$ mice, suggesting that CKα is essential for PC biosynthesis but is not necessarily rate-limiting.[8] Homologous knockout *Chkb*$^{-/-}$ did not cause embryonic lethality, but resulted in a form of muscular dystrophy associated with greatly reduced CK activity in the skeletal muscles of mouse hindlimbs in addition to forelimb bone deformity.[83] Further investigation determined that skeletal muscles of mouse hindlimbs expressed higher levels of CKβ than in the forelimbs, and *Chkb*$^{-/-}$ mice had reduced PC synthesis in the hindlimbs that contributed to the defects in skeletal muscle formation.[84] This highlights the role of CK as a contextual rate-limiting enzyme for PC synthesis resulting from differential expression

of CKα and CKβ in mammalian tissues. Furthermore, evidence suggests that CK promotes cancer cell survival independent of catalytic activity, suggesting additional functions of the enzyme yet to be described.[85]

CK kinase expression and activity is regulated by several mechanisms, including phosphorylation by various kinases. CK purified from *S. cerevisiae* is a substrate for protein kinase A (PKA) *in vivo* and *in vitro*. Conversely, alkaline phosphatase treatment of phosphorylated CK decreased enzyme activity by approximately 60%.[86] Two motifs for PKA in yeast CK were identified at Ser30 and Ser85, with serine-to-alanine mutants of Ser30 causing approximately 80% reduction of CK activity and 56% reduction of choline incorporation into PC.[87] Together, double mutants of Ser30 and Ser85 caused a 80-90% reduction for both CK activity and choline incorporation into PC. In another study, yeast CK Ser25 and Ser30 were identified as phosphorylation sites for protein kinase C.[88] The correlation between phosphorylation and increased enzyme activity highlights the importance of CK phosphorylation as a mechanism for regulating PC biosynthesis in *S. cerevisiae*.

Studies have also confirmed that phosphorylation of multiple serine residues enhance activity of human CKα and CKβ isoforms. Phosphorylation CK activity as assessed by isotope labelling was up-regulated in NIH-3T3 fibroblasts treated with serum or insulin in culture.[89] Similarly, NIH-3T3 fibroblasts treated with PMA and PDGF also showed enhanced CK activity (approximately 2-fold) in addition to a greater-than 2-fold induction of CK activity in K-ras and H-ras transformed cells.[90] PDGF-induced Ras-Raf1-MEK-MAPK pathway activation was blocked in NIH-3T3 fibroblasts treated with 3-

hemicholinium, an inhibitor of both CK and CHT, thus supporting a role for CK in regulating cell growth and proliferation in response to mitogens.[91 92]

CK is also regulated at the transcriptional level. Chemical stress-induced acute upregulation of CKα, but not CKβ, in mice injected with hepatotoxic carbon tetrachloride (CCl_4) and rats injected with mutagenic 3-methylcholanthrene.[80,81] In Hepa-1 cells, CCl_4 exposure induced c-jun translocation and binding to a distal Ap1 element in the promoter region of *Chka*, thus enhancing expression of both CKα mRNA and protein.[93] Two additional Sp1 binding sites in the *Chka* promoter region were also identified in that study. In addition to chemical-induced stress responses, CKα expression is upregulated in response hypoxia-induced stress. Hypoxia-inducible transcription factor 1α (HIF1α) is typically degraded by the proteasome under normoxic conditions, but hypoxia stabilizes and promotes HIF1α dimerization with its β subunit and translocation to the nucleus as part of a hypoxic stress response.[94] Seven hypoxia-response elements were identified in the promoter region of *Chka*. Thus cells grown under hypoxic conditions had increased CKα expression in addition to higher levels of PC synthesis.[95,96] Given that CKα is upregulated in a many cancers, its response to cellular stress suggests a role for the enzyme in promoting cancer cell survival and proliferation.[17,69,97–100] While CK isoforms are not typically rate-limiting in the CDP-choline pathway, the association of CK dysregulation and disfunction with various pathological outcomes highlights the importance of this enzyme and its role in PC biosynthesis.

1.3.3 CTP:phosphocholine cytidylyltransferase

PC biosynthesis is regulated by CCT, a member of the cytidylyltransferase family of enzymes that catalyzes the rate-limiting step cytidylation of phosphocholine in the CDP-choline pathway.[11] Two genes encode isoforms of CCT; *Pcyt1a and Pcyt1b. Pcyt1a en*codes CCTα, which is expressed ubiquitously in all mammalian tissues. CCTα knockout in mice *Pcyt1a*$^{-/-}$ is embryonic lethal during early development.[101] With a few exceptions, CCTα is expressed as a soluble dimer in the nucleus.[102] *Pcyt1b en*codes CCTβ, which has 3 splice variants that are all localized to the cytoplasm and display tissue-specific expression patterns.[103–105] CCTα is a 367 amino acid peptide consisting of an N-terminal nuclear localization signal (NLS) (N region), a catalytic domain (C domain), a membrane-binding domain (M domain) with an autoinhibitory (AI) helix, and a C-terminal disordered loop containing serine, threonine, and tyrosine residues that are targets for phosphorylation (P region) (Figure 1.4).[106–109]

Both the M domain and the P regions contribute to the mechanism of CCT regulation. The M domain is an amphipathic α-helix that reversibly embeds itself into membranes rich in type I lipids, such as fatty acids and anionic lipids, or type II lipids, such as conical shaped DAG and PE (**Figure 1.4**).[6,106,107,110–114] Type I lipids interact with the positively charged residues of the amphipathic helix while the smaller headgroups of type II lipids promote lateral packing that induces membrane stored curvature elasticity, exposing hydrophobic pockets to the nucleoplasm where neutral residues of the M domain helix associate.[12] This feature promotes the translocation of soluble dimers of CCTα to the inner nuclear membrane (INM) and induces a structural reorganization in the enzyme that increases the k_{cat}.[6,115,116] When soluble in the nucleoplasm, residues 236 through 272 of

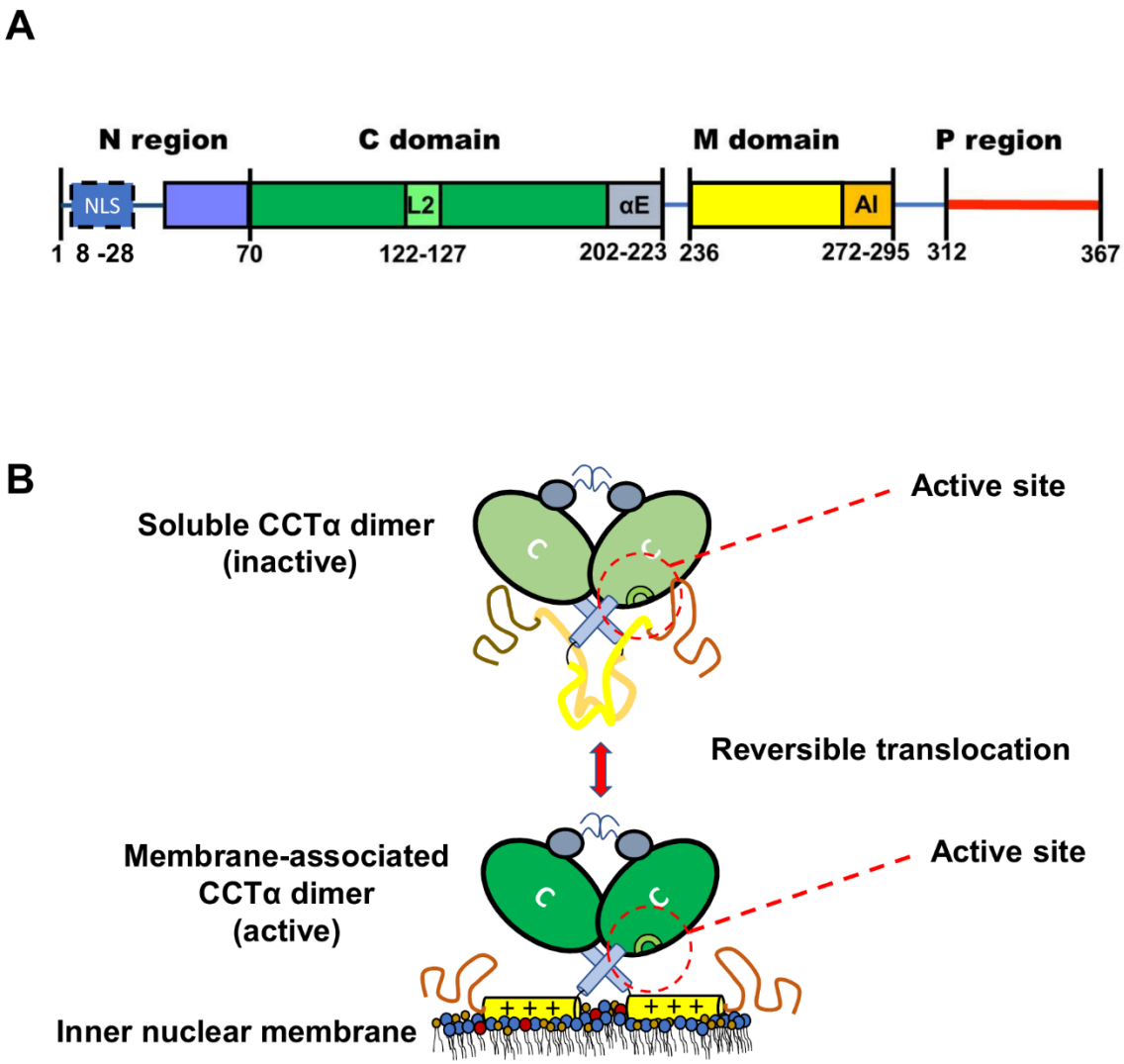

Figure 1.4. CCTα structure and membrane binding capability. A) A diagram of the protein domains of CCTα. B) Dimers of CCTα are inactive when soluble in the nucleoplasm resulting from the conformation of the enzyme αE helix and AI helix interfering with the active site. Anionic lipids and DAG promote the inducible amphipathic helix of M domain to embed into the inner nuclear membrane (INM), exposing the active site and promoting enzyme translocation Both diagrams are adapted from ref. 111.

the M domain form a flexible disordered segment that positions the AI helix segment from 272 to 295 within the proximity of the CCTα active site, significantly increasing the K_m and decreasing the k_{cat}.[117] This appears to be mediated in part by hydrogen bonding between carbonyl groups of the AI helix backbone and the ϵ-amino group of the catalytic residue Lys122.[118] Furthermore, residues Gly294 and Pro295 interact with the L2 loop at the opening of the catalytic site to possibly block access of Lys122 to CTP. Additional interactions between the AI helix and the αE helix adjacent to the C domain also contribute significantly to regulating the active site of CCTα.[117,118]

1.3.4 CCTα regulation is correlated with dephosphorylation

The C-terminal P region is a highly disordered and in humans contains up to 16 serine, threonine, and tyrosine residues that targets for phosphorylation.[11] The frequency of phosphorylation of each residue appears to be variable, with some residues more prominently phosphorylated than others.[119] The role of phosphorylation in CCTα regulation is not entirely understood. While activation and translocation of CCTα generally correlates with dephosphorylation of the P region, there is evidence that phosphorylation does not interfere with translocation to target membranes. On account of the disordered state of the P region, it has not been resolved in crystal structures of CCTα and thus it is unclear how the phosphorylated residues might interaction with the active site of the enzyme.[117]

The presence of multiple serine-proline repeats indicated that this region is targeted by proline-directed kinases. Casein kinase 2, Cdc2, and MAPK phosphorylated purified rat CCTα *in vitro*.[120,121] Insulin, EGF and TNFα treatment of cells increased

phosphorylation of CCTα through MAPK signalling.[121,122] *In vitro* assays showed that purified CCTα was negatively regulated by PKA phosphorylation and that dephosphorylation enhanced microsome-associated CCTα activity.[123,124] Similarly, c-jun N-terminal Kinase 1 and 2 (JNK1 and JNK2) phosphorylation of CCTα was also associated with a dose-dependent reduction in enzyme activity.[125] Overexpression of JNK2 in lung epithelial cells also increased phosphorylation of CCTα that was correlated with a 30% reduction in PC biosynthesis. These experiments suggest a link between the activation of CCTα at membranes and its dephosphorylation, but the exact mechanism for phospho-regulation is unclear.

Several studies have attempted to identify key regulatory phosphorylation sites in the P region of CCTα. A serine-to-alanine mutant at residue 315 (S315A) and a truncated CCTα mutant with residues 312-367 deleted (Δ312) had similar phosphocholine and CTP *Km* values relative to wild-type CCTα in the absence of lipid activation *in vitro*.[126] However, assaying the activity of these mutant enzymes when associated with DAG and PC liposomes demonstrated that the membrane-associated wild-type CCTα activity was stimulated to a lesser extent than Δ312. The *Km* values for both the S315A and Δ312 mutants were also consistently lower in response to lipid activation than the CCTα wild-type, which was significantly phosphorylated. Interestingly, despite containing only a single modification and significant amount of total phosphorylation, the S315A mutant response to lipid activators was intermediate between that of wild-type and Δ312, suggesting that desphosphorylation of Ser315 may be important for lipid-induced CCTα activation.

An additional study also compared the regulation of mutants containing either 5, 7 or 16 serine-to-alanine mutations (5SP-AP, 7SP-AP, or 16SA) and a 16 serine-to-glutamate (16SE) to the wild-type enzyme.[127] Wild-type CCTα and the mutants were overexpressed in CHO-MT58 cells, which expresses a temperature-sensitive CCTα that is degraded when the cells are cultured at 40ºC and thus serve as a useful model for studying temperature-permissive CCTα mutants. Both 5SP-AP and 7SP-AP mutants, each including a S315A mutation, had significantly reduced phosphorylation compared to wild-type CCTα. The 16SA mutant CCTα was completely dephosphorylated, indicating that the P region is the exclusive site CCTα phosphorylation. Furthermore, phosphopeptide mapping of trypsin-digested 5SP-AP and 7SP-AP mutants isolated from CHO-MT58 cells incubated with [^{32}P]phosphate showed only 2 and 1 phosphorylated peptides, respectively. This marked reduction in phosphorylation suggests that proline-directed kinases target these residues, and that these initial phosphorylation events may possibly serve to recruit additional kinases that phosphorylate other serine residues.

Interestingly, this same group reported that greater than 40% of the 16SA mutant CCTα was found in the membrane fraction isolated from untreated CHO-MT58 cells. By contrast, approximately 5% of both the 16SE mutant and wild-type CCTα were found in the membrane fraction of untreated CHO-MT58 cells, demonstrating that the 16SA mutant had a higher affinity the membrane. In agreement with those observations, the same group reported that 20% of CCTα truncated at residue 314 (Δ314) was membrane-associated in untreated cells.[128] No difference between mutant and wild-type CCTα translocation was observed in oleate-treated cells.[127,128] These data suggest that electrostatic interactions of

the P region alone contribute minimally to regulation of CCTα membrane association in CHO-MT58 cells.

Phosphorylated CCTα was found to translocate to total membranes isolated from PLC and oleate-treated rat hepatocytes.[129] Two-dimensional phosphopeptide mapping of CCTα purified from rat hepatocytes incubated with [^{32}P]phosphate demonstrated that four peptides were dephosphorylated while another peptide had increased phosphorylation following translocation induced by PLC or oleate treatments. Okadaic acid, which enhances phosphorylation of CCTα and inhibits PC biosynthesis, is an inhibitor of protein phosphatase 1 and 2a (PP1 & 2a).[130] While it is not known if CCTα is a substrate of either phosphatase *in vivo*, the catalytic subunit of PP1 was demonstrated to dephosphorylate CCTα *in vitro*.[131] It is therefore possible that okadaic acid induces CCTα phosphorylation indirectly by inhibiting either phosphatase. Taken together, these data suggest that phosphorylation of CCTα changes following translocation to membranes. While most sites in the P-region appear to be desphosphorylated after CCTα translocates to the membrane, some are phosphorylated. It has yet to be determined which S/T/Y residues are being phosphorylated or dephosphorylated when CCTα is localized at the membrane, highlighting the requirement for additional investigation of this post-translational modification of CCTα.

1.3.5 Transcriptional regulation of CCTα

Multiple transcriptional regulators for *Pcyt1a* have been reported in the literature. TEF-4 and Sp1 were identified as important co-activators with Ets1 of *Pyct1a* expression in COS-7 cells, whereas Net acted as a repressor of transcription.[132–134] Like CK, CCTα is

upregulated in response to H-ras-transformation.[120,135,136] Despite the presence of a sterol response element (SRE) in the promoter region, increased expression of constitutively sterol regulator element-binding protein (SREBP) 1a and 2 had no affect on *Pcyt1a* transcription and instead promoted PC biosynthesis through fatty acid synthesis production.[137] Increased CCTα activity and protein levels have been reported as part of the UPR, but given that no change in mRNA levels are observed, it appears the activity of the transcription factor X-box binding protein 1 (Xbp1) may instead contribute to reduction in CCTα turnover.[138,139] An early study identified bindings sites in the 200 bp promoter region of *Pcyt1a* for both Sp1(3 putative binding sites) and Ap1 (4 putative binding sites).[140] Overexpression of Sp1 and Sp3 were found to enhance *Pcyt1a* transcription in *Drosophila* SL-2 cells whereas Sp2 acted to repress transcription.[141] In contrast, overexpression of Sp2 and Sp3 in mouse embryonic fibroblasts (C3H10/T12) activated *Pyct1a* transcription whereas Sp1 did not. Sp1 and Sp3 were found to act synergistically in SL-2 cells while this same effect was not observed in C3H10/T12 cells. Interestingly, Sp1 interacted with the *Pcyt1a* promoter in C3H10/T12 cells during S phase.[142,143] When C3H10/T12 cells overexpressing Sp1 were transfected with plasmids encoding either cyclin A or Cdc2, transcription of *Pcyt1a* was enhanced, demonstrating that phosphorylated Sp1 activates expression of *Pcyt1a* as part of a mechanism regulating CCTα expression during progression in the cell cycle.[144] The timing of increased CCTα occurred prominently during S phase rather than G_1 phase, where PC demand is greatest.[23,142] This ensures that sufficient PC is generated for cell division.

1.3.6 Choline/choline-ethanolamine phosphotransferase

The terminal step of the CDP-choline pathway is catalyzed by CPT and CEPT that transfer phosphocholine from CDP-choline to the *sn*-3 position of DAG. CPT uses CDP-choline exclusively whereas CEPT uses both CDP-choline and CDP-ethanolamine as substrates.[7,145] Both CPT and CEPT are integral membrane proteins that have seven trans-membrane domains and are localized to the Golgi and the ER, respectively.[146] While CEPT appears to be ubiquitously expressed, CPT expression was significantly higher in the testis, colon, small intestines, heart, prostate, and spleen.[147] As was found for CCTα, expansion of the ER mediated by Xbp-1 increases activity of both CPT and CEPT significantly to meet the demands for PC required for ER membrane expansion.[139] The role of either enzyme in pathological contexts has received limited attention.

1.3.7 The role of the CDP-choline enzymes in cancer

Cancer is a disease characterized by dysregulation of cell proliferation and survival in response to extracellular input, unlimited cell division and tumor growth, tissue invasion and vascularization, and evasion of cell death.[148] Unlike normal cells, cancer cells are capable of growing detached from the extracellular matrix (ECM), allowing them to metastasize to other tissues and form secondary tumors. This is possible because cancer cells are capable of evading detachment-induced apoptosis, also called anoikis.[149] This form of apoptosis occurs when interactions between plasma membrane proteins and the scaffold of the ECM cease, thus allowing pro-apoptotic signals to promote anoikis.

With malignant transformation comes extensive transformation of lipid metabolism. Upregulation of choline metabolism in cancer cells has been recognized as a

major component of the lipogenic phenotype of cancer.[90,150–152] Both CKα and CCTα contribute cancer cell malignancy, and this is often associated with increased enzyme activity and protein expression resulting from oncogenic transformation. An initial report found that PLC-mediated production of DAG in H-ras-transformed 3T3-NIH cells was mainly derived from PC and resulted in accumulation of phosphocholine.[153] However, increased CK activity was also demonstrated to be a source of elevated pools of phosphocholine in H-ras-transformed 3T3-NIH cells.[90] Since these initial discoveries, there has been extensive investigations of CKα activity in cancer. CKα has been implicated in tumor promotion in endometrial cancer, prostate cancer, breast cancer, colon cancer, liver cancer, lung cancer, and ovarian cancer.[97,99,100,151,152,154–157] The prominence of CKα in cancer makes it a potential drug target for cancer treatment.

CCTα also contributes to malignant transformation. Upregulation of CCTα transcription was caused by MYC in diffuse large B-cell lymphoma (DLBCL), and this contributed to defects in mitophagy that interfered with tumor suppression via necroptosis.[158] From the same study, a screen of DLBCL patient samples revealed that high expression of MYC was correlated with upregulation of CCTα. *In vivo* tumor size of B-lymphoma was reduced by lipid-lowering berberine treatments and CCTα knockdown, inducing mitophagy-associated necroptosis. In H-ras-transformed C3H10T1/2 cells, increase p42/p44 MAPK signalling phosphorylated Sp3, thus increasing its activation of *Pcyt1a* transcription and protein expression.[135] However, much of the CCTα was observed to be phosphorylated and inactive in these cells. Our lab found that H-ras-transformed intestinal epithelial cells (IEC-ras) also had elevated CCTα protein expression, much of which appeared to soluble and inactive in the nucleus of these cells.[136] [^{3}H]Choline

labeling experiments demonstrated that adherent IEC-ras did not have increased PC synthesis relative to non-transformed IEC controls (IEC-18). However, lentiviral-mediated knockdown of CCTα in IEC-ras reduced tumor formation by ~50% relative to IEC-ras in subcutaneous xenograph tumor mouse models and reduced colony formation of cells cultured in soft agar. Since growth in agar prevents cell attachment and triggers anoikis, this suggested a possible role for CCTα in promoting malignancy. Additionally, [^{3}H]choline labeling demonstrated that PC biosynthesis was sustained in IEC-ras grown on agar. This was shown to be CCTα-dependent, further supporting the role of CCTα in promoting malignancy in H-ras-transformation. Intriguingly, IEC-ras grown on agar exhibited hyperphosphorylation of CCTα relative to cells cultured on plastic dishes. This result appears to call into question whether phosphorylation negatively regulates the catalytic activity of CCTα in IEC-ras that are detached from the ECM.

The mechanism for IEC-ras evasion of anoikis and the role of CCTα was further investigated. The autophagy pathway can contribute to promoting anoikis resistance, so our lab investigated whether CCTα promoted anoikis resistance by producing PC for membrane biogenesis for the autophagy pathway.[159,160] Knockdown of CCTα enhanced p62 accumulation in detached IEC-ras but not IEC-18, while an insignificant effect on LC3II accumulation was observed (Zetrini & Ridgway, data unpublished). The lack of significant changes of LC3II could indicate that flux of the autophagy pathway was unaffected, but the accumulation of p62 suggested autophagy might be impaired.[161] Pro-apoptotic Beclin-1 and PARP cleavage was enhanced in detached IEC-ras with knockdown of CCTα, indicating anoikis induction. Culturing cells in choline-free media induced both LC3II and p62 accumulation in IEC-ras but not IEC-18, highlighting a potential link

between *de novo* PC biosynthesis and autophagy in IEC-ras. Immunofluorescence showed that choline-depletion of IEC-ras caused accumulation of p62-containing puncta in the cells. Based on these data, further investigation was necessary to establish if the autophagy pathway was PC-dependent and involved in the CCTα-dependent anoikis resistance phenotype of IEC-ras.

1.4 Autophagy

1.4.1 Overview of the autophagy pathway

Autophagy is a mechanism for isolating and degrading intracellular materials in a lysosome-dependent manner. In macroautophagy (henceforth referred to as autophagy), double-membraned vesicles called autophagosomes sequester damaged organelles, protein aggregates, lipid droplets, and/or other intracellular materials before fusing with lysosomes where hydrolytic degradation occurs (**Figure 1.5**).[162] When intracellular amino acids, glucose, lipids, and oxygen levels are limiting, autophagy is induced as part of a stress response. Autophagosome biogenesis requires a host of autophagy-related (Atg) proteins and the induction of this pathway is tightly controlled by nutrient-sensing proteins like mTOR and AMP-activated protein kinase (AMPK).[163,164]

Lipids are crucial to each step of the autophagy pathway.[165] Phospholipids are reportedly involved in the regulation and initiation of autophagy while also acting to recruit proteins to the autophagosome and lysosome membranes that facilitate membrane expansion and fusion.[163,166] Autophagosome biogenesis occurs at multiple sites in yeast and mammalian cells, but the primary source of membrane lipids for autophagosome formation are sub-

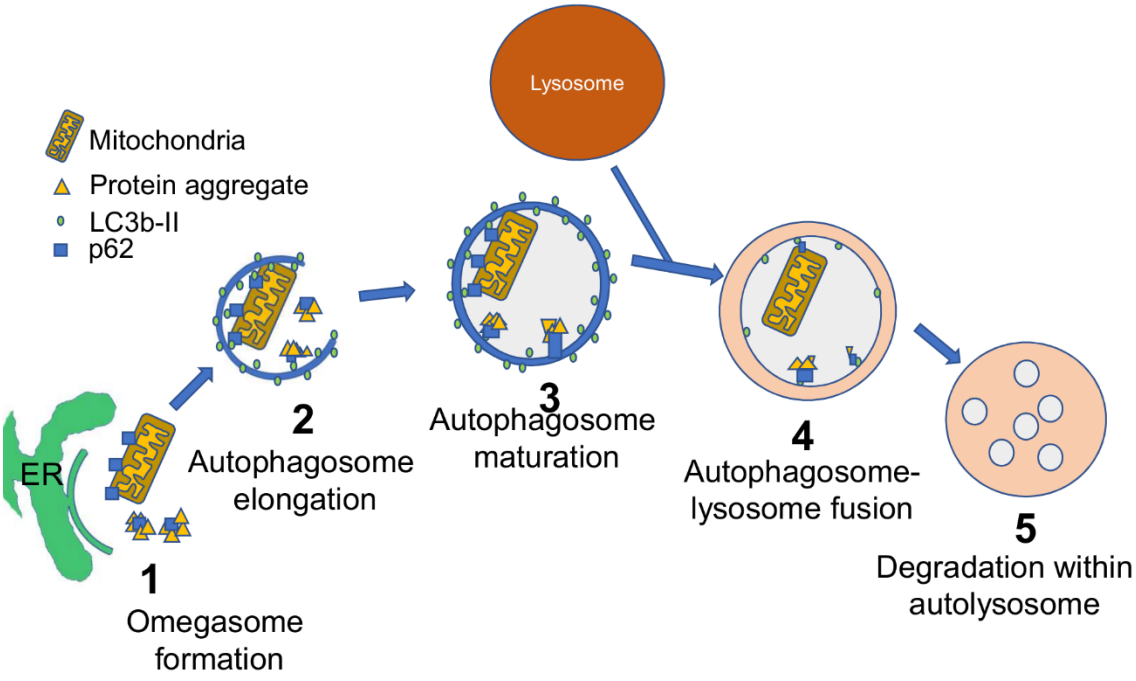

Figure 1.5. The autophagy pathway. 1) Autophagy initiation occurs at the ER membrane, beginning with omegasome formation that develops into the nascent phagophore. 2) Membrane elongation of the autophagosome that sequesters intracellular cargo through interactions between adapter protein p62 and PE-conjugated LC3b-II. 3) Autophagosomes form into double-membraned vesicles that deliver cargo for degradation. 4) Fusion between mature autophagosome and the lysosome produces the autolysosome compartment. 5) Degradation of the autophagosome cargo is carried out by acid hydrolases of the autolysosome.

domains of the ER and ER-organelle or ER-plasma membrane contact sites.[167–171] Additionally, *de novo* phospholipid biosynthesis has been observed in mouse hepatocytes following amino acid starvation, suggesting that these lipids might contribute to autophagosome membrane biogenesis.[172] Ultimately, autophagy can promote cell survival and maintain metabolic homeostasis under conditions of stress and limited nutrient availability. Depending on the context, autophagy has been shown to be both cancer-promoting and cancer-repressing under different circumstances.[173–175] In various cancers, autophagy is upregulated and appears to promote cancer cell survival, proliferation, and metastasis.[176–180] Autophagy has been shown to contribute to anoikis resistance in several cancer cell models, so our lab has investigated a possible link between CCTα-dependent anoikis resistance and the autophagy pathway in IEC-ras.[136,160] Our lab hypothesized that the absence of PC biosynthesis in IEC-ras would inhibit either autophagosome biogenesis or autophagosome-lysosome fusion, and this would contribute to sensitizing IEC-ras to anoikis.

1.4.2 The role of phospholipids in the autophagy pathway

Multiple nutrient-sensing pathways regulate autophagy activation and inhibition, and several lipid species are involved in facilitating signal transduction and effector protein function. As discussed previously, mTORC1 is a key negative regulator of canonical autophagy and is activated by lysosomal amino acid content as a means of sensing cellular nutrient levels. PA and PI3P are integral in the nutrient detection mechanism of mTORC1. The autophagy-initiating serine/threonine kinase activity of the UNC-51-like kinase (ULK1/Atg1) complex is typically inactivated by mTORC1 and its downstream kinases.[181] In contrast to mTORC1 negative regulatory activity, AMPK acts a sensor for

ATP:ADP:AMP ratios in the cell as a means of assessing cellular energy levels.[164] Activation of AMPK in response to low cellular energy levels initiates the autophagy pathway through several mechanisms, including ULK1 phosphorylation as described above. AMPK phosphorylates Ser91 and Ser94 of Beclin-1, a component of Vps34 complexes containing ATG14L required for autophagy initiation.[182] In addition to its positive regulatory effects, AMPK also phosphorylates Raptor and the TSC2 complex as means of promoting autophagy through mTORC1 activity inhibition.[183] Furthermore, AMPK phosphorylates Thr163 and Ser165 of Vps34 complexes lacking ATG14L, inhibiting PI3P generation necessary for mTORC1 activation.[182] Ultimately, generation of PI3P by different Vps34 complexes acts to promote or repress autophagy initiation.

Following initiation of the autophagy pathway, a pre-autophagic structure called the omegasome forms at the ER membrane.[162] PI3P generated by Vps34 is required for omegasome formation in the canonical autophagy pathway, but phosphatidylinositol 5-phosphate (PI5P) has also been shown to induce autophagy and is required for glucose-starvation induced autophagy.[167,184] Furthermore, PI5P in the absence of PI3P was sufficient for the recruitment of autophagy effector proteins typically associated with PI3P binding. Ultimately, both PI3P and PI5P serve as integral lipid mediators in the initial stages of autophagosome biogenesis, but the role of PI3P has been more thoroughly characterized in the literature.

PI3P also serves to recruit cytoplasmic mammalian WIPI proteins (homologs of yeast Atg18) as the omegasome forms the nascent autophagosome, a double-membraned structure known as the phagophore.[165,185] siRNA knockdown of mammalian WIPI200 in starved HEK293A cells resulted in significantly decreased microtubule-associated protein

1a/1b light chain 3 (LC3/Atg8) lipidation with PE, which is necessary for expansion of the nascent autophagosome and its eventual closure.[186–191] Additionally, WIPI200 binding to Atg16L1 of the Atg12-Atg5-AtgL complex was required for LC3 lipidation.[190] Both PI3P and PE at the autophagosome are thus important for the lipidation of LC3 on the maturing autophagosome.

LC3b is the best studied of the mammalian Atg8 family of proteins, which also includes the GABARAPs and GATE16.[161] LC3 is first processed via Atg4 and requires further processing from LC3I to LC3II for lipidation via Atg7 and Atg3 in a ubiquitin-like pathway that covalently joins the LC3II C-terminal glycine to the amino group of PE.[186,188] Working in parallel to the LC3 conjugation pathway, the Atg12-Atg5-Atg16 conjugation system is also required for expansion and elongation of the phagophore isolation membrane.[162,192] Once anchored to the autophagosome membranes, LC3 interacts with various adaptor proteins, such as sequestesome-1 (SQSTM1/p62), that sequester cargo within the growing autophagosome.[193] Both p62 and LC3b are useful protein markers for monitoring the autophagy pathway.[161]

Once autophagosomes mature, they deliver their cargo to lysosomes for degradation by heterotypic fusion to form autolysosomes in which hydrolytic enzymes degrade the materials sequestered by the autophagosome.[166] Fusion between lysosomes and autphagosomes requires both protein and lipid mediators. Phosphatidylinositol 4-phosphate (PI4P) generated by phosphatidylinositol 4-kinase Iiα (PI4KIIα) at GABARAP-positive autophagosomes was found to be necessary for heterotypic fusion between autophagosomes and lysosomes in HeLa cells.[194] PI3P and phosphatidylinositol 3,5-

bisphophate ($PI(3,5)P_2$) on both autophagosomes and lysosomes are also found to have important roles in autophagosome-lysosome fusion.[166,195]

Finally, PLD1-derived PA is involved in regulating the terminal step of autophagy. Knockdown of PLD1 similarly induced accumulation of p62 and LC3b-II in MDA-MB-231 breast cancer cells under low glucose conditions, suggesting AMPK-induced autophagy was inhibited.[196] A similar phenotype was observed in PLD1 knockout mice, associated with hepatic steatosis and accumulation of both p62 and LC3-II.[197] Treatment of PA was sufficient to restore autophagy in PLD1 knockout hepatocytes suggesting that PA derived from PC by PLD1 activity could be necessary for autophagy.

Currently, the role of PC in autophagy remains understudied. Activation of autophagy in FL83B mouse hepatoma cells increased [^{14}C]choline and [^{3}H]choline incorporation into PC by 2-fold and 3-fold, respectively.[172] Choline depletion inhibits PC synthesis and causes p62 and LC3b-II accumulation in IEC-ras, suggesting that PC is necessary for autophagy (Zetrini & Ridgway, unpublished). However, lentiviral knockdown CCTα in IEC-ras detached from the ECM resulted in p62 accumulation without concurrent LC3b-II accumulation. Similarly, CHO-MT58 cells when grown at a non-permissive temperature promoting CCTα degradation also only showed accumulation of p62 but not LC3b-II. With these data in mind, it was not clear whether our data supported our hypothesis that PC synthesis in IEC-ras was necessary for autophagy. For my study, I investigated the effects of choline depletion on autophagy in IEC-ras to test our hypothesis.

1.5 ER Stress Pathways

1.5.1 The unfolded protein response

Protein homeostasis at the ER is crucial for cell survival, as it is a major site of protein synthesis and folding. Three proteins are primarily responsible for induction of the unfolded protein response (UPR) at the ER membrane; inositol-requiring enzyme 1α (IRE1α), protein kinase RNA-like endoplasmic reticulum kinase (PERK), and activating transcription factor 6 (ATF6).[198] Together, these transmembrane proteins act in concert to restore ER homeostasis by inhibiting global protein translation while promoting the expression of protein chaperones that act to prevent the accumulation of harmful protein aggregates in the ER. If the UPR is incapable of resolving the burden of ER stress, the response will promote apoptosis by upregulating pro-apoptotic proteins such as CCAAT/enhancer-binding homologous protein (CHOP).

Dysregulation of ER lipid homeostasis and aberrant PC synthesis has been shown to promote ER stress. Overexpression of PEMT in Hepa1-6 cells decreased the activity of microsomal sarco/endoplasmic reticulum ATPase (SERCA), and this was linked to increased activation of IRE1α and PERK.[199] Adenovirus-mediated knockdown of PEMT obese mice restored hepatocyte PC-to-PE ratios in addition to alleviating ER stress and improving insulin sensitivity. Conversely, inhibition of PC synthesis in CHO-MT58 by temperature-sensitive promotion of CCTα degradation induced ER stress that culminated in apoptosis via CHOP induction.[16] Both IRE1α and PERK act as sensors of lipid bilayer stress independently of their ability to detect unfolded proteins through their luminal domains and this induces the UPR.[200,201] Similar to CCTα, IRE1α has an amphipathic helix

that embeds into the cytosolic surface of the ER membrane, promoting clustering of IRE1α in response to excessive lipid packing.[202] IRE1α clusters promotes the splicing of the *Xbp1* mRNA to promote its translation and subsequent upregulation of genes like *Pcyt1a* to restore lipid homeostasis at the ER.

The accumulation of p62 following inhibition of PC biosynthesis may also indicate the induction of other stress pathways. p62 was reported to transiently accumulate following activation of the UPR in bone marrow-derived macrophages.[203] p62 co-localized with ubiquitinated aggresome-like induced structures (ALIS), and the UPR response appeared to clear the ALIS through a lysosomal-dependent mechanism independent of the canonical autophagy pathway. Our observations that choline depletion also caused transient accumulation of p62 led us to consider a link between PC deficiency, the UPR, and p62 accumulation. PERK phosphorylation of eIF2α at Ser51 inhibits global mRNA translation in favor of promoting *ATF4* mRNA translation.[204,205] ATF4 in turn upregulates a host of UPR-related proteins as part of the UPR. Interestingly, both ATF and CHOP were shown to significantly upregulate genes of the autophagy pathway, including LC3b and p62.[206] It seemed plausible that ER stress induced by either choline depletion or shCCTα might be responsible for our observations in IEC-ras.

1.5.2 The Keap1-Nrf2 pathway

Finally, another stress pathway that involves p62 is the Keap1-Nrf2 pathway, which protects the cell against oxidative stress.[207] When oxidative stress is absent, Keap1 binds to and promotes the proteosomal degradation of Nrf2. However, in conditions of oxidative stress, several Keap1 cysteine residues are oxidized causing a conformational

change, thus Nrf2 evades degradation.[208] As a transcription factor, Nrf2 promotes gene expression of anti-oxidative enzymes like glutathione *S*-transferase as part of an anti-oxidative stress response. It has previously been demonstrated that p62 expression is upregulated as part of this response.[209] Nrf2 and p62 compete for binding of Keap1, thus increasing p62 expression promotes p62-mediated sequestration of Keap1 to enhance the oxidative stress response.[210]

With this in mind, we considered that choline depletion could be triggering an oxidative stress response that in turn elevated p62 levels. mTORC1 was previously found to phosphorylate p62 at Ser351 and this promoted p62-mediated selective autophagy of protein aggregates (aggrephagy), damaged mitochondria (mitophagy), and bacteria (xenophagy) in mouse embryonic fibroblast cells.[211] LC3b-II accumulation typically lags behind the transient p62 accumulation in choline-depleted IEC-ras, so it seemed possible that we were observing autophagy induction resulting in the clearance of the accumulated p62. However, no one has reported a link between PC deficiency and the Keap1-Nrf2 pathway, requiring further investigation.

1.6 Research objectives and rationale for investigation

For this research, I focused primarily on investigating two problems: 1) The role of phosphorylation in the regulation of CCTα and 2) the mechanism by CCTα in promoting survival of IEC-ras. Understanding the relationship of CCTα activity and anoikis could provide us with a better understanding of cancer cell survival and metastasis while also

providing a future therapeutic target for cancer treatment. I worked on three overlapping projects throughout the duration of this investigation, summarized as follows:

1) Validation of phospho-specific antibodies for CCTα and use these to investigate CCTα regulation. Our collaborator Stephen Pelech has provided us with anti-pCCT rabbit polyclonal antibodies raised against key residues that are phosphorylated on CCTα. In this investigation, I used human and rat cells lines and treated them with oleate or depleted them of choline to activate and promote INM localization of CCTα to assess changes in phosphorylation of Ser315/Ser319 and Tyr359/Ser362.

2) Determine if choline depletion causes p62 and LC3b-II accumulation in human cancer cells. I attempted to identify a human cancer cell line that could be used to study the role of CCTα in promoting cancer cell survival and proliferation.

3) Determine the mechanism of choline depletion and CCTα-induced p62 accumulation in IEC-ras. Using choline depletion and CCTα knockdown in IEC-ras, I attempted to establish a mechanism by which CCTα promotes survival of IEC-ras. Because p62 accumulates under these conditions, my investigation focused on the autophagy, Keap1-Nrf2, and PERK-eIF2α-ATF4-CHOP pathways, all of which involve p62.

Chapter 2: Materials and Methods

2.1 Materials

Rabbit anti-pCCT Ser315/Ser319, Tyr359/Ser362, and Thr342/Ser343 polyclonal antibodies were provided by our collaborator Steven Pelech (Kinexus, Vancouver, BC). Rabbit anti-CCTα polyclonal antibody was produced and purchased from Genscript (Scotch Plains, NJ). Rabbit anti-p62 polyclonal antibody (cat: ab91562) was purchased from Abcam (Cambridge, MA). Rabbit anti-LC3B (cat: NB1002220) was purchased from Novus Biologicals (Littleton, CO). Mouse anti-Nrf2 monoclonal antibody (cat: MAB3925) was purchased from R&D Systems (Minneapolis, MN). Rabbit anti-ATF4 monoclonal antibody (cat: D4B8), rabbit anti-CHOP monoclonal antibody (cat: D46F1), rabbit anti-eIF2α polyclonal antibody (cat: 9722), rabbit anti-phospho-eIF2α Ser51 polyclonal antibody (cat: 9721), rabbit anti-p62 polyclonal antibody (cat: 5114), rabbit anti-PDI polyclonal antibody (cat: 2446), and rabbit anti-GRP78 monoclonal antibody (cat: 3177) were all purchased from Cell Signaling Technology (Danvers, MA). Alexa Fluor® 488 goat anti-rabbit secondary antibody, Alexa Fluor® 594 goat anti-mouse secondary antibody, Alexa Fluor® 800cw goat anti-rabbit secondary antibody, Alexa Fluor® IRDye 680LT goat anti-mouse secondary antibodies, and Odyssey Blocking Buffer in TBS were purchased from LI-COR (Lincoln, NE). Nitrocelluose membrane (0.2-µm) , 40% acrylamide/Bis solution (29:1), ammonium persulfate, tetramethylethylenediamine, and Tween 20 were purchased from Bio-Rad (Hercules, CA). Hank's Buffered Saline Solution (HBSS), Dulbecco's modified Eagle's medium (DMEM), alpha-modified Eagle's Medium (α-MEM), fetal bovine serum (FBS), puromycin, Triton X-100, Pierce BCA Protein Assay Kit, paraformaldehyde, and Lipofectamine2000 were purchased from Thermo Fisher

Scientific (Waltham, MA). Lentivial pLKO.1 shNT and shCCTα plasmids, chloroquine disphosphate, choline chloride, MG-132, Mowiol® 4-88, oleic acid, fatty acid-free bovine serum albumin (BSA), and tunicamycin were purchased from Millipore-Sigma (St. Louis, MO). SeaPlaque® GTG Agarose was purchased from FMC BioProducts (Rockland, ME). QIAfilter Plasmid Midi kits were purchased from Qiagen (Missisauga, ON). pBABE mCherry-eGFP-LC3 was a gift from Jayanta Debnath (Addgene plasmid #22418).

2.2 Cell Culture

IEC-18, IEC-ras33 and IEC-ras34 cells were cultured in IEC-MEM (α-MEM containing 5% fetal bovine serum (FBS), D-glucose (3.6 g/L), insulin (12.74 μg mL^{-1}), and glutamine (2.92 mg mL^{-1})). HEK293T, HCT116, HKH2, HKE3, HeLa, F8, Caco2, and Caco2-CCTαKO cells were cultured in DMEM containing 10% FBS. All cells were cultured in 5% CO_2 at 37°C except for MDA-MB-453, which were maintained without CO_2. Caco2-CCTαKO cells were provided generously by Kyle Lee and generated as previously described (Lee & Ridgway, in press). For choline depletion experiments, cells were treated with choline-free DMEM (CF-DMEM) containing 5% or 10% dialyzed FBS depending on the cell line used. 50 mL of FBS was dialyzed (10,000 molecular weight cut-off) against 2 L of PBS at 4°C overnight. Cells treated with HBSS were incubated at 37°C without CO_2.

2.3 Plasmid transfection of HeLa cells

HeLa cells were plated at 200,000 per 60-mm dish and allowed to reach 70% confluence. Transfection reagents were prepared by mixing 4 μL of lipofectamine per 2

μg plasmid DNA in 400 μL of DMEM per dish and incubated for 30 minutes at room temperature. Transfection mixtures were added to 3 mL of DMEM containing 10% FBS, and HeLa cells were incubated overnight at 37ºC with 5% CO_2. Transfection media was removed and replaced with fresh DMEM containing 10% FBS for an additional 24 h before harvesting cells.

2.4 Retroviral and lentiviral production and cell transduction

Retrovirus was produced in HEK293T cells (70% confluent in 10-cm dishes) by co-transfecting with polyethyleneimine (PEI) complexed with 3 μg of pBABE-puro mCherry-eGFP-LC3B and plasmids encoding packaging factors pΔ8.2 and pVSV-G. Virus-containing IEC-MEM was collected and filtered through a 0.45-micron polysterene filter. IEC-ras34 (80% confluent in IEC-MEM in 10-cm dishes) were transduced overnight with 8 mL of retrovirus-containing IEC-MEM with 4 μg mL^{-1} polybrene. After transduction, cells were selected with 5 μg μL^{-1} puromycin for up to 48 h.

Lentivirus was produced in HEK293T cells (70% confluent in 10-cm dishes) co-transfected with PEI complexed with 3μg of pLKO.1-shRNA and plasmids encoding packaging factors psPAX.2 and pMD2.G. pLKO.1 shNT: 5'-CCGCCAACAA-GATGAAGAGCACCAACTCGAGTTGGTGCTCTTCATCTTGTTGTTTTT-3'. pLKO.1-shCCT1 5'-CCGGCCTAAGGACATCTACAAGAACTCGAGTTCTTTGTA-GATGTCCTTAGGTTTTTG-3'. Virus-containing IEC-MEM was collected and filtered through a 0.45-micron polysterene filter. To produce stable knockdown of CCTα in IEC-ras34, 1 mL of virus-containing media was combined with 3 mL of IEC-MEM containing 10 μg mL^{-1} polybrene, and this media was added to cells in 60-mm dishes at approximately

60-70% confluent. Cells were incubated overnight and selected for 48 h with 10 μg mL^{-1} puromycin. After selection, the cells were maintained in IEC-MEM at 3 μg mL^{-1} puromycin.

2.5 SDS-PAGE and immunoblotting of cell lysates

Prior to harvesting cells, media was removed and cells were washed once with ice-cold PBS. Whole-cell lysates were then collected in SDS reducing buffer (62.5 mM Tris-HCL pH 6.8, 10% glycerol, 2% SDS, 0.05% bromophenol blue, and 5% β-mercaptoethanol). For preparing detergent lysates, cells were scraped and collected 1 mL of ice-cold PBS pelleted by centrifugation at 3000 rpm for 1 minute, and then solubilized with 0.1% Triton X-100 in PBS for 20 minutes on ice. Detergent lysates were then centrifuged at 13,000 rpm at 4ºC in a microcentrifuge to remove insoluble cellular debris. Protein concentration was determined using Thermofisher BCA protein assay kits. All samples were stored at -20ºC.

Prior to electrophoresis, whole-cell lysates were subjected to sonication for 7 sec and then heated to 90ºC for 3 minutes. Similarly, detergent lysates were heated to 90ºC following the addition of an appropriate amount of SDS gel-loading buffer. Samples were separated in SDS-polyacrylamide gels (8%, 12%, or 15%) at 100 V in SDS-PAGE running buffer (3 mM SDS, 200 mM glycine, 25 mM Tris-base). Proteins were transferred to nitrocellulose membranes submerged in transfer buffer (25 mM Tris-base, 192 mM glycine, 20% (v/v) methanol) at 100 V for 1 h.

Nitrocellulose membranes were incubated in blocking buffer (1:5 dilution of Licor Odyssey blocking buffer in TBS-Tween (20 mM Tris-base, pH of 7.4, 500 mM NaCl,

0.05% Tween 20)) for 60 min at room temperature or 4ºC overnight with gentle shaking. Primary antibody incubations were carried out as described in figure legends. Secondary antibody incubations (1:15,000 for GAR800 and 1:20000 GAM680 in blocking buffer) were for 1 h at room temperature. Nitrocellulose membranes were scanned using a Licor Odyssey and fluorescence was quantified using Licor Odyssey software v3.0 .

2.6 Immunofluorescence

Cells seeded on 1-mm glass coverslips were fixed with 4% (*w/v*) paraformaldehyde in PBS for 15 min with gentle shaking and permeabilized with 0.5% Triton X-100 in PBS at 4ºC for 15 min. Coverslips were blocked overnight at 4ºC with 1% bovine serum albumin (BSA) in PBS. For primary antibody incubation, anti-CCTα (1:500 to 1:1000), anti-pCCTα Ser315/Ser319 (1:500-1:1000), anti-pCCTα Tyr359/Ser362 (1:500), and anti-lamin A/C (1:250-1:500) were prepared with 1% BSA in PBS and coverslips were placed on 100 µL aliquots of antibody solution on a parafilm surface in humid chamber for 2.5 to 4 h at room temperature or overnight at 4ºC. For secondary antibody incubation, goat anti-rabbit conjugated to AlexaFluro488 (1:4000) and goat anti-mouse conjugated to AlexaFluro594 (1:4000) were prepared with 1% BSA in PBS and added 2 mL to coverslips in six-well dishes for 1 h at room temperature. Coverslips were mounted on glass slides using Mowiol and cells were imaged using a Zeiss LSM 510 Meta laser scanning confocal microscope with 100X Plan APOCHROMAT lens, Argon 488/HeNe 548 lasers, and Zeiss LSM 5 software.

2.7 Measuring autophagic flux in IEC-ras34

IEC-ras34 stably expressing mCherry-EGFP-LC3B were incubated with CF-DMEM containing 5% dialyzed FBS for 24 h at 37ºC in 5% CO_2 with or without supplements of 50 μM choline, and with or without a 50 μM chloroquine treatments for 12 h. Cells were fixed with 4% (*w/v*) paraformaldehyde, mounted on glass slides using Mowiol, and imaged using a Zeiss LSM 510 Meta laser scanning confocal microscope with 100X Plan APOCHROMAT lens, Argon 488/HeNe 548 lasers, and Zeiss LSM software.

Yellow and red puncta were quantified using 'Colocalization' and 'Analyze Particles' plugins using ImageJ software v.1.8.0. To count yellow puncta (autophagosomes), the 'Colocalization' plugin generated an image from overlapping signals of the red and green channels of LSM files converted to greyscale 8-bit images. A threshold was applied to each image and the 'Analyze Particles' plugin counted the signal for puncta in the field of cells. Red puncta were counted similarly using grey 8-bit images of the red channel from each LSM file. The total number of puncta counted in each image was divided by the number of cells in the field to give average yellow and red puncta per cell per image (989 cells from 3 separate experiments).

2.8 Measuring ER stress in IEC-ras cultured on agarose

To investigate cellular responses to detachment-independent growth, 60-mm dishes were coated with 3 mL of 1% (*w*/v) SeaPlaque® agarose in α-MEM and allowed to set for 30 min. IEC-ras34 cells (100,000 to 150,000 cells per dish) stably expressing pLKO.1 shNT or shCCTα were added in 2 mL of IEC-MEM to each dish and incubated at 37ºC for

up 72 h or 12 h, respectively. For controls, cells were cultured in 60-mm dishes for 72 h with or without a 10 μg mL^{-1} tunicamycin treatment for 12 h prior to harvesting.

2.9 Oleate treatment of cultured cells

Oleate/BSA (6.6/1) complexes were prepared by dissolving 45 mg of oleic acid in 1 mL of ethanol. 50 μL of 5 M NaOH was added the mixture and the ethanol was evaporated under a stream of nitrogen. The oleate was then dissolve in 5 mL of 150 mM NaCl and heated for 4 min at 60ºC prior to adding 6.25 mL of chilled 24% (*w/v*) BSA dissolved in 150 mM NaCl. The mixture was stirred for 10 min and the volume was adjusted to 12.5 mL total with 150 mM NaCl to produce a final oleate concentration of 12.7 mM.

Cells were cultured in 35-mm dishes until 50-80% confluent and media was replaced with serum-free DMEM or α-MEM prior to timed additions of oleate/BSA (300 μM or 500 μM). For oleate pre-treatment experiments, cells were cultured as previously described before incubating in the presence of 500 μM oleate/BSA in serum-free DMEM or α-MEM for 30 minutes. After 30 minutes, oleate-containing media was replaced with serum-free DMEM or α-MEM for the timepoints indicated in the figure legends.

2.10 Statistical analysis

Statistical significance of data was determined from 3 or more independent experiments using a two-tailed student t-test analysis computed with GraphPad Prism 6.0 software. Error bars represent standard error of the mean (SEM) or standard deviation

(SD) as indicated in figure legends. Significance is reported for p-values determined to be <0.05 (*), 0.01 (**), and 0.001 (****).

Chapter 3: Results

3.1 Using phospho-specific antibodies to monitor CCTα phosphorylation

3.1.1 Oleate induces dephosphorylation of CCTα at Ser315/Ser319 but not Tyr359/Ser362

To study CCTα regulation by phosphorylation, I used phospho-specific antibodies raised against phospho-Ser315/Ser319 and phospho-Tyr359/Ser362 peptides (**Figure 3.1**). Significant sequence homology was observed in alignments of CCTα and CCTβ at the Ser315/Ser319 site suggesting probable cross-reactivity of antibody binding to this motif. To validate the specificity of these antibodies, rat CCTα and β isoforms were overexpressed in HeLa cells and probed with the phospho-specific antibodies. Anti-p-Ser315/Ser319 detected overexpressed CCTα-V5 and CCTβ-MYC-FLAG (**Figure 3.2A**) whereas anti-p-Tyr359/Ser362 did not. To demonstrate the specificity of anti-p-Ser315/Ser319 for phosphorylated residues, CCTα-V5 with 16 serine residues mutated to alanine (16SA) was overexpressed in HeLa cells. Not surprisingly, anti-p-Ser315/Ser319 did not detect this dephosphorylated mutant (**Figure 3.2B**). Looking at reactivity of the antibody with endogenous CCT isoforms, I compared Caco-2 cells to Caco-2 cells in which CCTα was knock-out using CRISPR-cas9 (Lee & Ridgway, in press) and found that both anti-p-Ser315/Ser319 and anti-p-Tyr359/Ser362 detected the remaining endogenous CCTβ isoform (**Figure 3.3**). These data suggest that these two antibodies could be useful for detecting changes in phosphorylation status of CCTα and CCTβ in response to activation and translocation to the INM.

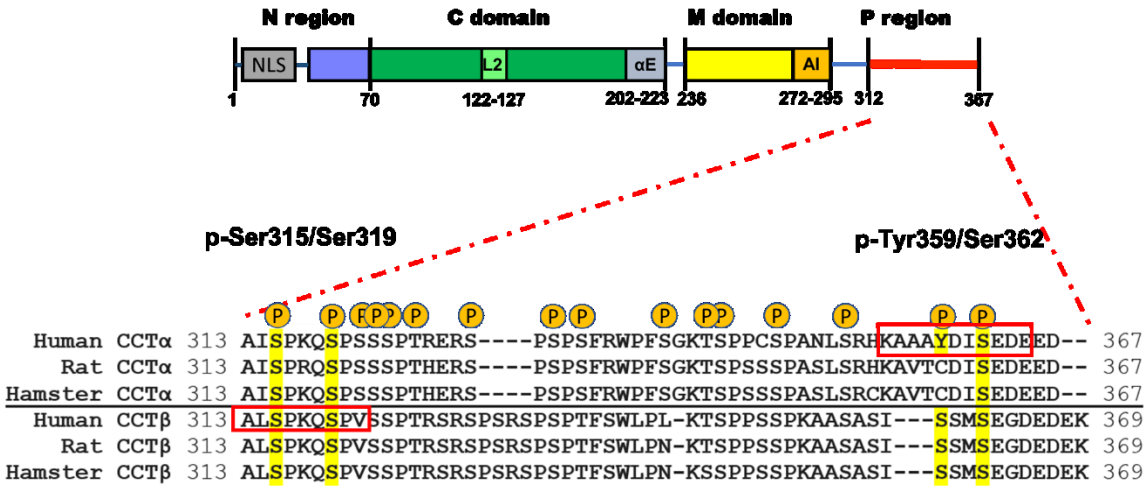

Figure 3.1. Target residues of anti-pCCT antibodies raised against p-Ser315/Ser319 and p-Tyr359/Ser362. Rabbit polyclonal antibodies were raised against phosphorylated peptides outlined in red corresponding to human CCTβ p-Ser315/Ser319 and human CCTα p-Tyr359/Ser362 (phosphorylated residues highlighted in yellow).

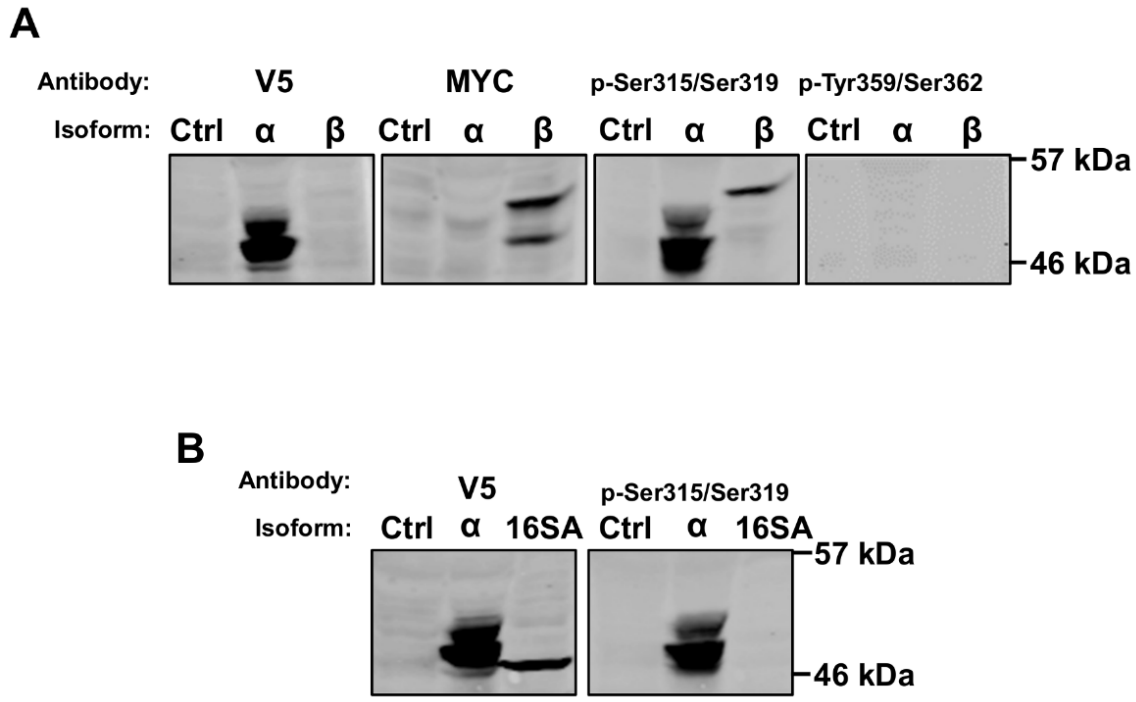

Figure 3.2. Anti-p-Ser315/Ser319 but not anti-p-Tyr359/Ser362 detects both overexpressed CCT isoforms in HeLa cells. A) HeLa cells were transfected with rat CCTα-V5 or rat CCTβ-MYC-FLAG. **B)** HeLa cells were also transfected with rat CCTα-V5 or rat CCTα-V5 16SA. After 48 h, whole-cell lysates were collected and protein resolved by SDS-PAGE, transferred to nitrocellulose and immunoblotted with anti-V5 (1:1000), anti-MYC (1:1000), anti-p-Tyr359/Ser362 (1:1000), and anti-p-Ser315/Ser319 (1:1000).

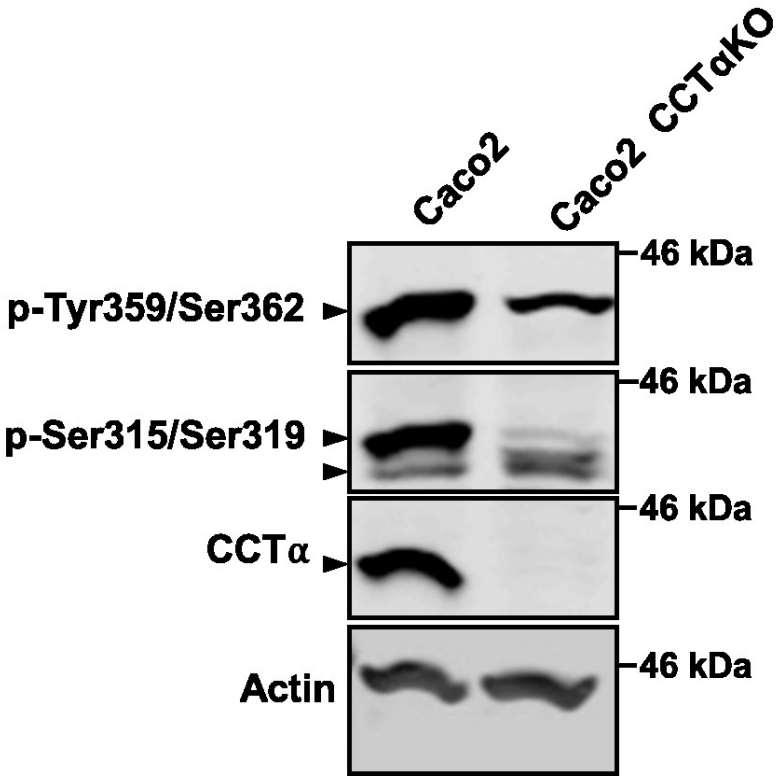

Figure 3.3. Anti-p-Ser315/Ser319 and anti-p-Tyr359/Ser362 detect endogenous CCT isoforms in Caco2 and Caco2 CCTαKO cells. Caco-2 and Caco-2 CCTαKO cells were cultured in 60-mm dishes until 70% confluent. Whole-cell lysates were collected and resolved by SDS-PAGE. Protein was transferred to nitrocellulose and immunoblotted with anti-CCTα (1:500), anti-pCCT-Tyr359/Ser362 (1:1000), and anti-pCCT-Ser315/Ser319 (1:1000).

Anionic lipids such as oleate stimulate dephosphorylation and translocation of CCTα to the INM in HeLa and CHOK1 cells.[212,213] This phenotype is also associated with a 100-fold increase enzyme activity, thus suggesting a link between CCTα translocation, phosphorylation, and regulation. To determine if either anti-p-Ser315/Ser319 or anti-p-Tyr359/Ser362 could detect changes in CCTα phosphorylation following enzyme activation, I treated HeLa cells with oleate/BSA (500 μM). The anti-p-Ser315/Ser319 signal decreased significantly as early as 15 min after oleate/BSA addition and was sustained for 60 min (**Figure 3.4**). However, the anti-p-Tyr359/Ser362 signal increased slightly by 15 minutes and returned to baseline by 30 minutes. Oleate/BSA (500 μM) induced dephosphorylation of Ser315/Ser319 in both F8 human fibroblasts and Caco-2 cells, whereas no consistent changes occurred in Tyr359/Ser362 phosphorylation (**Figure 3.5 & 3.6**).

In agreement with previous studies, oleate/BSA treatments stimulated CCTα translocation to the INM in HeLa cells and F8 fibroblasts as assessed by confocal microscopy (**Figure 3.7 & 3.8**). Anti-p-Ser315/Ser319 detected primarily nucleoplasmic staining and did not detect CCTα at the INM in oleate/BSA-treated cells (**Figure 3.9**), providing evidence that CCTα is dephosphorylated upon translocation to the INM. In non-human cell lines, oleate/BSA treatment also induced dephosphorylation at Ser315/Ser319 but not Tyr359/Ser362 in IEC-ras34 as assessed by Western blot (**Figure 3.10**) and this coincided with translocation of CCTα to the INM in and decreased nuclear p-Ser315/Ser319 signal in IEC-18, IEC-ras33, and IEC-ras34 (**Figure 3.11**).

Given that INM-associated CCTα appeared to be dephosphorylated in response to oleate/BSA treatment, I sought to characterize the response of CCTα after removing oleate

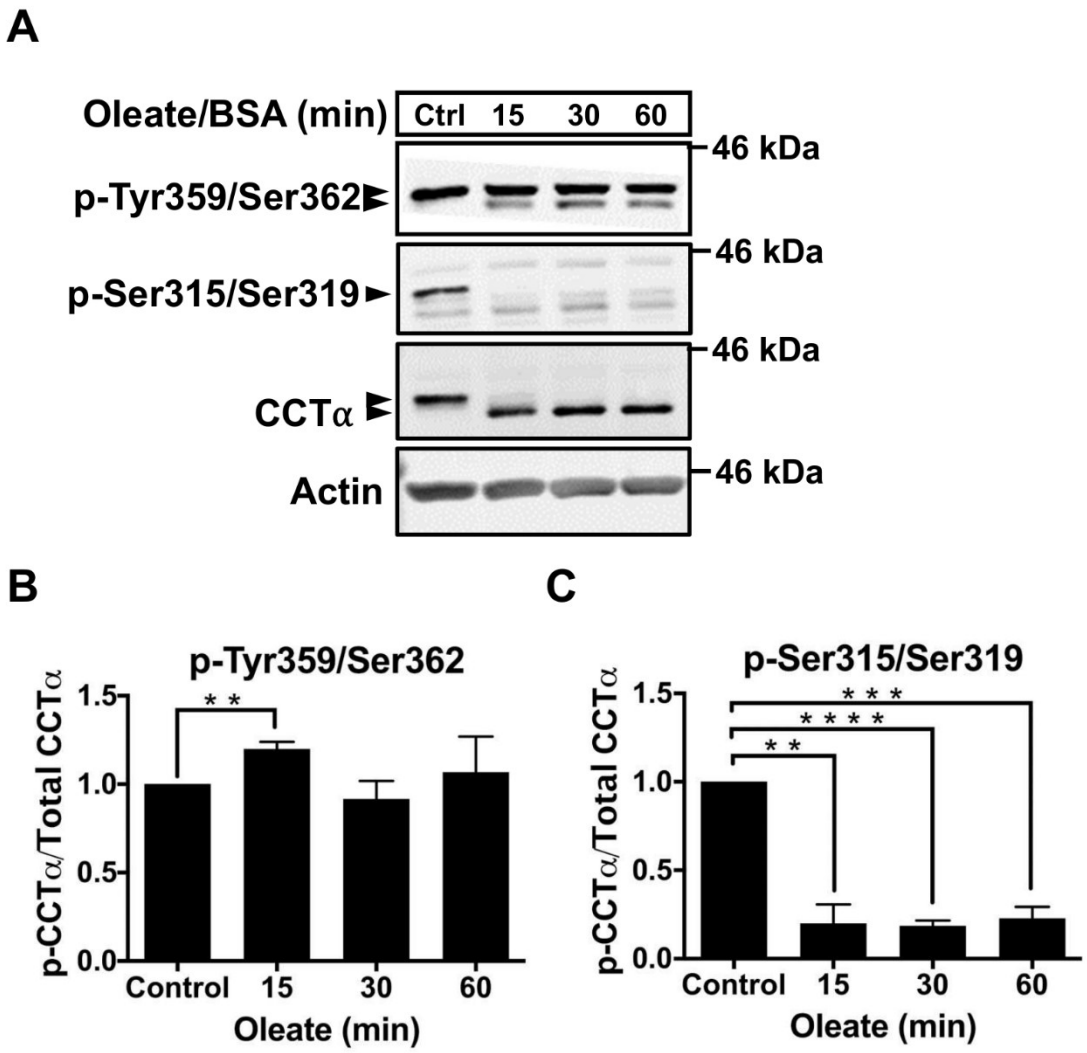

Figure 3.4. Oleate treatment induces dephosphorylation of Ser315/Ser319 but not Tyr359/Ser362 in HeLa cells. HeLa cells were cultured in 35-mm dishes to until approximately 50-80% confluent. Media was replaced with serum-free DMEM (control) and treated with 500 μM oleate/BSA was added to each dish for 15, 30, or 60 min. Whole-cell lysates were collected as described in Section 2.5, resolved by SDS-PAGE. Protein was transferred to nitrocellulose and immunoblotted with anti-CCTα (1:500), anti-p-Tyr359/Ser362 (1:1000), and anti-p-Ser315/Ser319 (1:1000). Phosphorylation was quantified relative to total CCTα protein. Results are the mean and SEM of three experiments.

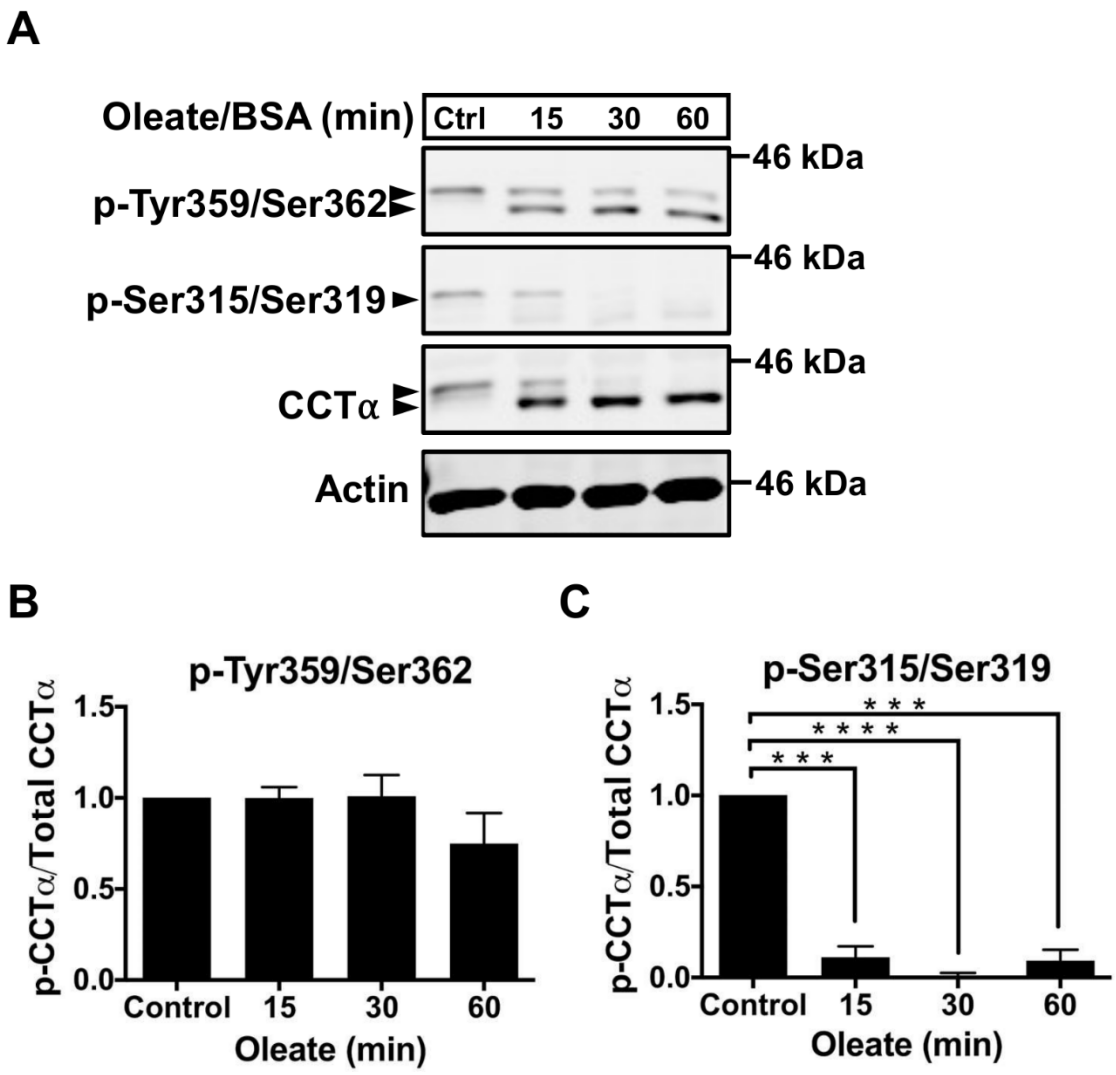

Figure 3.5. Oleate treatment induces dephosphorylation of Ser315/Ser319 but not Tyr359/Ser362 in F8 human fibroblasts. F8 human fibroblasts were cultured in 35-mm dishes until approximately 70% confluent. Media was replaced with serum-free DMEM (control) and 500 μM oleate/BSA was added to each dish for 15, 30, or 60 min. Whole-cell lysates were collected as described in Section 2.5 and resolved by SDS-PAGE. Protein was transferred to nitrocellulose and immunoblotted with anti-CCTα (1:500), anti-p-Tyr359/Ser362 (1:1000), and anti-p-Ser315/Ser319 (1:1000). Phosphorylation was quantified relative to whole CCTα protein. Results are the mean and SEM of three experiments.

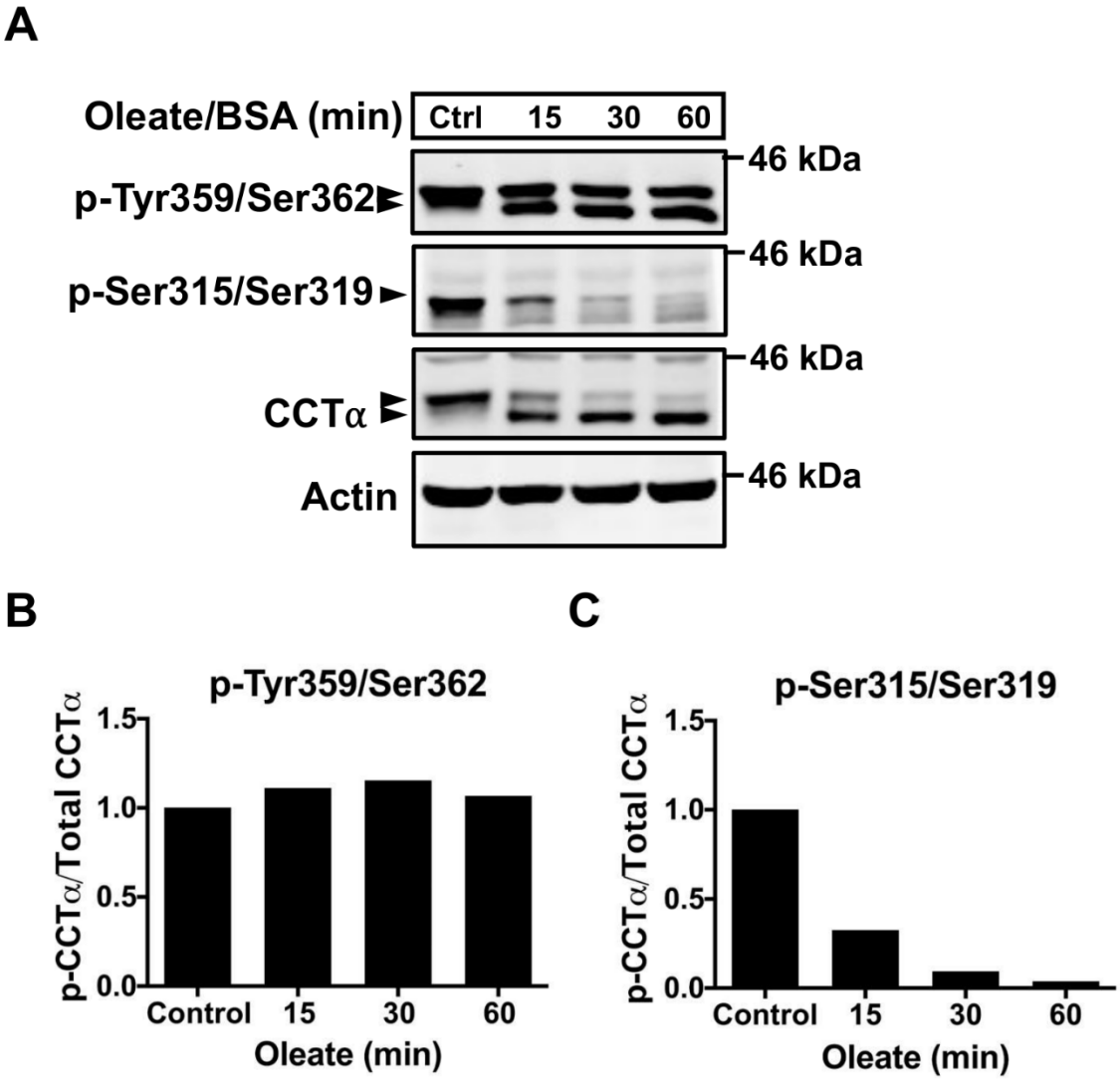

Figure 3.6. Oleate treatments induce dephosphorylation of Ser315/Ser319 but not Tyr359/Ser362 in Caco2 cells. Caco2 cells were cultured in 35-mm dishes until approximately 70% confluent. Media was replaced with serum-free DMEM (control) and 500 μM oleate/BSA was added to each dish for 15, 30, or 60 min. Whole-cell lysates were collected as described in Section 2.5 and resolved by SDS-PAGE. Protein was transferred to nitrocellulose and immunoblotted with anti-CCTα (1:500), anti-p-Tyr359/Ser362 (1:1000), and anti-p-Ser315/Ser319 (1:1000). Results are from a single experiment.

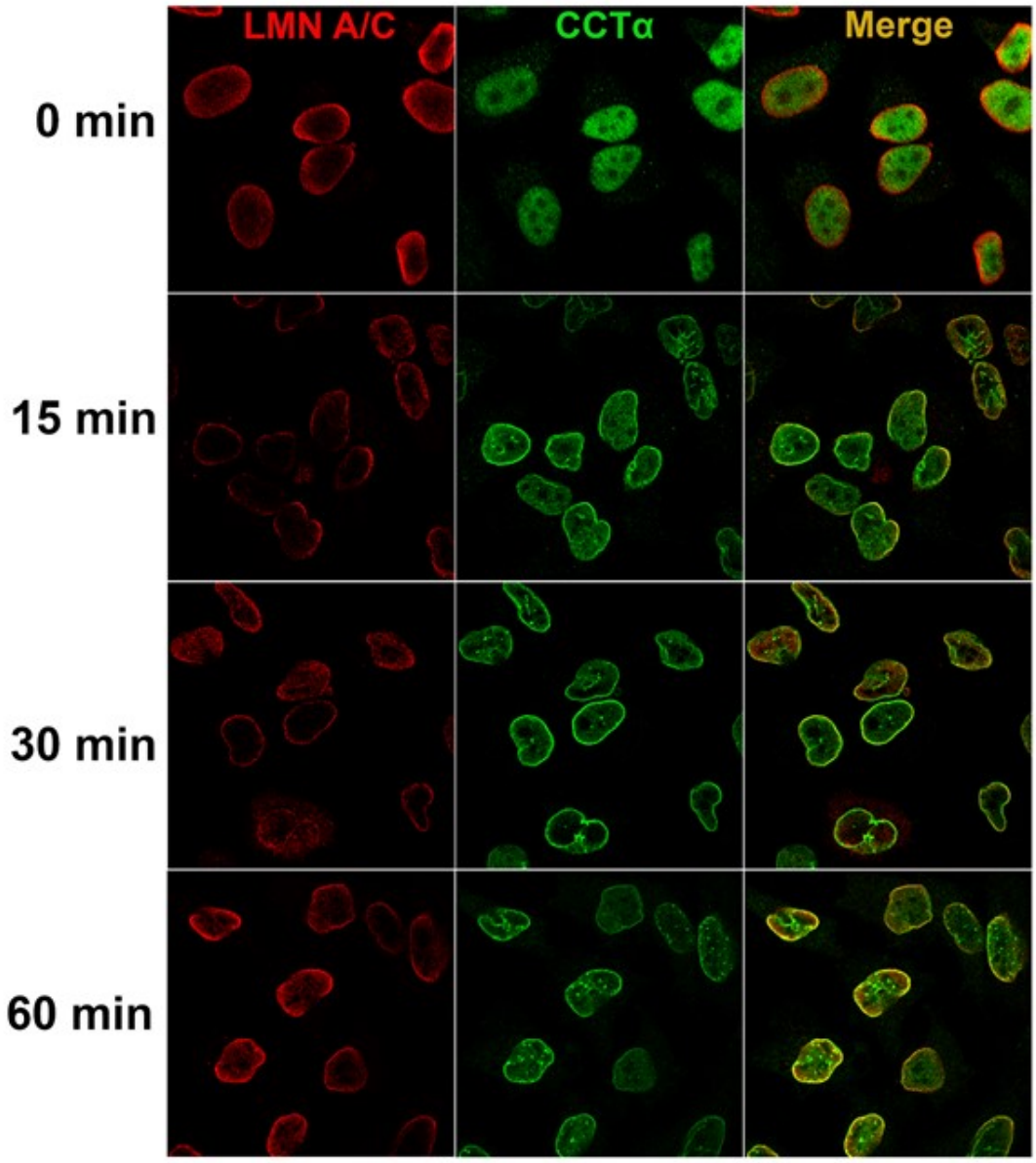

Figure 3.7. Oleate induces translocation of CCTα in HeLa cells. HeLa cells were cultured in 35-mm dishes with 1.0 mm coverslips until approximately 50-80% confluent. Media was replaced with serum-free DMEM (0 min) and 500 μM oleate/BSA was added to each dish for 15, 30, or 60 min. Cells were fixed and permeabilized as described in Section 2.6. and were probed with anti-CCTα (1:500) and anti-lamin A/C (1:500).

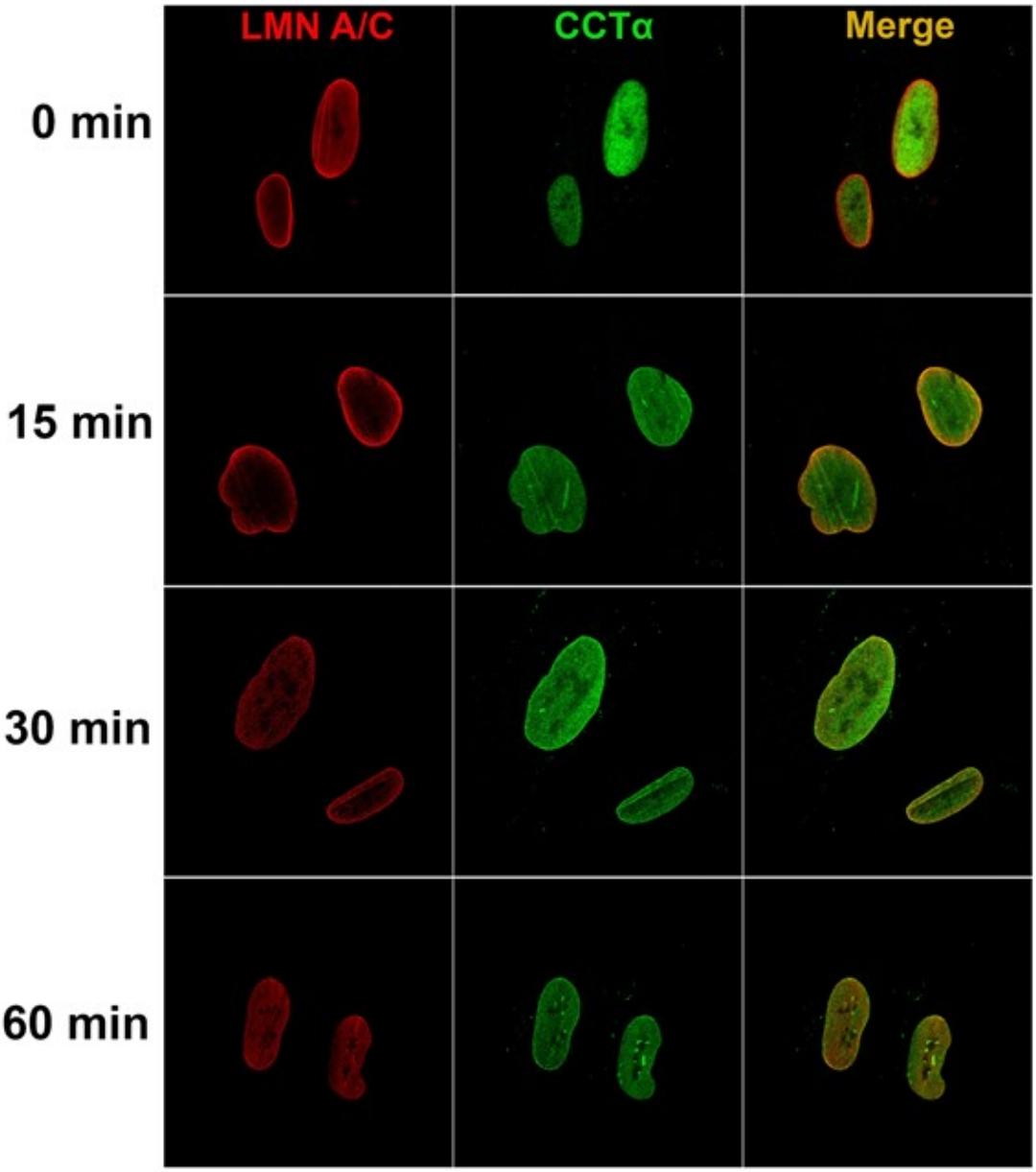

Figure 3.8. Oleate induces translocation of CCTα in F8 human fibroblasts. F8 cells were cultured in 35-mm dishes with 1.0 mm coverslips until approximately 50% confluent. Media was replaced with serum-free DMEM (0 min) and 300 µM oleate/BSA was added to each dish for 15, 30, or 60 min. Cells were fixed and permeabilized as described in Section 2.6. and were probed with anti-CCTα (1:500) and anti-lamin A/C (1:500).

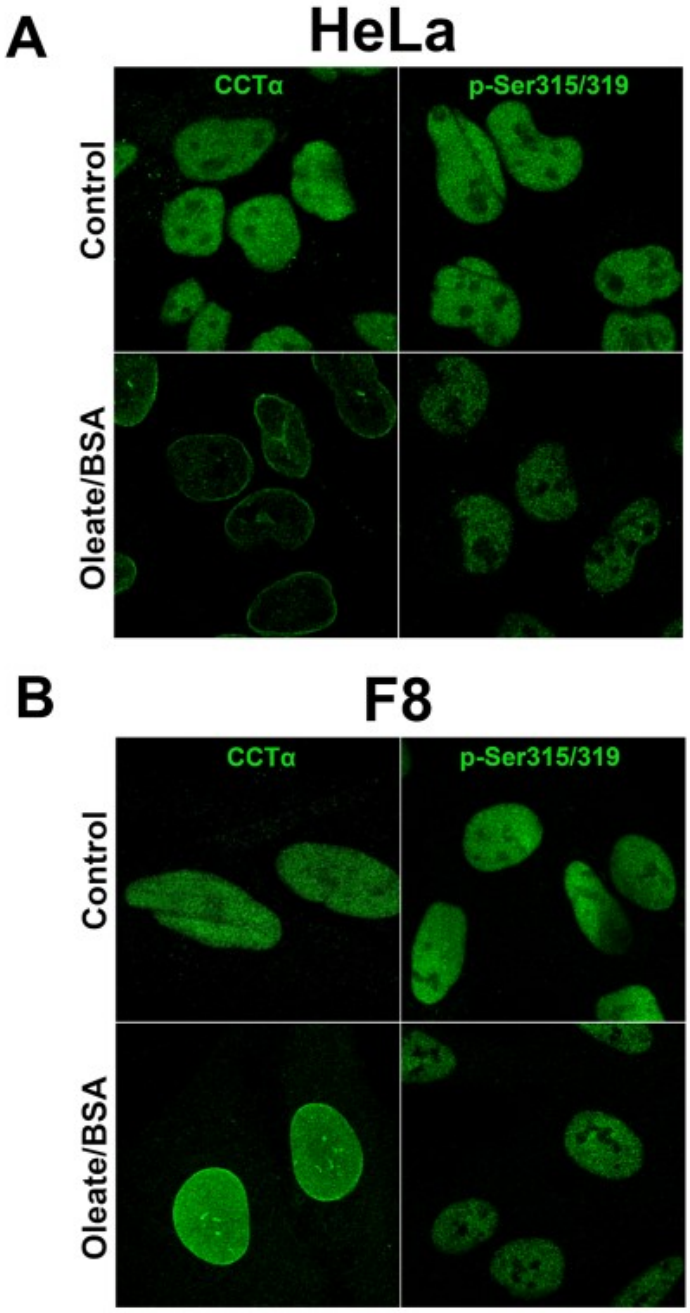

Figure 3.9. Oleate-induced translocated CCTα is dephosphorylated at Ser315/Ser319 in HeLa cells and F8 human fibroblasts. (A) HeLa cells and **(B)** F8 human fibroblasts were cultured in 35-mm dishes with 1.0 mm coverslips until approximately 50-80% confluent. Media was replaced with serum-free DMEM with no addition or treated with 500 μM oleate/BSA for 30 min. Cells were fixed and permeabilized as described in Section 2.6. and were probed with anti-CCTα (1:500) or anti-p-Ser315/Ser319 (1:500).

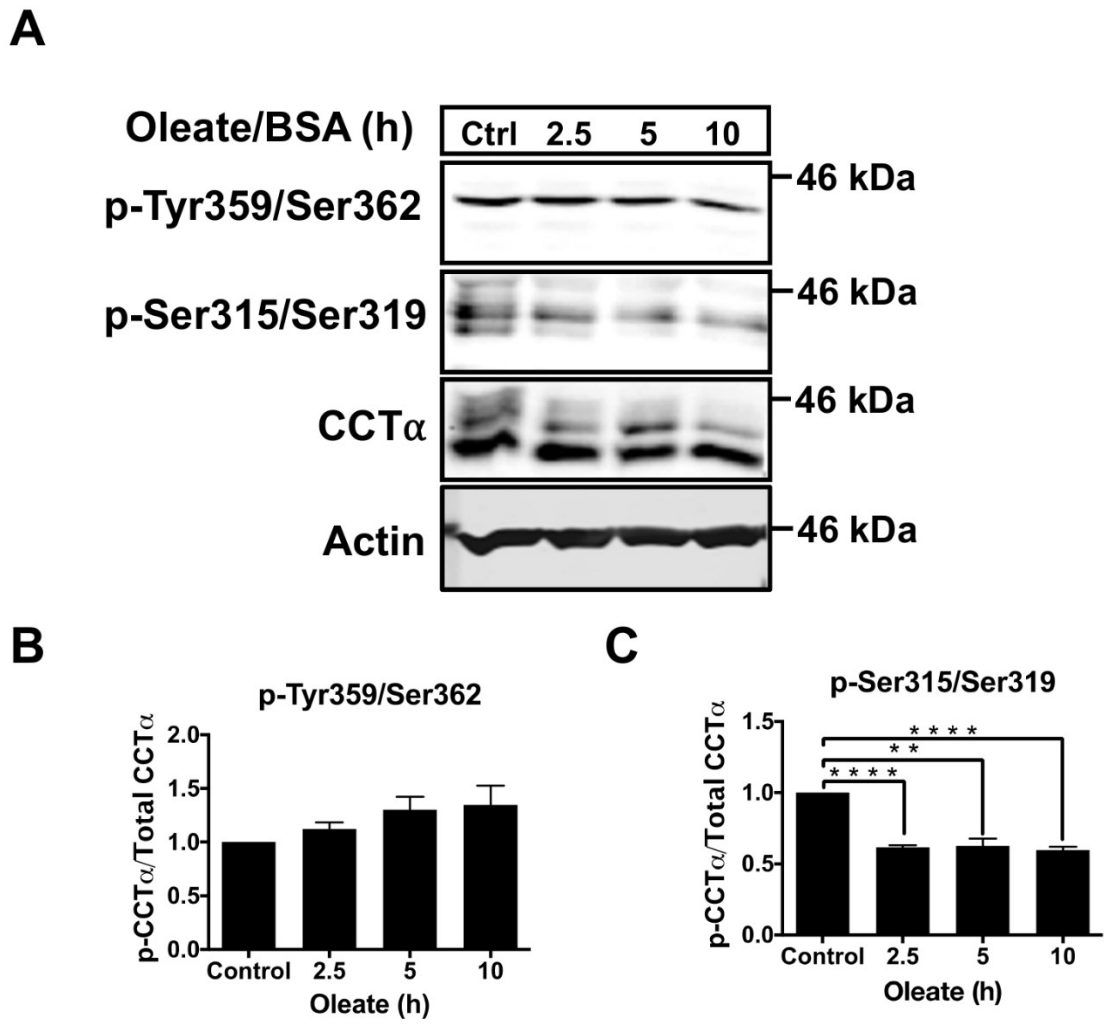

Figure 3.10. Oleate treatment induces dephosphorylation of Ser315/Ser319 but not Tyr359/Ser362 in IEC-ras34 cells. IEC-ras34 were cultured in 35-mm dishes until 70-80% confluence. Media was replaced with IEC-MEM (control) 300 μM oleate/BSA was added to each dish for 2.5, 5, or 10 h. Whole-cell lysates were collected as described in Section 2.5, resolved by SDS-PAGE, transferred to nitrocellulose and immunoblotted with anti-CCTα (1:500), anti-pCCT-Tyr359/Ser362 (1:1000), and anti-p-Ser315/Ser319 (1:1000). Phosphorylation was quantified relative to whole CCTα protein. Results are the mean and SEM of three experiments.

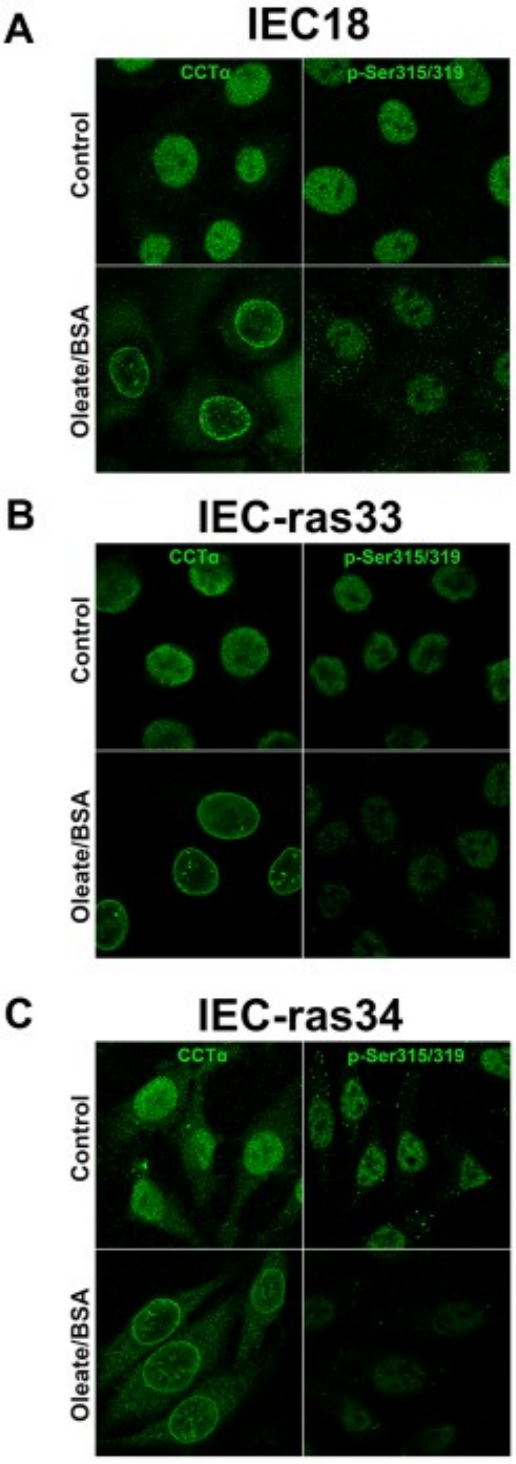

Figure 3.11. Oleate treatment induces translocation and dephosphorylation of Ser315/Ser319 in IEC-18, IEC-ras33, and IEC-ras34 cells. (A) IEC-18 and **(B & C)** IEC-ras cells were cultured in 35-mm dishes until 50-70% confluent. Media was replaced with serum-free α-MEM with either no addition (control) or 300 μM oleate/BSA for dish for 60 min. Cells were fixed and permeabilized as described in Section 2.6. and were probed with anti-CCTα (1:500) or anti-p-Ser315/Ser319 (1:500).

from culture. Replacing oleate/BSA-containing media was found to increase phosphorylation of Ser315/Ser319 around 30 min post-oleate removal in HeLa cells and around 60 min post-oleate removal in F8 human fibroblasts (**Figure 3.12 & 3.13**). CCTα began to dissociate from the INM by 30 min in both HeLa and F8 cells and this correlated with increased anti-p-Ser315/Ser319 signal intensity in the nucleus (**Figure 3.14**). Taken together, these data suggest the Ser315/Ser319 is re-phosphorylated when CCTα dissociates from the INM.

3.1.2 Choline depletion induces dephosphorylation of CCTα at Ser315/Ser319 in IEC-ras

Choline depletion deprives the CDP-choline pathway of exogenous substrate, resulting in decreased membrane PC and increased DAG that promotes CCTα translocation and activation.[6,214–216] Relevant to our interest in the role of the CDP-choline pathway in ras-transformation, I compared CCTα activation by choline depletion in non-transformed IEC-18 and ras-transformed IEC-ras33 and ras34 cell lines. As expected, choline depletion for up to 24 h triggered significant dephosphorylation of Ser315/Ser319 in IEC-ras33 and ras34 but not IEC-18 (**Figure 3.15**). CCTα remained soluble and diffuse in the nucleus of IEC-18 cells whereas CCTα translocated to the NE and to the nucleoplasmic reticulum in IEC-ras34 (**Figure 3.16**). These data are consistent with the results for oleate stimulation in IEC-ras and further support the conclusion that activation of CCTα at the INM is associated with dephosphorylation at Ser315/Ser319.

Previous studies have shown that autophagy initiation promotes PC synthesis in FL83B mouse hepatoma cells.[172] I was interested in determining whether or not starvation-induced autophagy affected phosphorylation of CCTα. IEC-ras34 were starved with

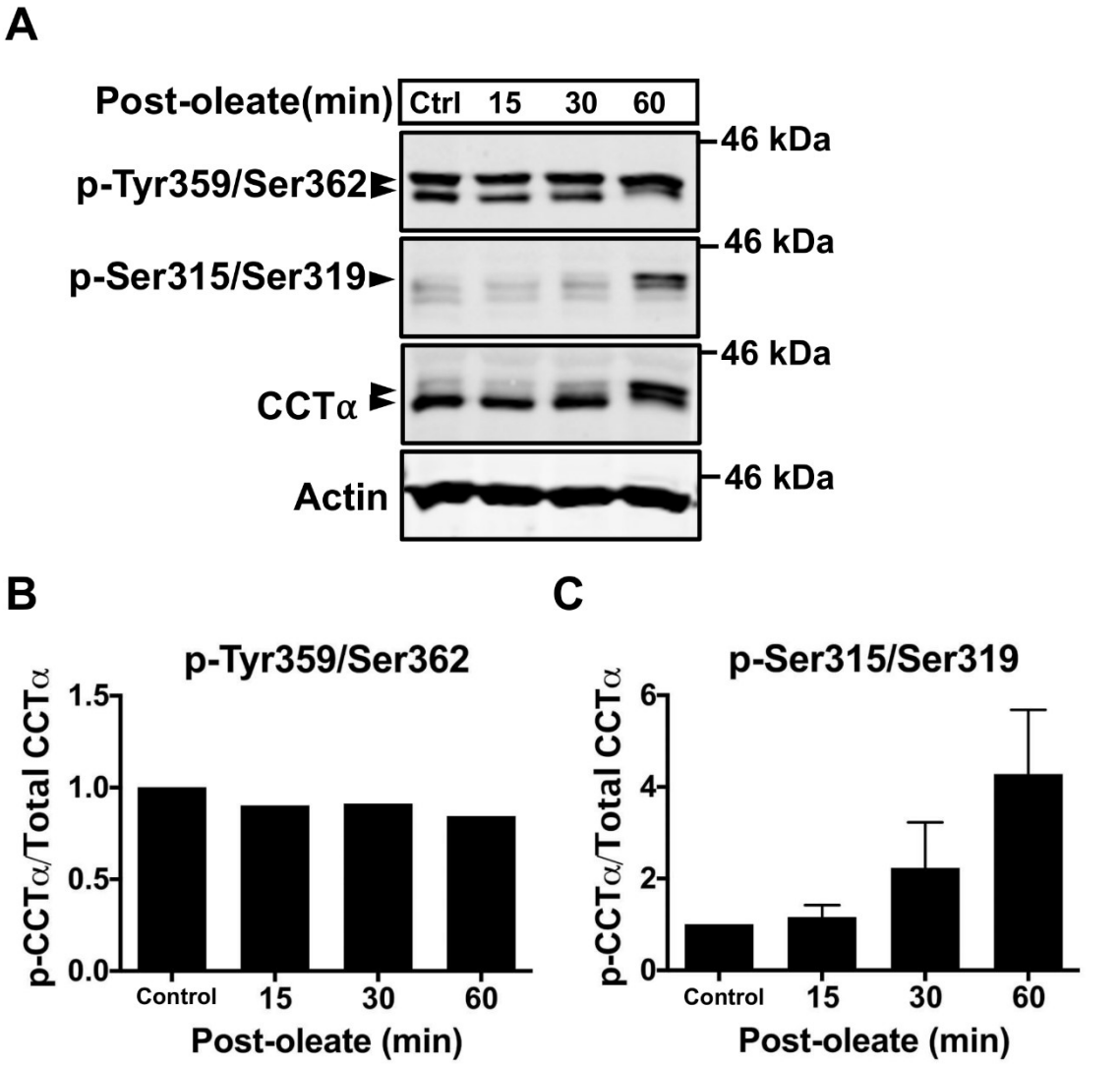

Figure 3.12. Removing oleate from culture induces CCTα phosphorylation in HeLa cells. HeLa cells were cultured in 35-mm dishes for 48 h. Media was replaced with serum-free DMEM and the cells were treated with 300 μM oleate/BSA for 30 min (control). Oleate-containing media was then replaced with fresh serum-free DMEM and cells were incubated for 15, 30, and 60 min. Whole-cell lysates were collected as described in Section 2.5, resolved by SDS-PAGE, transferred to nitrocellulose and immunoblotted with anti-CCTα (1:500), anti-pCCT-Tyr359/Ser362 (1:1000), and anti-pCCT-Ser315/Ser319 (1:1000). Phosphorylation was quantified relative to whole CCTα protein. Results from panel A) and C) are the mean and SEM of three experiments.

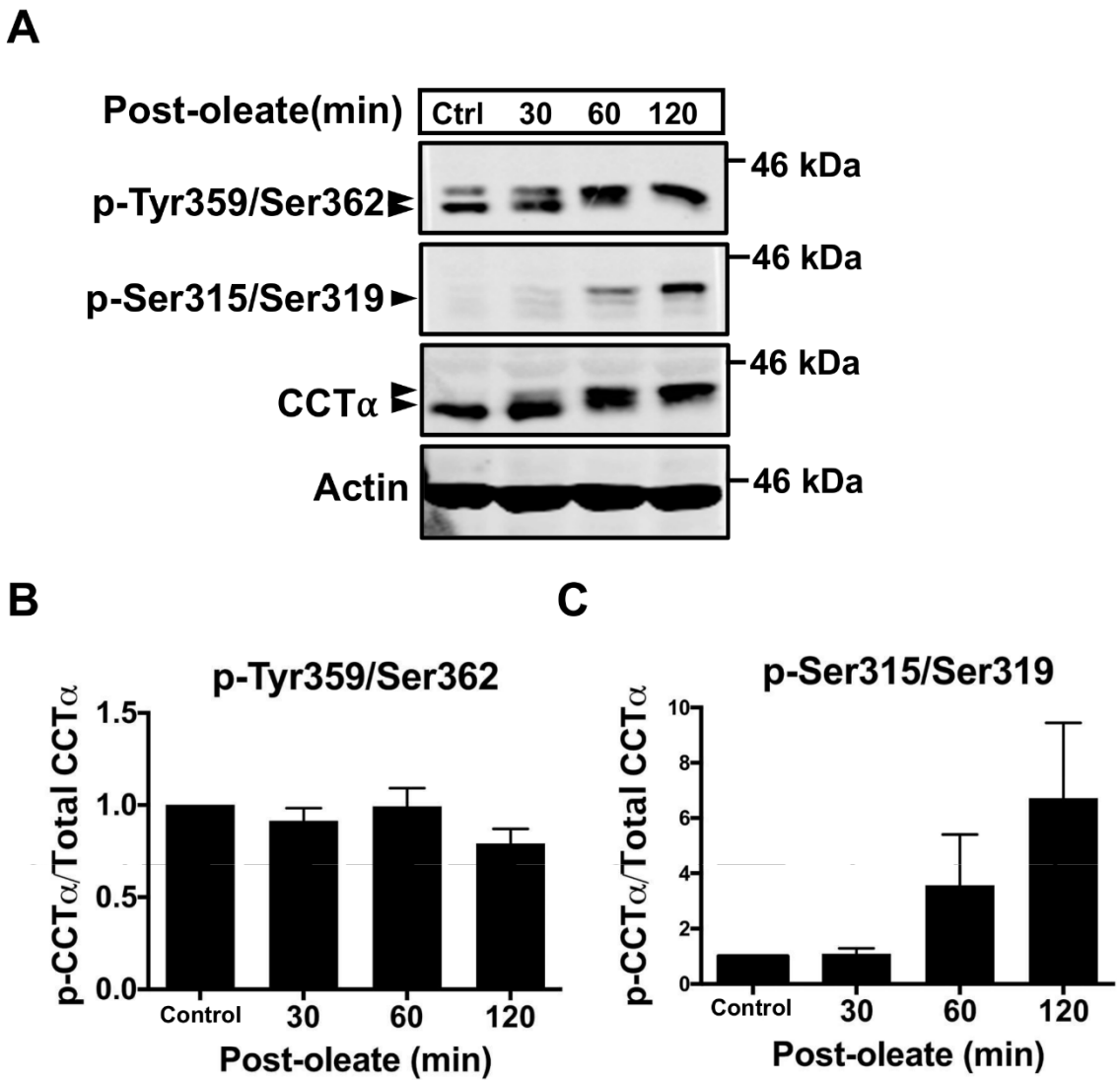

Figure 3.13. Removing oleate from culture induces CCTα phosphorylation in F8 human fibroblasts. F8 human fibroblasts were cultured in 35-mm dishes for 48 h. Media was replaced with serum-free DMEM and the cells were treated with 300 μM oleate/BSA for 30 min (control). Oleate-containing media was then replaced with fresh serum-free DMEM and cells were incubated for 15, 30, and 60 min following removal of oleate/BSA. Whole-cell lysates were collected as described in Section 2.5, resolved by SDS-PAGE. Protein was transferred to nitrocellulose and immunoblotted with anti-CCTα (1:500), anti-pCCT-Tyr359/Ser362 (1:1000), and anti-pCCT-Ser315/Ser319 (1:1000). Phosphorylation was quantified relative to whole CCTα protein. Results are the mean and SEM of three experiments.

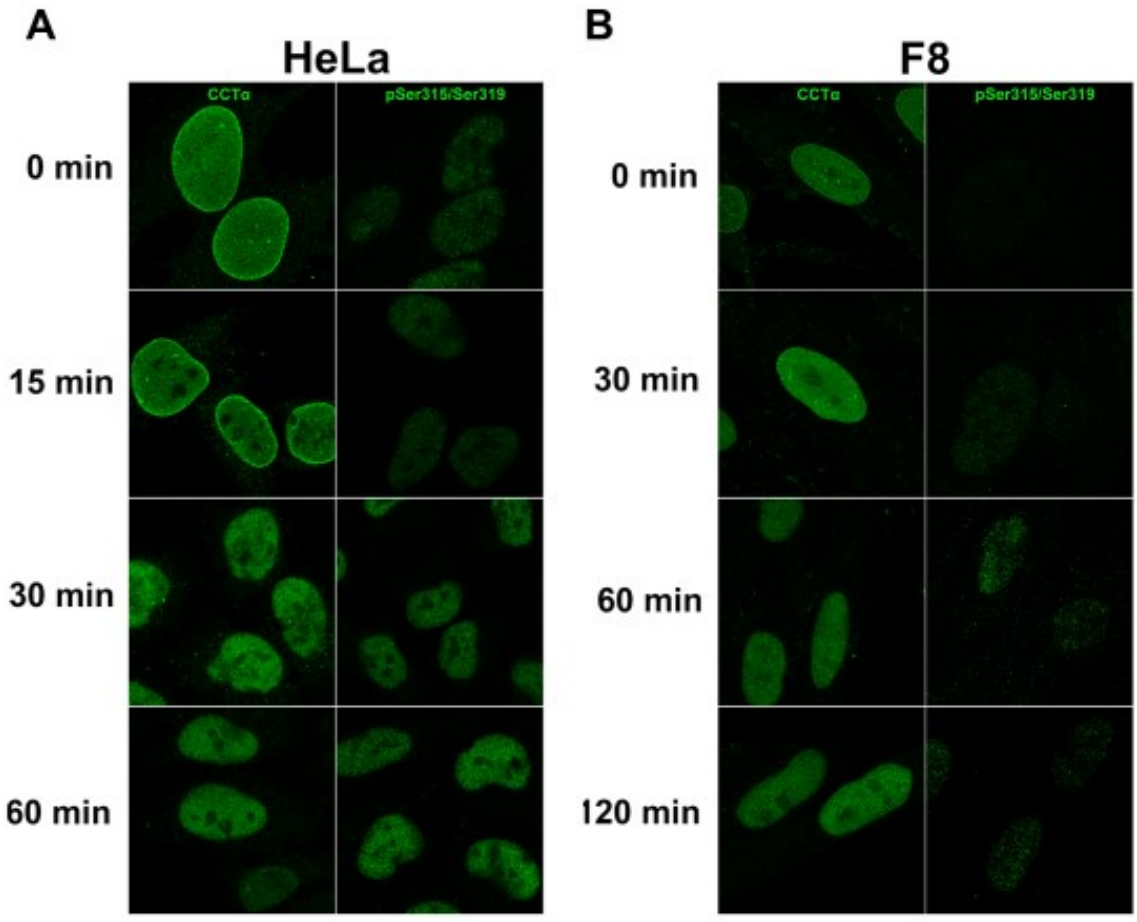

Figure 3.14. Oleate removal from HeLa cells and F8 human fibroblasts induces CCTα dissociation from the NE. (A) HeLa cells or **(B)** F8 human fibroblasts were cultured in 35-mm dishes for 48 h. Media was replaced with serum-free DMEM and the cells were treated with 300 μM oleate/BSA for 30 min (0 min). Oleate-containing media was then replaced with fresh serum-free DMEM and cells were incubated for 30, 60 and 120 min following removal of oleate/BSA. Cells were fixed and permeabilized as described in Section 2.6. and were probed with anti-CCTα (1:500) and anti-pCCT-Ser315/Ser319 (1:500).

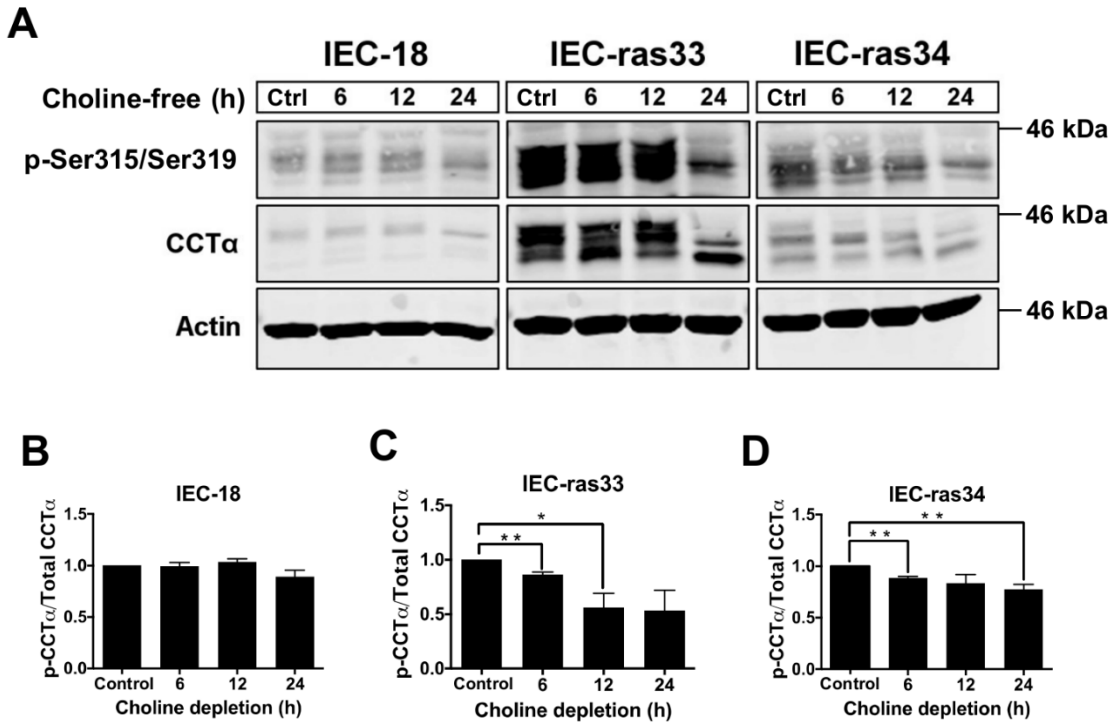

Figure 3.15. Choline depletion induces CCTα dephosphorylation in IEC-ras but not IEC-18. IEC-18, IEC-ras33, and IEC-ras34 were cultured in 35-mm dishes for 24-36 h prior to experiment. Media was replaced with choline free-DMEM with 5% dialyzed FBS for 6, 12, and 24 h. For a control, cells were cultured for 24 h with choline-free DMEM (CF-DMEM) supplemented with 50 μM choline. Whole-cell lysates were collected as described in Section 2.5, resolved by SDS-PAGE. Protein was transferred to nitrocellulose and immunoblotted with anti-CCTα (1:1000), anti-pCCT-Tyr359/Ser362 (1:1000), and anti-pCCT-Ser315/Ser319 (1:1000). Phosphorylation was quantified relative to whole CCTα protein. Results are the mean and SEM of three experiments.

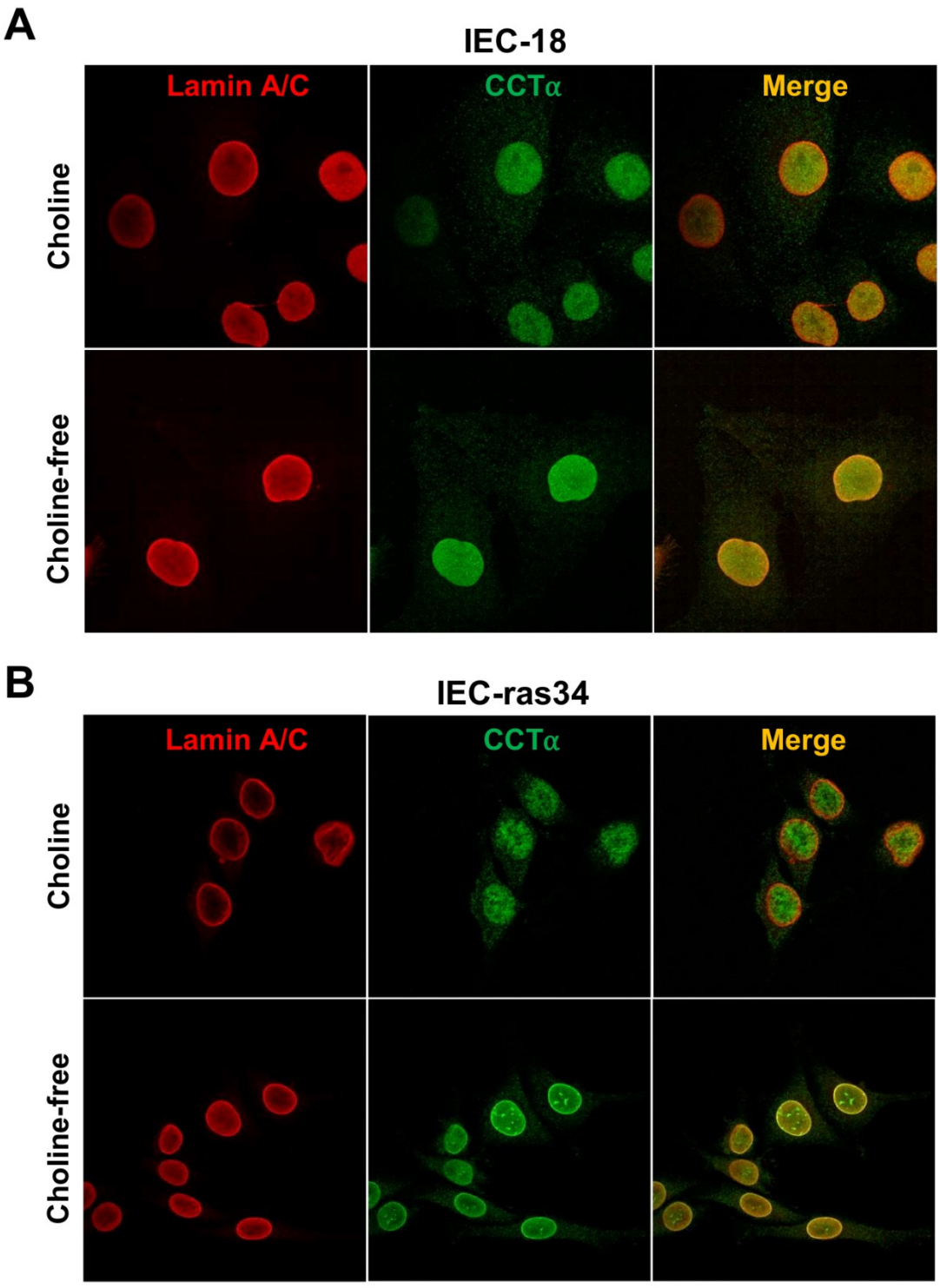

Figure 3.16. Choline depletion induces CCTα translocation in IEC-ras34 but not IEC-18. (A) IEC-18 and **(B)** IEC-ras34 were seeded onto 1.0 mm coverslips in 35-mm dishes and cultured for 24 h. Media was replaced with CF-DMEM with 5% dialyzed FBS for 24 h with or without 50 µM choline. Cells were fixed and permeabilized as described in Section 2.6. and were probed with anti-CCTα (1:1000) and anti-lamin A/C (1:500).

HBSS, a potent inhibitor of mTORC1 activity via amino acid and mitogen starvation, to see if autophagy activation might stimulate CCTα dephosphorylation over a 6-hour period. HBSS contains no choline or growth factors known to stimulate PC biosynthesis, so IEC-ras34 were incubated in HBSS with or without choline (50 μM). HBSS treatment alone decreased phosphorylation of Ser315/Ser319 in IEC-ras34 relative to control, HBSS with choline slightly increased phosphorylation at this site (**Figure 3.17**). Once again, no statistically significant difference was found in the phosphorylation of Tyr359/Ser362. Confocal microscopy confirmed that CCTα translocated to the INM following HBSS treatment, and anti-pCCT Ser315/Ser319 did not detect membrane-associated CCTα at the same time points (**Figure 3.18**). These data suggest that HBSS induces choline depletion of IEC-ras, significantly stimulating CCTα translocation and dephosphorylation of Ser315/Ser319 but not Tyr359/Ser362.

3.1.3 CCTα is phosphorylated at Ser315/Ser319 in IEC-ras grown detached from the ECM

Having shown that CCTα activation is correlated with Ser315/Ser319 dephosphorylation, I next sought to study CCTα phosphorylation in response to detachment-induced PC biosynthesis in IEC-ras34. As discussed previously, malignant cells survive detachment from the ECM through evasion of anoikis and lentiviral knockdown of CCTα in IEC-ras34 sensitized these cells to anoikis.[136] It was also shown that IEC-ras34 grown on agarose had sustained PC synthesis whereas non-malignant IEC-18 did not. Interestingly, CCTα appeared to be hyperphosphorylated during IEC-ras34 growth on agarose, indicating potential contradicting mechanisms for regulating CCTα activity under different conditions.[136] I also found that there was increased phosphorylation

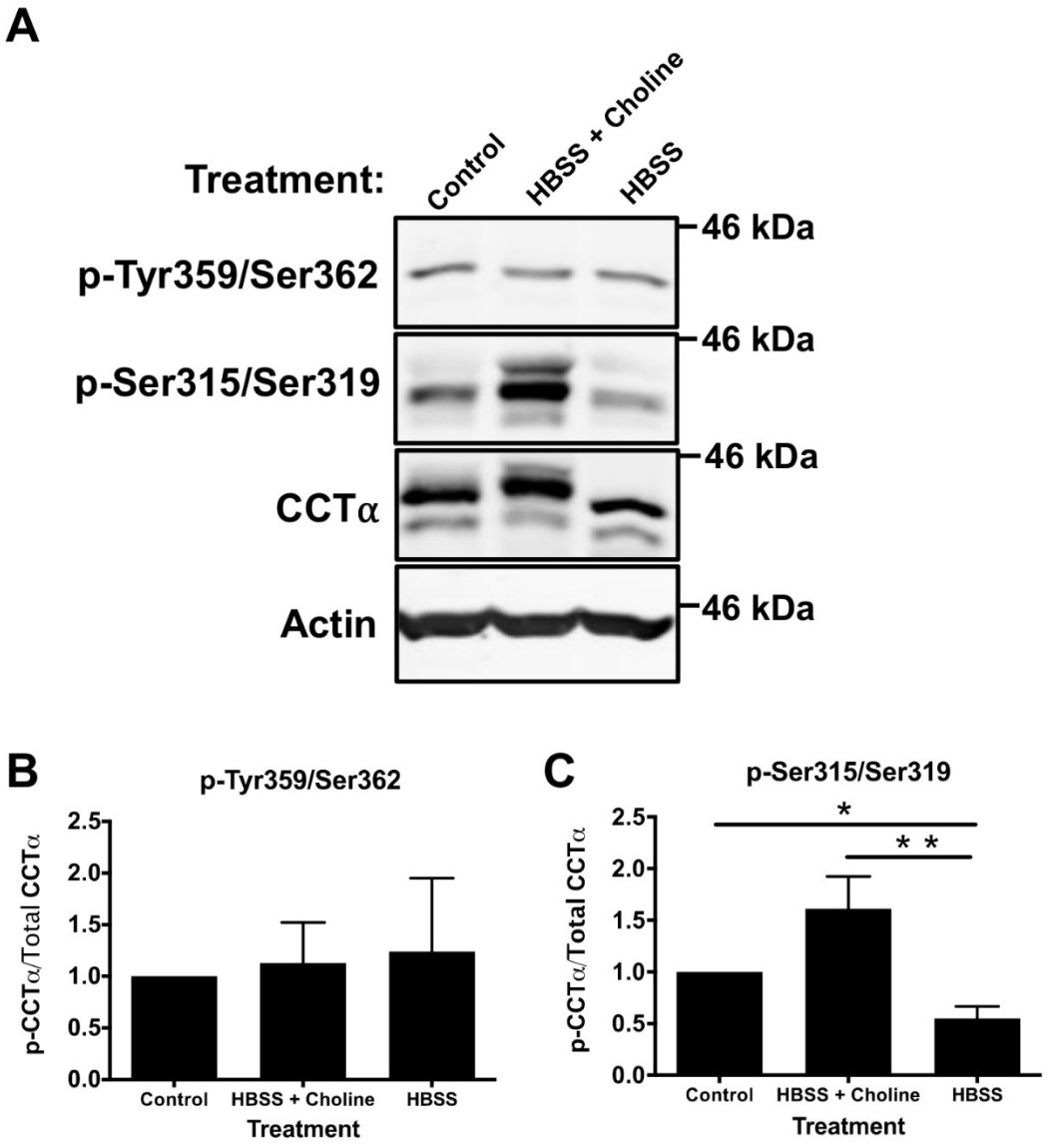

Figure 3.17. HBSS-induced dephosphorylation of Ser315/Ser319 is choline-dependent in IEC-ras34. IEC-ras34 were cultured in 35-mm dishes until 70-80% confluent. Media was replaced with either IEC-MEM (Control), HBSS with 50 μM choline, or HBSS for up to six hours. Whole-cell lysates were collected as described in Section 2.5, resolved by SDS-PAGE. Protein was transferred to nitrocellulose and immunoblotted with anti-CCTα (1:500), anti-pCCT-Tyr359/Ser362 (1:1000), and anti-pCCT-Ser315/Ser319 (1:1000). Phosphorylation was quantified relative to whole CCTα protein. Results are the mean and SEM of five experiments.

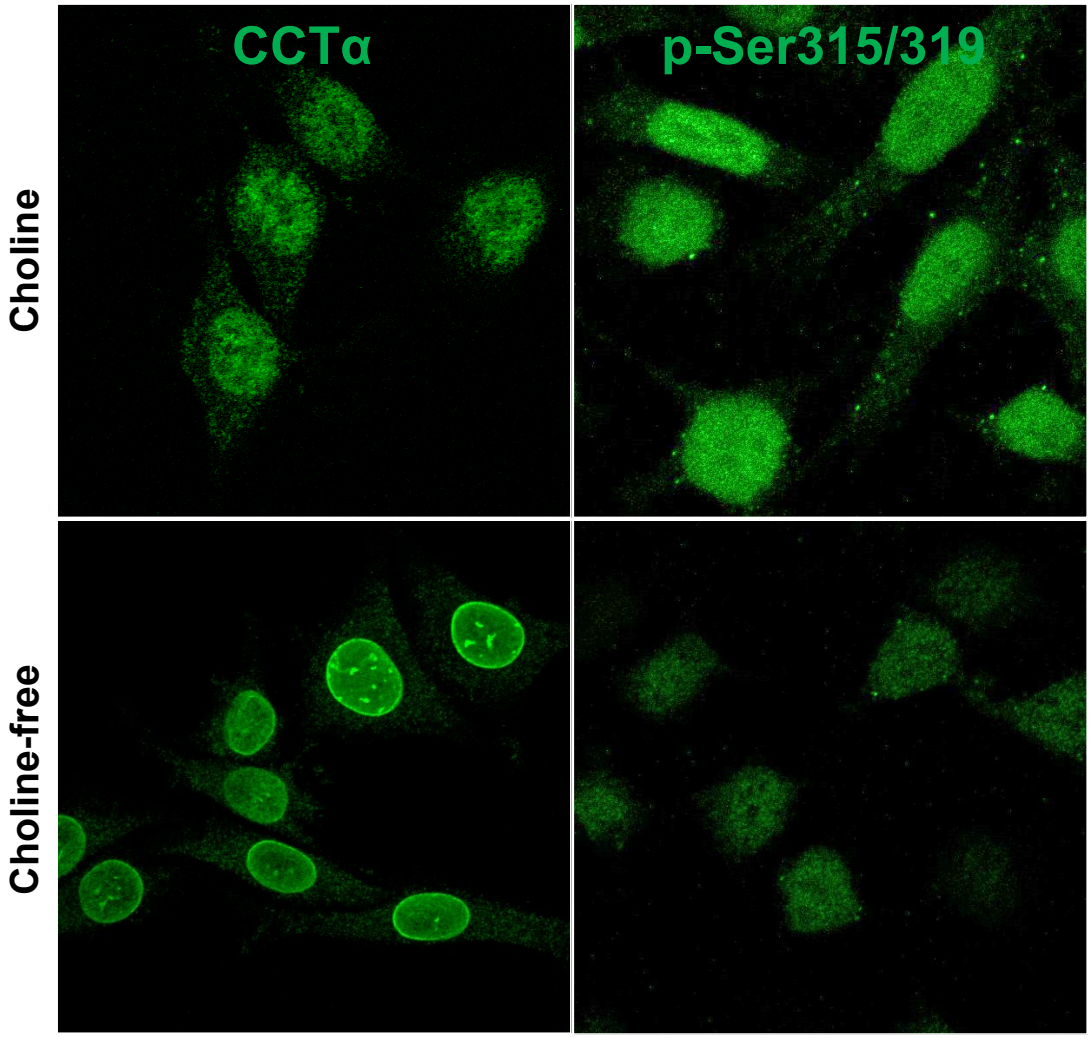

Figure 3.18. HBSS treatments induces translocation of CCTα in choline-dependent manner in IEC-ras34. IEC-ras34 were seeded on 1.0-mm coverslips and cultured in 35-mm dishes until 50% confluent. Media was replaced with either HBSS with or without 50 μM of choline for up to six hours. Cells were fixed and permeabilized as described in Section 2.6. and were probed with anti-CCTα (1:1000) or anti-pSer315/Ser319 (1:1000).

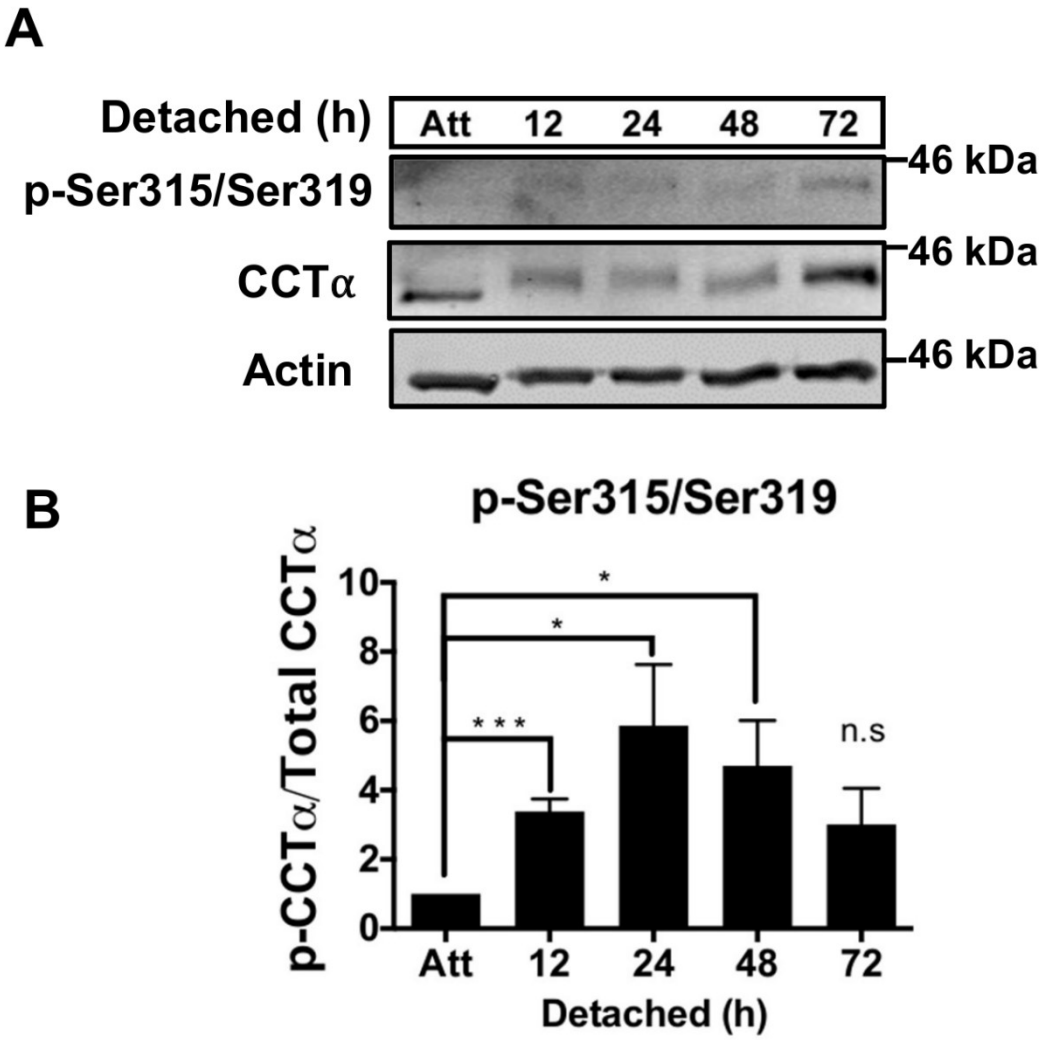

Figure 3.19. Detachment-independent growth is associated with increased phosphorylation of CCTα at Ser315/Ser319. Up to 100,000 IEC-ras34shNT cells were cultured for up to 72 h in 2 mL of IEC-MEM added to 60-mm dishes lined with 3 mL of 1% SeaPlaque® agarose. Detergent lysate sample concentrations were measured as described previously in Section 2.6 and resolved with SDS-PAGE, transferred to nitrocellulose, and immunoblotted for whole CCTα (1:500), p-Tyr359/Ser362 (1:1000), and p-Ser315/Ser319 (1:1000). Phosphorylation was quantified relative to whole CCTα protein. Results are the mean and SEM of four experiments.

of Ser315/Ser319 in IEC-ras34shNT grown on SeaPlaque® agarose as early 12 h and peaked by 24 h (**Figure 3.19**). These data indicate that phosphorylation of Ser315/Ser319 does not inhibit PC biosynthesis in IEC-ras grown detached from the ECM.

3.2 Investigating the role of PC biosynthesis in promoting cancer cell survival

3.2.1 Choline depletion does not cause p62 or LC3b-II accumulation in HCT116 cells

Choline depletion was previously shown to induce accumulation of p62 and LC3b-II in IEC-ras, suggesting that lack of PC synthesis inhibited autophagy (Zetrini & Ridgway, data unpublished). I confirmed that choline depletion of IEC-ras induced accumulation p62 by 12 and 24 h followed by a decline around 48 h (**Figure 3.20**). LC3b-II accumulated at 24 h and remained elevated until 48 h. I next sought to determine if this phenotype was relevant to a human cancer cell line. Choline depletion of HCT116 and K-ras-negative HKH2 and HKE3 did not induce p62 accumulation over 48 h (**Figure 3.21A**). Similar experiments also showed no accumulation of LC3b-II following a 24 h choline depletion (**Figure 2.1B)**. Taken together, I could not confirm that this phenotype occurs in HCT116 cells.

3.2.2 Choline depletion does not affect autophagic flux in IEC-ras

Inhibition of autophagosome-lysosome fusion causes LC3b-positive autophagosomes to accumulate as a result of blocking autophagic flux. I tested to see if choline depletion affected autophagic flux by stably expressing mCherry-eGFP-LC3 in IEC-ras34 to identify and separately quantify autophagosomes and autolysosomes.[161] This method relies on a dual-tagged LC3b protein being incorporated into autophagosomes. Both eGFP and mCherry proteins are stable in the autophagosome environment, but the

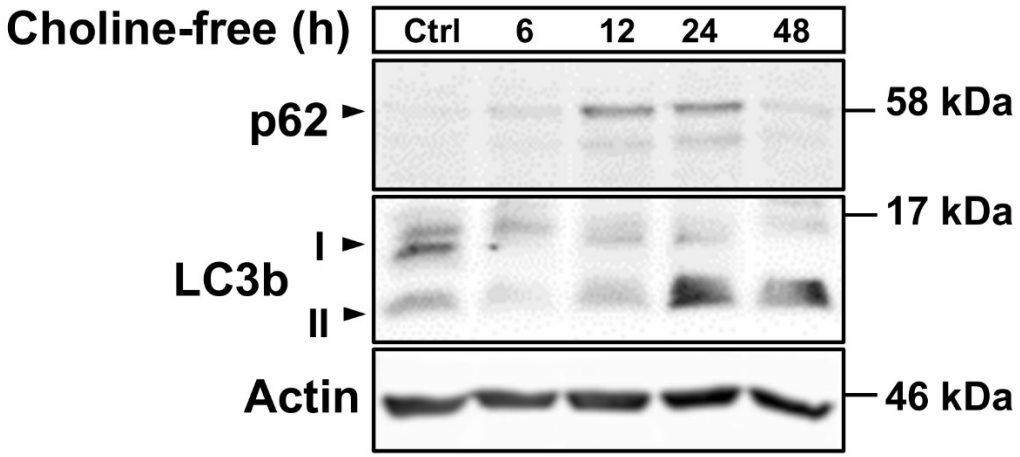

Figure 3.20. Choline depletion induces both p62 and LC3b-II accumulation in IEC-ras34. IEC-ras 34 were cultured in 35-mm dishes and treated with CF-DMEM with 5% dialyzed FBS for up to 48 h. For a control, cells were treated with CF-DMEM with 5% dialyzed FBS and 50 μM choline for up to 48 h Whole-cell lysates were collected and resolved with SDS-PAGE and transferred to nitrocellulose. Immunoblotting with anti-p62 (1:500) and anti-LC3b (1:1000).

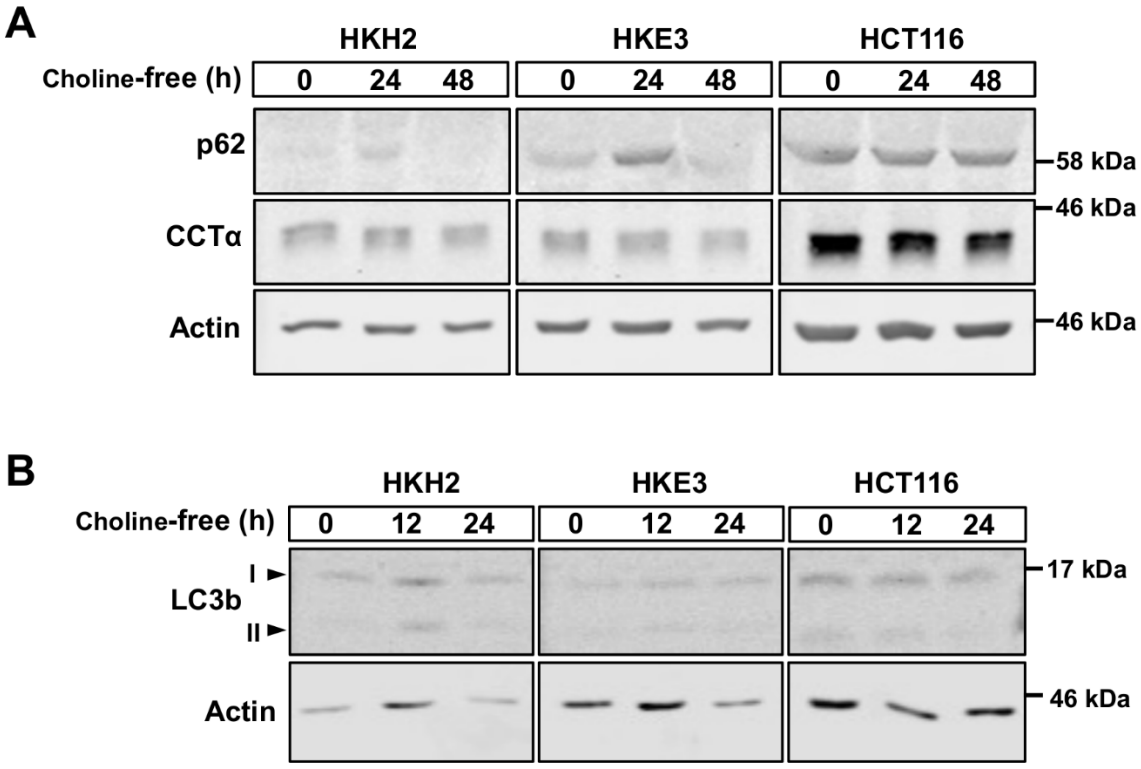

Figure 3.21. Choline depletion does not induce p62 of LC3 accumulation in human cancer cells. HCT116, HKE3, and HKH2 cells were cultured on 35-mm dishes and treated with CF-DMEM with 5% dialyzed FBS for up to **(A)** 48 h or **(B)** 24 h. Whole-cell lysates were collected and resolved with SDS-PAGE. Protein was transferred to nitrocellulose and immunoblotted with **(A)** anti-p62 (1:1000) and anti-CCTα (1:1000) or **(B)** LC3b (1:1000). Results are representative of two experiments.

autolysosome environment destabilizes the eGFP protein more readily. This causes the green eGFP signal to diminish and thus allows one to differentiate between autophagosomes and autolysosomes. IEC-ras34-mCherry-eGFP-LC3 were cultured in the presence or absence of choline for 24 h, either with or without chloroquine for 12 h. Quantification of autophagosomes and autolysosomes revealed that there was no significant effect of choline depletion on autophagic flux at these time points (**Figure 3.22**), suggesting that the accumulation of p62 in response to choline depletion is in response to another pathway activated in IEC-ras.

3.2.3 Choline depletion and CCTα knockdown does not induce the UPR through PERK-eIF2α-ATF4-CHOP in IEC-ras

p62 is involved in multiple stress pathways that promote cell survival or apoptosis depending on the conditions.[207,217] As discussed in Section 1.4.1, p62 mRNA and protein levels were transiently upregulated in bone marrow-derived macrophages following induction of ER stress.[203] The formation of p62-containing ALIS in the cytoplasm co-localized with ubiqitinated proteins. We previously found that choline depletion also triggered the formation of p62-rich puncta in the cytoplasm of IEC-ras, suggesting a possible link between the UPR and choline depletion (Zetrini & Ridgway, unpublished). To test this, I compared the accumulation of ubiquitinated proteins in IEC-18 and IEC-ras33 and ras34 in the presence or absence of choline for 24 h. While both IEC-ras had higher total ubiquitinated proteins compared to IEC-18, choline depletion produced no significant effect (**Figure 3.23**). Furthermore, the expression of the ER chaperones PDI and GRP78 was unaffected. Choline depletion also did not induce eIF2α phosphorylation or ATF4 and CHOP expression in IEC-ras. (**Figure 3.24 & 3.25**). Collectively, these data

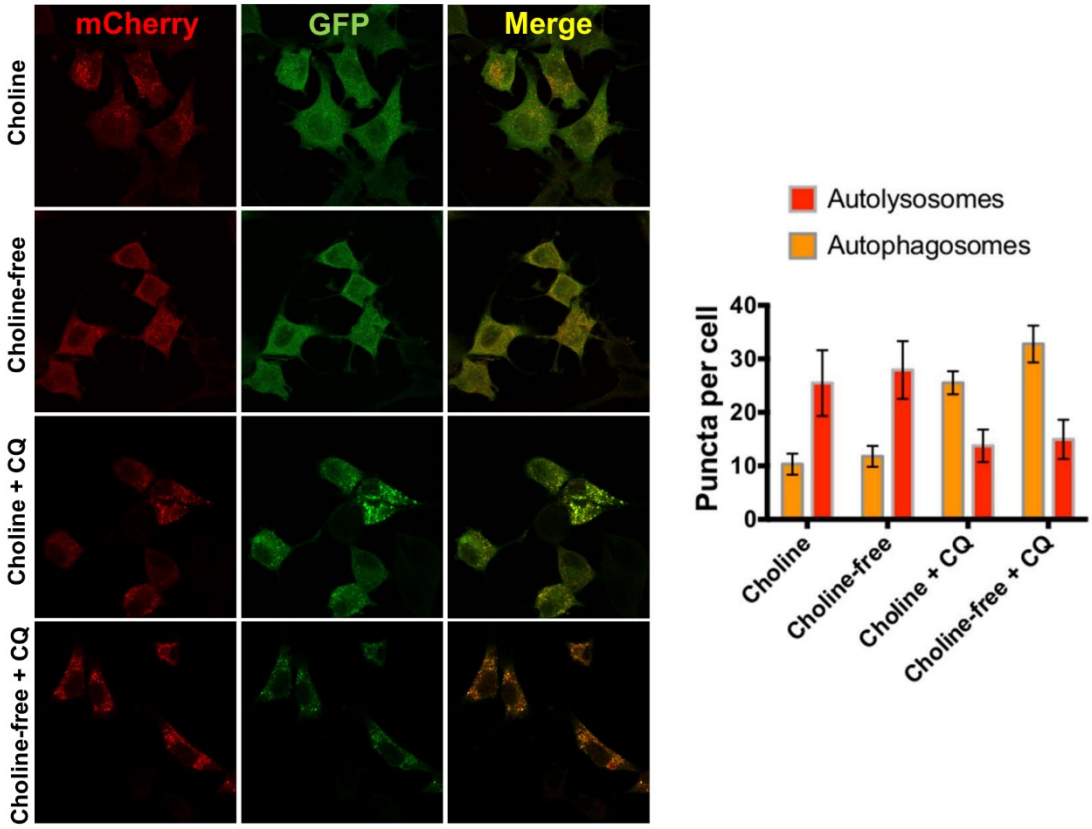

Figure 3.22. Choline depletion does not significantly affect autophagic flux in IEC-ras34. IEC-ras34 stably expressing mCherry-eGFP-LC3b were seeded onto 1.0 mm coverslips and cultured in 35-mm dishes. Cells were treated with CF-DMEM with 5% dialyzed FBS with or without 50 µM choline for 24 h. Additionally, cells were treated similarly but with or without the addition of 50 µM chloroquine for 12 h. Cells were fixed as described in Section 2.6 and imaged using confocal microscopy. Data are representative of three separate experiments (total of 989 cells).

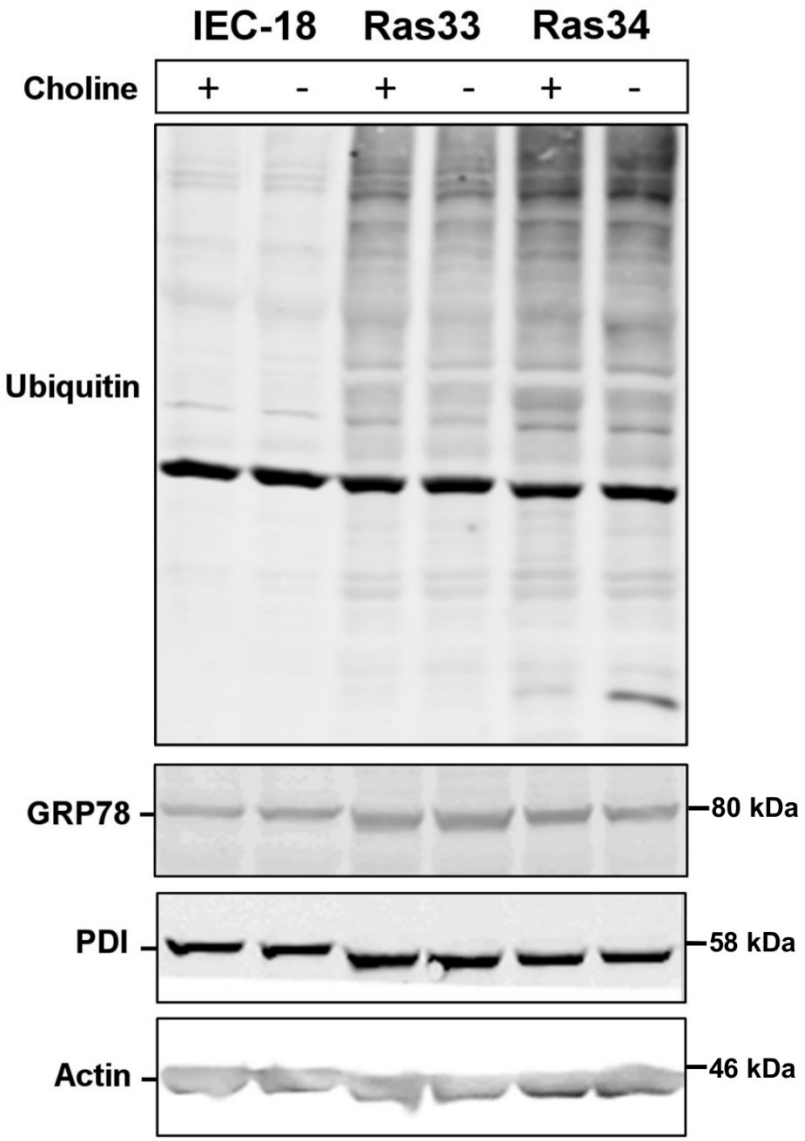

Figure 3.23. Choline depletion does not induce ER chaperone expression or increased ubiquitination in IEC-ras34. IEC-18, IEC-ras33, and IEC-ras34 were cultured in 35-mm dishes until 50% confluent and then cultured in CF-DMEM with 5% dialyzed FBS in the presence of absence of 50 μM choline for 24 h. Whole-cell lysates were collected and resolved with SDS-PAGE, transferred to nitrocellulose and immunoblotted with anti-Ubiquitin (1:1000), anti-GRP78(1:1000), and anti-PDI (1:1000).

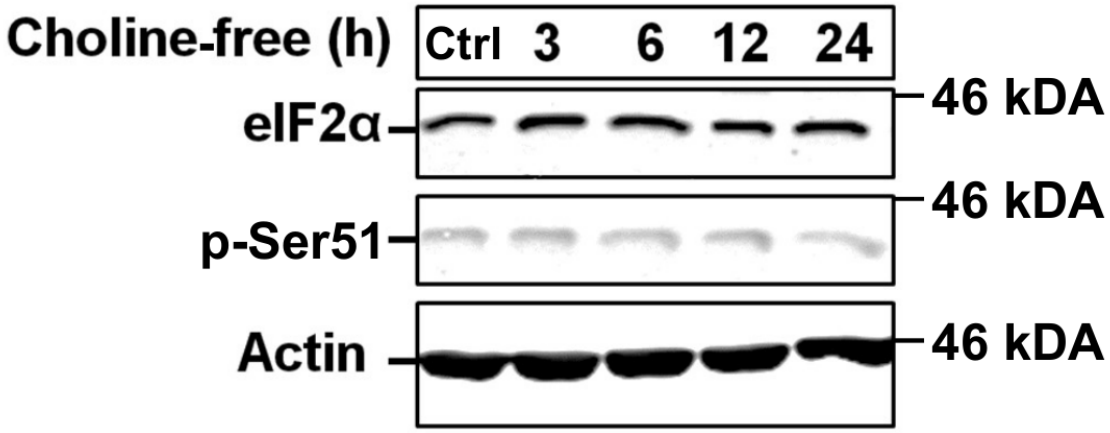

Figure 3.24. Choline depletion does not induced phosphorylation of eIF2α Ser51 in IEC-ras34. IEC-ras34 were cultured in 35-mm dishes until 50% confluent and then cultured in CF-DMEM with 5% dialyzed FBS for up to 24 h. Whole-cell lysates were collected and resolved with SDS-PAGE, transferred to nitrocellulose and immunoblotted with anti-eIF2α (1:1000) and anti-eIF2α pSer51 (1:1000).

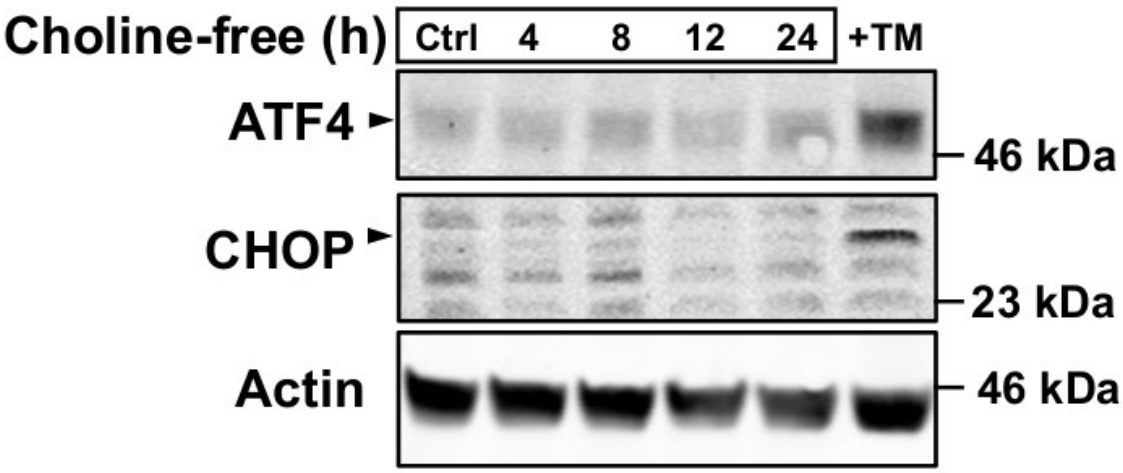

Figure 3.25. Choline depletion does not induce ATF4 or CHOP expression in IEC-ras34. IEC-ras34 were cultured in 35-mm dishes until 50% confluent and then cultured in CF-DMEM with 5% dialyzed FBS for up to 24 h. As a positive control, cells were also cultured in the presence of 10 mg mL^{-1} tunicamycin (+TM) for 8 h. Whole-cell lysates were collected and resolved with SDS-PAGE, transferred to nitrocellulose and immunoblotted with anti-ATF4 (1:1000) and anti-CHOP (1:1000). Results are representative of two experiments.

suggest that the choline depletion-induced p62 accumulation in IEC-ras is not caused by induction of the UPR through the PERK-eIF2α-ATF4-CHOP pathway.

Our previous data in showed p62 accumulation alongside PARP and Beclin cleavage in IEC-ras34 with lentiviral knockdown of CCTα and cultured on agarose (Zetrini & Ridgway, unpublished). This suggested that CCTα conferred anoikis resistance and that p62 accumulation might be involved with promoting anoikis in the absence of sufficient PC synthesis. Given that sustained ER stress can promote apoptosis through ATF4-CHOP, I used lentivirus to mediate shRNA knockdown of CCTα in IEC-ras34 and cultured them on agarose to see if this pathway was affected. Knockdown efficiency was approximately 75% efficient shCCTα relative to shNT controls (**Figure 3.26a**). However, ATF4 or CHOP were not induced during this time when compared with tunicamycin controls (**Figure 3.27b**).

3.2.4 Choline depletion does not induce the Keap1-Nrf2 pathway in IEC-ras

In the case of the Keap1-Nrf2 pathway, p62 sequesters Keap1 and promotes translocation of Nrf2 to the nucleus where it upregulates genes such as p62 and Nrf2 as a part of a feedback loop in response to oxidative stress.[209] If p62 accumulation was the result of Nrf2 activity, one would expect that Nrf2 expression might likewise be increased following choline depletion in IEC-ras. Depriving IEC-ras of choline for up to 24 h did not induce accumulation of Nrf2, suggesting that it was unlikely to be involved in this response to choline depletion (**Figure 3.27**). In summary, none of the known stress response pathways that regulate p62 expression were activated in response to choline depletion in IEC-ras34.

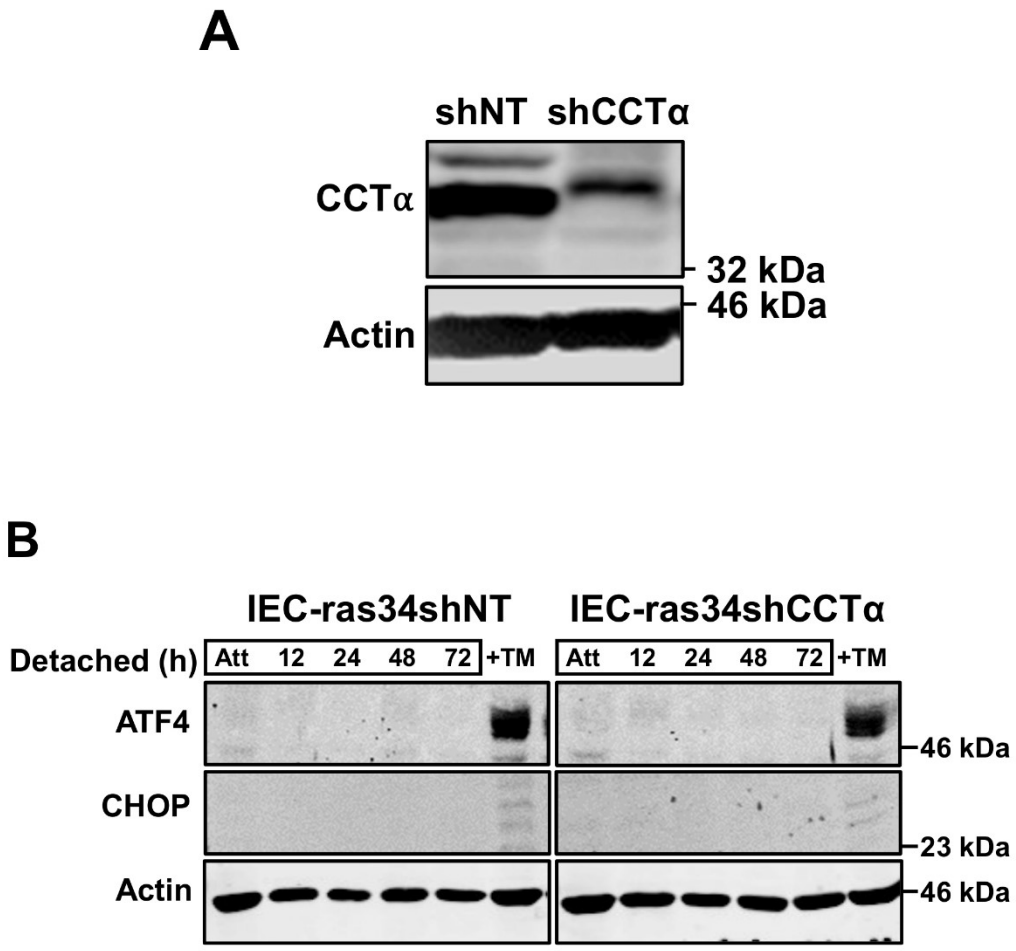

Figure 3.26. Detachment-independent growth is not associated with increased ATF4 or CHOP expression in IEC-ras34shCCTα. (A) IEC-ras34 were treated with lentivirus encoding shCCTα or non-target (shNT). (**B)** IEC-ras34shNT and IEC-ras34shCCTα were cultured for up to 72 h in 2 mL of IEC-MEM on 60-mm dishes lined with 3 mL of 1% SeaPlaque® agarose. Detergent lysate sample concentrations were measured as described previously in Section 2.6 and resolved with SDS-PAGE, transferred to nitrocellulose, and immunoblotted for ATF4 (1:500) and CHOP (1:500). Results are representative of three experiments.

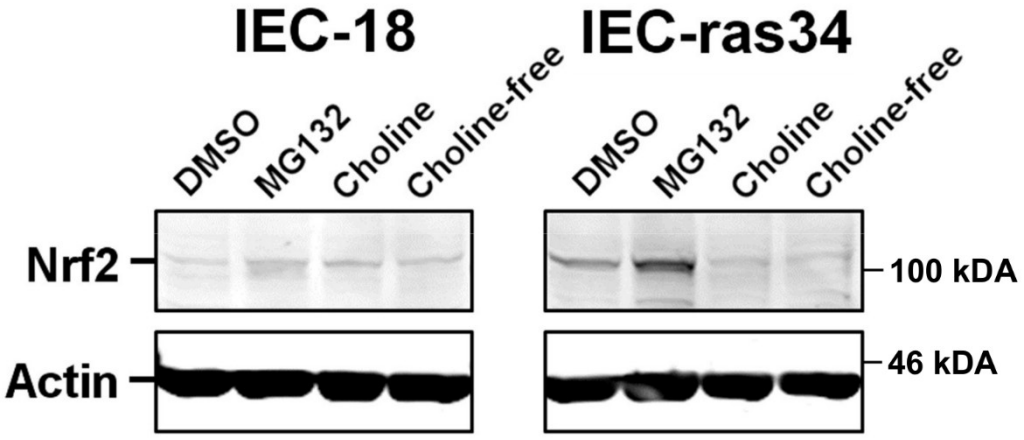

Figure 3.27. Choline depletion does not induce the Keap1-Nrf2 pathway in IEC-18 or IEC-ras34. IEC-18 and IEC-ras34 were cultured on 35-mm dishes for 48 h before replacing media with either CF-DMEM with 5% dialyzed FBS, with or without a 50 µM choline, and incubated for up to 24 h. As a positive control, cells cultured in DMEM with 5% dialyzed FBS were either treated with DMSO or MG132 for 4 h prior to the end of the experiment. Whole-cell lysates were collected and resolved with SDS-PAGE and transferred to nitrocellulose. Immunoblotting with anti-Nrf2 (1:500). Results are representative of two similar experiments.

Chapter 4: Discussion

4.1 CCTα activity is correlated with phosphorylation at Ser315/Ser319

In 1982**,** Pelech & Vance demonstrated that phosphorylation was negatively correlated with CCTα activity.[124] While the correlation between phosphorylation and CCTα inhibition has been well established both *in vitro* and *in vivo*, a precise mechanism for phospho-regulation remains elusive. Phosphorylation does not prevent CCTα from translocating to the INM, thus electrostatic antagonism between the hyperphosphorylated P region, the amphipathic helix of the M domain, and the INM seems unlikely to have a significant contribution to this mechanism.[128,129] Conversely, truncations of CCTα removing the P region primarily enhance the affinity of the enzyme for lipid activators like DAG and oleate.[126,218] As indicated in the previously cited reports, dephosphorylation of CCTα is proposed to occur after translocation to the NE, suggesting that the P region acts as an additional regulatory module for membrane-associated CCTα activity. One may consider that the M domain acts as the threshold sensor for changes in lipid content at the INM, whereas the P region may act to fine tune regulation of enzyme activity.[126]

Previous studies of CCTα phosphorylation at specific residues have primarily relied on overexpressed mutants.[119,126,218] In this study, I have demonstrated the utility of phospho-specific antibodies for characterizing changes in phosphorylation of endogenous CCTα in response to oleate treatments and choline depletion. Both anti-p-Ser315/Ser319 and anti-p-Tyr359/Ser362 detected endogenous CCTα and CCTβ in Caco2 cell lysates (**Figure 3.3**). Immunofluorescence confocal microscopy confirmed that anti-p-Ser315/Ser319 detected CCTα in the nucleus, although some cytoplasmic staining is indicative that CCTβ is detected given that the antibody was shown to detect both

overexpressed CCT isoforms in HeLa cells by immunoblotting (**Figure 3.2**). While anti-p-Tyr359/S362 detected endogenous CCT isoforms, it did not detect overexpressed rat CCT isoforms in HeLa cells (**Figure 3.2**). Given the proximity of the C-terminal V5 and MYC-FLAG epitopes to this phosphorylation site, this may have blocked the binding of anti-p-Tyr359/S362.

Oleate treatment consistently stimulated dephosphorylation of Ser315/Ser319 within 15 minutes in several human cell lines (**Figure 3.4, 3.5 & 3.6**). The presence of oleate had a sustained effect on both dephosphorylation of Ser315/Ser319 and translocation of CCTα to the INM (**Figure 3.7 & 3.8**). Similar results were also found for rat IEC-ras (**Figure 3.10 & 3.11**), demonstrating that this phenotype is conserved. The anti-p-Tyr359/Ser362 signal was inconsistent across most cells that were tested, with only a significant increase in signal following oleate treatment identified in HeLa cells after 15 minutes (**Figure 3.4**).

Removal of oleate from cells caused CCTα to gradually dissociation from the NE (**Figure 3.14**) as well as increased phosphorylation of Ser315/Ser319 (**Figure 3.12 & 3.13**). The effect of oleate removal on phosphorylation of Ser315/Ser319 was not statistically significant in either HeLa or F8 human fibroblasts, but a clear trend emerged in both cell lines. By 30 minutes, CCTα had mostly dissociated from the INM in HeLa cells, but phosphorylation occurred more slowly until 60 minutes. A similar trend was observed in F8 human fibroblasts, although the response was even more gradual. These data indicate that phosphorylation of Ser315/Ser319 does not occur immediately following CCTα dissociation from the INM, which is in agreement with a previous report using [^{32}P] labeling to measure total CCTα phosphorylation following oleate removal.[212] Future

experiments should include longer time points to determine a maximum for Ser315/Ser319 phosphorylation after oleate is removed.

Choline depletion of IEC-ras caused Ser315/Ser319 dephosphorylation as assessed by Western blot in IEC-ras (**Figure 3.15**). Dephosphorylation was associated with CCTα translocation in IEC-ras34, neither of which was observed in the non-malignant IEC-18. This could suggest that choline turnover is greater in IEC-ras, but this is contrary to previous reports that [^{3}H]choline incorporation into the CDP-choline pathway was not increased.[136] Despite there being no differences in PC synthesis, differences in INM lipid content of IEC-18 and IEC-ras could explain this discrepancy. Cancer cells typically have increased *de novo* fatty acid synthesis compared to non-cancer cells, and it is possible that the abundance of fatty acids and subsequent synthesis of DAG could promote increased sensitivity of CCTα for membrane binding.[219] Fatty acid synthase was upregulated in K-ras-positive lung adenocarcinoma cells of mice, and DESI mass spectrometry analysis showed that lung adenocarcinoma cells of mice had a significantly altered lipid profile compared to normal lung epithelial cells. Further investigations should characterize the lipid profiles of IEC-18 and IEC-ras to determine if H-ras-transformation promotes increased CCTα sensitivity to lipid activators because of increased synthesis of other membrane lipids.

HBSS-induced Ser315/Ser319 dephosphorylation and translocation of CCTα in IEC-ras34 appears to be choline-dependent (**Figure 3.17 & 3.18**). This treatment caused decreased Ser315/Ser319 phosphorylation to the same degree as oleate treatments, while HBSS supplemented with 50 μM choline induced Ser315/Ser319 phosphorylation in IEC-ras34 compared to cells cultured in whole media. Presumably, HBSS-starved IEC-ras34

are depleted of choline and unable to maintain PC homeostasis, thus elevated DAG produced by PC turnover and would promotes the translocation of CCTα to the NE. However, it not known how HBSS might affect signal transduction pathways that would promote CCTα dephosphorylation in this context. Activation of PP2a in response to amino acid and serum starvation could be one possibility. Hui *et al.* reported that inhibition of PP2a by PLD1 was mTOR dependent in both MDA-MB-231 and MCF7 breast cancer cell lines.[220] As okadaic acid is an inhibitor of PP2a and also prevents CCTα dephosphorylation, it is possible HBSS inhibits mTOR activity that suppresses PP2a leading to dephosphorylation of membrane-associated CCTα.[129] However, this explanation is not entirely sufficient. Choline supplementation of HBSS-treated cells prevented CCTα translocation and increased phosphorylation of Ser315/Ser319 in IEC-ras34, suggesting that CCTα activity is significantly reduced (**Figure 3.17 & 3.18**). If this were the case, it might suggest that only a small pool of active CCTα is required to maintain PC homeostasis, but further experiments will be required to address this problem.

This investigation is not the first to have identified the correlation between Ser315 phosphorylation and lipid-induced CCTα activation. It was previously reported that lipid-induced activation of mutant CCTα S315A was greater than that of wild-type CCTα.[126] A single S315A mutation reduced ERK-mediated phosphorylation of CCTα by nearly 50% *in vitro*.[221] In the same study, co-transfection of mouse lung epithelial (MLE) cells with constitutively active MEK1 increased overexpressed His-tagged CCTα phosphorylation while decreasing PC synthesis. Interestingly, an overexpressed S315A mutant was completely resistant MEK1-mediated phosphorylation and thus prevented subsequent reduction in PC synthesis. Taken together with my data, there appears to be a strong

correlation between CCTα lipid-induced activation and dephosphorylation of Ser315. It is unclear if the Tyr359/Ser362 site correlates significantly with CCTα regulation under any circumstances.

Perhaps the most interesting finding was that CCTα is phosphorylated at Ser315/319 in IEC-ras grown detached from the ECM (**Figure 3.19**). Our lab previously reported that growth on agarose promoted hyperphosphorylation of CCTα, yet they also observed sustained PC synthesis for up to 72 h.[136] Knockdown of CCTβ had no affect on PC synthesis under these conditions, highlighting the importance of CCTα in this response. Because phosphorylation does not prevent translocation of CCTα, further experiments should be done to characterize whether CCTα is translocated to the NE in IEC-ras34 grown on agarose. Despite previous reports demonstrating a correlation between decreased activity and increased phosphorylation, the overexpression of CCTα in the context of ras-transformation may be sufficient to compensate for the hyperphosphorylation. However, CCTα overexpression alone was not sufficient to promote anoikis resistance in non-malignant IEC-18.[136]

Some weaknesses of this investigation are apparent upon analysis of the Western blots using the phospho-specific antibodies. Cross-reactivity of these antibodies to both CCTα and CCTβ may be interfering with accurate quantification of Tyr359/Ser362 phosphorylation in human cell lines. While total CCTα migrates further as a single band in oleate-treated human cells, the anti-p-Tyr359/Ser362 signal consists of two bands; one that remains stationary across all time point, and second band that matches the migration of CCTα. In IEC-ras34, only a single band is detected with the anti-p-Tyr359/Ser362 antibody regardless of treatment, suggesting that this antibody does not detect rat CCTα

and more likely detects CCTβ (**Figure 3.11**). This is not surprising, as residue 359 in rat CCTα is a cysteine instead of a tyrosine, while residue 359 in rat CCTβ is a serine (**Figure 3.1**).

Comparing Ser315/Ser319 phosphorylation between IEC-ras34-shNT and IEC-ras34-shCCTα, I have determined that a portion of the anti-p-Ser315/Ser319 signal may correspond to CCTβ isoforms or other non-specific binding (**Figure 4.1**). A region of multiple lightly-visible bands detected by anti-p-Ser315/Ser319 (indicated by arrow 1) were found to decrease by approximately 77% in IEC-ras34shCCTα relative to the same bands in IEC-ras34shNT, matching the decrease of total CCTα. The fourth band of anti-p-Ser315/Ser319 (indicated by arrow 4) also decreased approximately 77% in knockout cells. Conversely, the signal for a second band of anti-p-Ser315/Ser319 (indicated by arrow 2) only decreased by approximately 50% in the knockout cells relative to the same band detected by total anti-CCTα. Signal for the third band of anti-p-Ser315/Ser319 (indicated by arrow 3) only slightly decreased in knockout cells and no specific band corresponding to this arrow is detected with the antibody for total CCTα. This suggests signal overlap of CCT isoforms detected with anti-p-Ser315/Ser319 for bands 2 and 3 is unreliable for quantifying changes in the phosphorylation of CCTα, whereas bands 1 and 4 are likely specific to CCTα and therefore reliable. Unfortunately, I was unable to consistently resolve defined CCTα bands in many experiments, thus highlighting the importance of properly resolving CCTα by SDS-PAGE for accurate quantification.

Finally, total anti-CCTα detected a fifth band (indicated by arrow 5) that was not detected with anti-p-Ser315/Ser319 in cells treated with oleate/BSA or HBSS, thus indicating the major dephosphorylated species of activated CCTα (**Figure 4.1**).

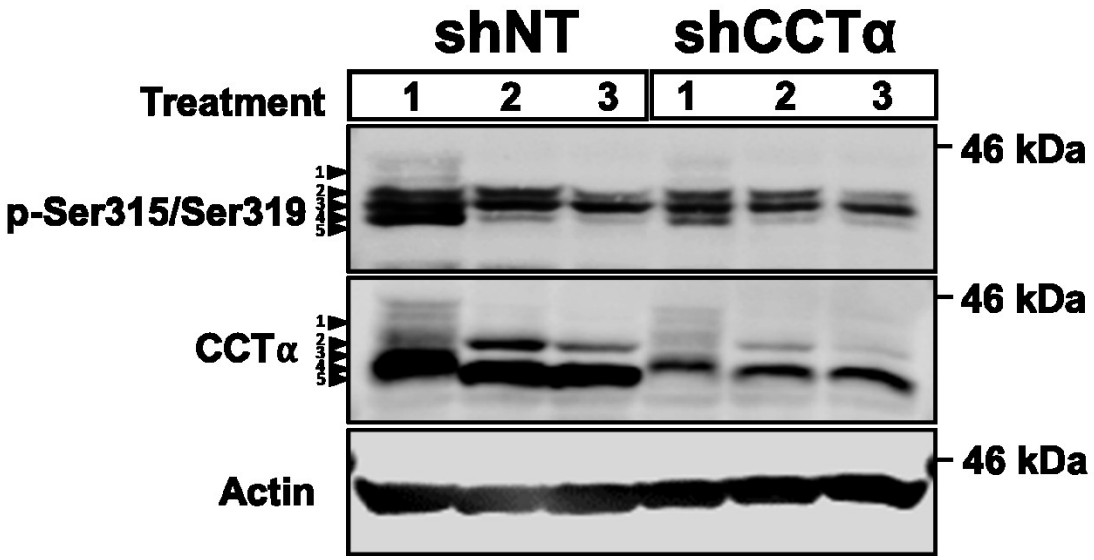

Figure 4.1. Overlapping bands of CCTα and CCTβ determined using lentiviral knockdown of CCTα in IEC-ras34. IEC-ras34 were treated with lentivirus encoding shCCTα or non-target (shNT). These cells were treated with 1) α-MEM, 2) HBSS and 3) oleate/BSA for 5 h. Whole-cell lysates were collected as described in Section 2.5 and resolved by SDS-PAGE. Protein was transferred to nitrocellulose and immunoblotted with anti-CCTα (1:500), and anti-p-Ser315/Ser319 (1:1000). Corresponding bands between anti-p-Ser315/Ser319 and total anti-CCTα were identified based on molecular weight and indicated with arrows.

Interestingly, band 1 and band 4 of total CCTα disappears following CCTα activation while band 2 becomes more prominent. Unfortunately, the overlap of anti-p-Ser315/Ser319 signals for both CCT isoforms prevents accurate quantification, but band 2 could possibly correspond to a pool of soluble CCTα that is phosphorylated at Ser315/Ser319. Future studies of CCTα phosphor-regulation should attempt to better characterize the different pools of CCTα in IEC-ras, as it may provide clues for different levels of phosphorylation and the affect this has on enzyme activity. To do this, it would be necessary to knockdown CCTβ in IEC-ras to accurately quantify changes in anti-p-Ser315/Ser319.

4.2 Choline depletion and CCTα knockdown induce p62 accumulation by an unknown mechanism

This investigation failed to determine the role of CCTα in promoting cell survival in the context of anoikis. Our hypotheses considered three pathways that are involved in regulating cell survival under conditions of stress: 1) autophagy, 2) the unfolded protein response, and 3) the Keap1-Nrf2 pathway. In my hands, I was unable to demonstrate a correlation between choline depletion or CCTα knockdown with alterations to any markers from these pathways. Based on measurements of autophagic flux using IEC-ras34-mCherry-eGFP-LC3b, no significant changes in autophagy were observed following 24 h of choline depletion (**Figure 3.22**). Additionally, I did not observe p62 or LC3b-II accumulation in choline-depleted HCT116, which is a human colorectal carcinoma cell line (**Figure 3.21**). However, CCTα knockdown or knockout in a human cancer cell line would serve as a better model for studying the role of CCTα in promoting cancer cell survival.

While there was no observed accumulation of ATF4, CHOP, or Nrf2 in either IEC-ras34sh NT or IEC-ras34shCCTα when grown detached from the ECM, these pathways have been previously implicated in anoikis resistance.[222] Targeting cancer cell anoikis resistance is a promising area of therapeutic development.[149] For example, microRNA targeting of genes responsible for epithelial-to-mesenchymal transition (EMT) with miR-200c sensitized breast cancer cells to anoikis in addition to inhibiting cell motility.[223] If CCTα is relevant to human cancer cell anoikis resistance, targeting its activity might provide therapeutic benefit by preventing metastasis.

4.3 Conclusions

This investigation has validated the use of a phospho-specific antibody for detecting changes in phosphorylation of Ser315/Ser319. Ultimately, CCTα activation by oleate treatments and choline depletion was associated with decreased phosphorylation at Ser315/Ser319. In IEC-ras cultured in detached conditions, CCTα was found to have increased phosphorylation at Ser315/Ser319 despite previous reports indicating sustained PC synthesis in these conditions. This is the first study to show changes in phosphorylation at Ser315/Ser319 upon lipid activation of CCTα and I demonstrated the utility of studying CCTα phospho-regulation using these phospho-specific antibodies. Further studies are required to determine both the mechanism CCTα in promoting anoikis resistance in IEC-ras and the possibility that this phenotype is exhibited by other cancers.

References

1. Keenan, T. W. & Morre, D. J. Phospholipid class and fatty acid composition of Golgi apparatus isolated from rat liver and comparison with other cell fractions. *Biochemistry* **9,** 19–25 (1970).

2. Van Meer, G., Voelker, D. R. & Feigenson, G. W. Membrane lipids: Where they are and how they behave. *Nat. Rev. Mol. Cell Biol.* **9,** 112–124 (2008).

3. Esko, J. D., Nishijima, M. & Raetz, C. R. Animal cells dependent on exogenous phosphatidylcholine for membrane biogenesis. *Proc. Natl. Acad. Sci. U. S. A.* **79,** 1698–702 (1982).

4. Pérez-Gil, J. Structure of pulmonary surfactant membranes and films: The role of proteins and lipid-protein interactions. *Biochim. Biophys. Acta - Biomembr.* **1778,** 1676–1695 (2008).

5. Holthuis, J. C. M. & Menon, A. K. Lipid landscapes and pipelines in membrane homeostasis. *Nature* **510,** 48–57 (2014).

6. Haider, A. *et al.* PCYT1A Regulates Phosphatidylcholine Homeostasis from the Inner Nuclear Membrane in Response to Membrane Stored Curvature Elastic Stress. *Dev. Cell* **45,** 481–495.e8 (2018).

7. Kennedy, E. P. & Weiss, S. B. The function of cytidine coenzymes in the biosynthesis of phospholipides. *J. Biol. Chem.* **222,** 193–214 (1956).

8. Wu, G. & Vance, D. E. Choline kinase and its function. *Biochem. Cell Biol.* **88,** 559–564 (2010).

9. Okuda, T. *et al.* Identification and characterization of the high-affinity choline transporter. *Nat. Neurosci.* **3,** 120–125 (2000).

10. Yuan, Z. Genomic organization, promoter activity, and expression of the human choline transporter-like protein 1. *Physiol. Genomics* **26,** 76–90 (2006).

11. Cornell, R. B. & Ridgway, N. D. CTP:phosphocholine cytidylyltransferase: Function, regulation, and structure of an amphitropic enzyme required for membrane biogenesis. *Prog. Lipid Res.* **59,** 147–171 (2015).

12. Lagace, T. A. & Ridgway, N. D. The role of phospholipids in the biological activity and structure of the endoplasmic reticulum. *Biochim. Biophys. Acta - Mol. Cell Res.* **1833,** 2499–2510 (2013).

13. Vance, D. E. Phospholipid methylation in mammals: From biochemistry to physiological function. *Biochim. Biophys. Acta - Biomembr.* **1838,** 1477–1487 (2014).

14. Jacquemyn, J., Cascalho, A. & Goodchild, R. E. The ins and outs of endoplasmic reticulum-controlled lipid biosynthesis. *EMBO Rep.* **18,** 1905–1921 (2017).

15. Testerink, N., van der Sanden, M. H. M., Houweling, M., Helms, J. B. & Vaandrager, A. B. Depletion of phosphatidylcholine affects endoplasmic reticulum morphology and protein traffic at the Golgi complex. *J. Lipid Res.* **50,** 2182–2192 (2009).

16. van der Sanden, M. H. M., Houweling, M., van Golde, L. M. G. & Vaandrager, A. B. Inhibition of phosphatidylcholine synthesis induces expression of the endoplasmic reticulum stress and apoptosis-related protein CCAAT/enhancer-binding protein-homologous protein (CHOP/GADD153). *Biochem. J.* **369,** 643–650 (2003).

17. Sanchez-Lopez, E. *et al.* Choline kinase inhibition induces exacerbated endoplasmic reticulum stress and triggers apoptosis via CHOP in cancer cells. *Cell Death Dis.* **4,** e933-11 (2013).

18. Kuge, O., Nishijima, M. & Akamatsu, Y. Phosphatidylserine biosynthesis in cultured Chinese Hamster Ovary cells. *J. Biol. Chem.* **261,** 5795–5798 (1986).

19. Stone, S. J. & Vance, J. E. Phosphatidylserine synthase-1 and -2 are localized to mitochondria-associated membranes. *J. Biol. Chem.* **275,** 34534–34540 (2000).

20. Shiao, Y.-J., Lupo, G. & Vance, J. E. Evidence that phosphatidylserine is imported into mitochondria via a mitochondria-associated membrane and that the majority of mitochondrial phosphatidylethanolamine is derived from decarboxylation of phosphatidylserine. *J. Biol. Chem.* **270,** 11190–11198 (1995).

21. Slotte, P. J. Biological functions of sphingomyelins. *Progress* **52,** 424–437 (2013).

22. Ullman, M. D. & Radin, N. S. The Enzymatic Formation of Sphingomyelin from Ceramide and Lecithin in Mouse Liver and Enzymatic Lecithin Formation in Mouse of Sphingomyelin Liver * from Ceramide. *J. Biol. Chem.* **249,** 1506–1512 (1974).

23. Jackowski, S. Coordination of membrane phospholipid synthesis with the cell cycle. *J. Biol. Chem.* **269,** 3858–67 (1994).

24. Bartz, R. *et al.* Lipidomics reveals that adiposomes store ether lipids and mediate phospholipid traffic . *J. Lipid Res.* **48,** 837–847 (2007).

25. Krahmer, N. *et al.* Phosphatidylcholine synthesis for lipid droplet expansion is mediated by localized activation of CTP:Phosphocholine cytidylyltransferase. *Cell Metab.* **14,** 504–515 (2011).

26. Pol, A., Gross, S. P. & Parton, R. G. Biogenesis of the multifunctional lipid droplet: Lipids, proteins, and sites. *J. Cell Biol.* **204,** 635–646 (2014).

27. Aitchison, A. J., Arsenault, D. J. & Ridgway, N. D. Nuclear-localized CTP:phosphocholine cytidylyltransferase regulates phosphatidylcholine synthesis required for lipid droplet biogenesis. *Mol. Biol. Cell* **26,** 2927–2938 (2015).

28. Cole, L. K., Vance, J. E. & Vance, D. E. PC biosynthesis and lipoprotein metabolism.pdf. *Biochim. Biophys. Acta* **1821,** 754–761 (2012).

29. Jacobs, R. L., Devlin, C., Tabas, I. & Vance, D. E. Targeted deletion of hepatic CTP:phosphocholine cytidylyltransferase α in mice decreases plasma high density and very low density lipoproteins. *J. Biol. Chem.* **279,** 47402–47410 (2004).

30. Jacobs, R. L., Lingrell, S., Zhao, Y., Francis, G. A. & Vance, D. E. Hepatic CTP:phosphocholine cytidylyltransferase-α is a critical predictor of plasma high density lipoprotein and very low density lipoprotein. *J. Biol. Chem.* **283,** 2147–2155 (2008).

31. Payne, F. *et al.* Mutations disrupting the Kennedy phosphatidylcholine pathway in humans with congenital lipodystrophy and fatty liver disease. *Proc. Natl. Acad. Sci.* **111,** 8901–8906 (2014).

32. Billah, M. M. & Anthes, J. C. The regulation and cellular functions of phosphatidylcholine hydrolysis. *Biochem. J.* **269,** 281–291 (1990).

33. Kishimoto, A., Takai, Y., Mori, T., Kikkawa, U. & Nishizuka, Y. Activation of calcium and phospholipid-dependent protein kinase by diacylglyercol, its possible realtion to phosphatidylinositol turnover. *J. Biol. Chem.* **255,** 2273–2276 (1980).

34. Kishimoto, A., Iwasa, Y., Kawahara, Y., Mori, T. & Nishizuka, Y. Calcium-dependent activation of a multifunctional protein kinase by membrane phospholipids. *J. Biol. Chem.* **254,** 3692–3695 (1979).

35. Monick, M. M. *et al.* A Phosphatidylcholine-Specific Phospholipase C Regulates Activation of p42/44 Mitogen-Activated Protein Kinases in Lipopolysaccharide-Stimulated Human Alveolar Macrophages. *J. Immunol.* **162,** 3005–3012 (1999).

36. Uhing, R. J., Prpic, V., Hollenbach, P. W. & Adams, D. O. Involvement of protein kinase C in platelet-activating-factor-stimulated diacylglycerol accumulation murine peritoneal macrophages. *J. Biol. Chem.* **264,** 9224–9230 (1989).

37. Sebaldt, R. J., Adams, D. O. & Uhing, R. J. Quantification of contributions of phospholipid precursors to diradylglycerols in stimulated mononuclear phagocytes. *Biochem J* **284 (Pt 2,** 367–375 (1992).

38. Xia, L., Zhang, D., Wang, C., Wei, F. & Hu, Y. PC-PLC is involved in osteoclastogenesis induced by TNF-α through upregulating IP3R1 expression. *FEBS Lett.* **586,** 3341–3348 (2012).

39. Sebaldt, R. J., Prpic, V., Hollenbach, W., Adams, D. O. & Uhing, R. J. IFN-gamma potentiates the accumulation of diacylglycerol in murine macrophages. *J. Immunol.* **145,** 684–689 (1990).

40. Mufson, R. A., Gubina, E., Rinaudo, M. & Baxter, G. A phosphatidylcholine phospholipase C inhibitor, D609, blocks interleukin-3 (IL-3)-induced bcl-2 expression but not c-myc expression in human IL-3-dependent cells. *Exp. Cell Res.* **240,** 228–235 (1998).

41. Martinson, E. A., Goldstein, D. & Brown, J. H. Muscarinic Receptor Activation of Phosphatidylcholine Hydrolysis. *Biochemistry* **264,** 14748–14754 (1989).

42. Cai, H. *et al.* Hydrolysis of phosphatidylcholine is stimulated by Ras proteins during mitogenic signal transduction. *Mol. Cell. Biol.* **12,** 5329–5335 (1992).

43. Cai, H. *et al.* Hydrolysis of phosphatidylcholine couples Ras to activation of Raf protein kinase during mitogenic signal transduction. *Mol. Cell. Biol.* **13,** 7645–51 (1993).

44. Büscher, D., Hipskind, R. A., Krautwald, S., Reimann, T. & Baccarini, M. Ras-dependent and -independent pathways target the mitogen-activated protein kinase network in macrophages. *Mol. Cell. Biol.* **15,** 466–75 (1995).

45. van Dijk, M. C., Muriana, F. J., de Widt, J., Hilkmann, H. & van Blitterswijk, W. J. Involvement of phosphatidylcholine-specific phospholipase C in platelet-derived growth factor-induced activation of the mitogen-activated protein kinase pathway in Rat-1 fibroblasts. *J. Biol. Chem.* **272,** 11011–6 (1997).

46. English, D., Cui, Y. & Siddiqui, R. A. Messenger functions of phosphatidic acid. *Chem. Phys. Lipids* **80,** 117–132 (1996).

47. Fang, Y., Bachmann, R., Flanigan, A. & Chen, J. Phosphatidic Acid – Mediated Mitogenic Activation of mTOR Signaling. *Science (80-.).* **294,** 1942–1946 (2001).

48. Pleskot, R., Li, J., Žárský, V., Potocký, M. & Staiger, C. J. Regulation of cytoskeletal dynamics by phospholipase D and phosphatidic acid. *Trends Plant Sci.* **18,** 496–504 (2013).

49. Yuan, H. X., Xiong, Y. & Guan, K. L. Nutrient Sensing, Metabolism, and Cell Growth Control. *Mol. Cell* **49,** 379–387 (2013).

50. Foster, D. A. Phosphatidic acid and lipid-sensing by mTOR. *Trends Endocrinol. Metab.* **24,** 272–278 (2013).

51. Fingar, D. C. *et al.* mTOR Controls Cell Cycle Progression through Its Cell Growth Effectors S6K1 and 4E-BP1 / Eukaryotic Translation Initiation Factor 4E mTOR Controls Cell Cycle Progression through Its Cell Growth Effectors S6K1 and 4E-BP1 / Eukaryotic Translation Initiation. *Mol. Cell. Biol.* **24,** 200–216 (2004).

52. Fang, Y. *et al.* PLD1 Regulates mTOR Signaling and Mediates Cdc42 Activation of S6K1. *Curr. Biol.* **13,** 2037–2044 (2003).

53. Yoon, M. S., Du, G., Backer, J. M., Frohman, M. A. & Chen, J. Class III PI-3-kinase activates phospholipase D in an amino acid-sensing mTORC1 pathway. *J. Cell Biol.* **195,** 435–447 (2011).

54. Xu, L. *et al.* Phospholipase D mediates nutrient input to mammalian target of rapamycin complex 1 (mTORC1). *J. Biol. Chem.* **286,** 25477–25486 (2011).

55. Han, J. M. *et al.* Leucyl-tRNA synthetase is an intracellular leucine sensor for the mTORC1-signaling pathway. *Cell* **149,** 410–424 (2012).

56. Yoon, M. S. *et al.* Leucyl-tRNA Synthetase Activates Vps34 in Amino Acid-Sensing mTORC1 Signaling. *Cell Rep.* **16,** 1510–1517 (2016).

57. Mérida, I. *et al.* Diacylglycerol kinases in cancer. *Adv. Biol. Regul.* **63,** 22–31 (2017).

58. Pettitt, T. R., Saqib, K. M., Shimwell, N. & Wakelam, M. J. O. Phospholipase D1b and D2a generate structurally identifical phosphatidic acid species in mammalian cells. *Biochem. J.* **360,** 707–715 (2001).

59. Yoon, M. S. *et al.* Rapid mitogenic regulation of the mTORC1 Inhibitor, DEPTOR, by phosphatidic acid. *Mol. Cell* **58,** 549–556 (2015).

60. Amandi-Burgermeister, E., Tibes, U., Kaiser, B. M., Friebe, W. G. & Scheuer, W. V. Suppression of cytokine synthesis, integrin expression and chronic inflammation by inhibitors of cytosolic phospholipase A2. *Eur J Pharmacol* **326,** 237–250 (1997).

61. Ricciotti, E. & Fitzgerald, G. A. Prostaglandins and inflammation. *Arterioscler. Thromb. Vasc. Biol.* **31,** 986–1000 (2011).

62. Sharma, J. N. & Mohammed, L. A. The role of leukotrienes in the pathophysiology of inflammatory disorders: Is there a case for revisiting leukotrienes as therapeutic targets? *Inflammopharmacology* **14,** 10–16 (2006).

63. Gill, P., Jindal, N. L., Jagdis, A. & Vadas, P. Platelets in the immune response: Revisiting platelet-activating factor in anaphylaxis. *J. Allergy Clin. Immunol.* **135,** 1424–1432 (2015).

64. Saunders, L. P. *et al.* Kinetic analysis of autotaxin reveals substrate-specific catalytic pathways and a mechanism for lysophosphatidic acid distribution. *J. Biol. Chem.* **286,** 30130–30141 (2011).

65. Lin, M. E., Herr, D. R. & Chun, J. Lysophosphatidic acid (LPA) receptors: Signaling properties and disease relevance. *Prostaglandins Other Lipid Mediat.* **91,** 130–138 (2010).

66. Gomez-Cambronero, J. Phosphatidic acid, phospholipase D and tumorigenesis. *Adv. Biol. Regul.* **54,** 197–206 (2014).

67. Abalsamo, L. *et al.* Inhibition of phosphatidylcholine-specific phospholipase C results in loss of mesenchymal traits in metastatic breast cancer cells. *Breast Cancer Res.* **14,** R50 (2012).

68. Paris, L. *et al.* Phosphatidylcholine-specific phospholipase C inhibition reduces HER2-overexpression, cell proliferation and in vivo tumor growth in a highly tumorigenic ovarian cancer model. *Oncotarget* **8,** 55022–55038 (2017).

69. Glunde, K., Bhujwalla, Z. M. & Ronen, S. M. Choline metabolism in malignant transformation. *Nat. Rev. Cancer* **11,** 835–848 (2011).

70. Okuda, T. & Haga, T. Functional characterization of the human high-affinity choline transporter. *FEBS Lett.* **484,** 92–97 (2000).

71. Simon, J. R. & Kuhar, M. J. High Affinity Choline Uptake: Ionic and Energy Requirements. *J. Neurochem.* **27,** 93–99 (1976).

72. O'Regan, S. & Meunier, F. M. Selection and characterization of the choline transport mutation suppressor from Torpedo electric lobe, CTL1. *Neurochem. Res.* **28,** 551–555 (2003).

73. Traiffort, E., Ruat, M., O'Regan, S. & Meunier, F. M. Molecular characterization of the family of choline transporter-like proteins and their splice variants. *J. Neurochem.* **92,** 1116–1125 (2005).

74. Yuan, Z., Tie, A., Tarnopolsky, M. & Bakovic, M. Genomic organization, promoter activity, and expression of the human choline transporter-like protein 1. *Physiol. Genomics* **26,** 76–90 (2006).

75. Roth, M., Obaidat, A. & Hagenbuch, B. OATPs, OATs and OCTs: The organic anion and cation transporters of the SLCO and SLC22A gene superfamilies. *Br. J. Pharmacol.* **165,** 1260–1287 (2012).

76. Wittenberg, J. & Kornberg, A. Choline phosphokinase. *J. Biol. Chem.* **202,** 431–444 (1953).

77. Porter, T. J. & Kent, C. Purification and Characterization from Rat Liver of Choline/Ethanolamine Kinase. *J. Biol. Chem.* **265,** 414–422 (1990).

78. Kozo, I., Kaname, I., Keiko, T. & Yasuo, N. Evidence for the existence of multiple forms of choline (ethanolamine) kinase in rat tissues. *Biochim. Biophys. Acta - Lipids Lipid Metab.* **833,** 1–8 (1985).

79. Aoyama, C., Yamazaki, N., Terada, H. & Ishidate, K. Structure and characterization of the genes for murine choline / ethanolamine kinase isozymes α and β. *J. Lipid Res.* **41,** 452–464 (2000).

80. Uchida, T. Regulation of choline kinase r: Analyses of alternatively spliced choline kinases and the promoter region. *J. Biochem.* **116,** 508–518 (1994).

81. Aoyama, C., Ohtani, A. & Ishidate, K. Expression and characterization of the active molecular forms of choline/ethanolamine kinsae-alpha and -beta in mouse tissues, including carbon tetrachloride-induced liver. *Biochem. J.* **363,** 777–784 (2002).

82. Wu, G., Aoyama, C., Young, S. G. & Vance, D. E. Early embryonic lethality caused by disruption of the gene for choline kinase α, the first enzyme in phosphatidylcholine biosynthesis. *J. Biol. Chem.* **283,** 1456–1462 (2008).

83. Sher, R. B. *et al.* A rostrocaudal muscular dystrophy caused by a defect in choline kinase beta, the first enzyme in phosphatidylcholine biosynthesis. *J. Biol. Chem.* **281,** 4938–4948 (2006).

84. Wu, G., Sher, R. B., Cox, G. A. & Vance, D. E. Differential expression of choline kinase isoforms in skeletal muscle explains the phenotypic variability in the rostrocaudal muscular dystrophy mouse. *Biochim. Biophys. Acta - Mol. Cell Biol. Lipids* **1801,** 446–454 (2010).

85. Falcon, S. C. *et al.* A non-catalytic role of choline kinase alpha is important in promoting cancer cell survival. *Oncogenesis* **2,** e38-4 (2013).

86. Kim, K. H. & Carman, G. M. Phosphorylation and regulation of choline kinase from Saccharomyces cerevisiae by protein kinase A. *J. Biol. Chem.* **274,** 9531–9538 (1999).

87. Yu, Y., Sreenivas, A., Ostrander, D. B. & Carman, G. M. Phosphorylation of Saccharomyces cerevisiae choline kinase on Ser 30 and Ser 85 by protein kinase A regulates phosphatidylcholine synthesis by the CDP-choline pathway. *J. Biol. Chem.* **277,** 34978–34986 (2002).

88. Choi, M. G., Kurnov, V., Kersting, M. C., Sreenivas, A. & Carman, G. M. Phosphorylation of the yeast choline kinase by protein kinase C: Identification of Ser25 and Ser30 as major sites of phosphorylation. *J. Biol. Chem.* **280,** 26105–26112 (2005).

89. Warden, C. H. & Friedkin, M. Regulation of choline kinase activity and phosphatidylcholine biosynthesis by mitogenic growth factors in 3T3 fibroblasts. *J. Biol. Chem.* **260,** 6006–6011 (1985).

90. Macara, I. G. Elevated phosphocholine concentration in ras-transformed NIH 3T3 cells arises from increased choline kinase activity, not from phosphatidylcholine breakdown. *Mol. Cell. Biol.* **9,** 325–8 (1989).

91. Jiménez, B., del Peso, L., Montaner, S., Esteve, P. & Lacal, J. C. Generation of phosphorylcholine as an essential event in the activation of Raf-1 and MAP-kinases in growth factors-induced mitogenic stimulation. *J. Cell. Biochem.* **57,** 141–149 (1995).

92. Chang, C. C., Few, L. L., Konrad, M. & See Too, W. C. Phosphorylation of human choline kinase beta by protein kinase A: Its impact on activity and inhibition. *PLoS One* **11,** 1–23 (2016).

93. Aoyama, C., Ishidate, K., Sugimoto, H. & Vance, D. E. Induction of choline kinase alpha by carbon tetrachloride (CCl4) occurs via increased binding of c-jun to an AP-1 element. *Biochim. Biophys. Acta - Mol. Cell Biol. Lipids* **1771,** 1148–1155 (2007).

94. Ziello, J. E., Jovin, I. S. & Huang, Y. Hypoxia-Inducible Factor (HIF)-1 regulatory pathway and its potential for therapeutic intervention in malignancy and ischemia. *Yale J. Biol. Med.* **80,** 51–60 (2007).

95. Bansal, A., Harris, R. A. & DeGrado, T. R. Choline phosphorylation and regulation of transcription of choline kinase α in hypoxia. *J. Lipid Res.* **53,** 149–157 (2012).

96. Glunde, K. *et al.* Hypoxia Regulates Choline Kinase Expression through Hypoxia-Inducible Factor-1 Signaling in a Human Prostate Cancer Model. *Cancer Res.* **68,** 172–180 (2008).

97. Nakagami, K. *et al.* Increased choline kinase activity and elevated phosphocholine levels in human colon cancer. *Japanese J. Cancer Res.* **90,** 419–424 (1999).

98. Gallego-Ortega, D. *et al.* Differential role of human choline kinase α and β enzymes in lipid metabolism: Implications in cancer onset and treatment. *PLoS One* **4,** (2009).

99. Gallego-Ortega, D., Gómez del Pulgar, T., Valdés-Mora, F., Cebrián, A. & Lacal, J. C. Involvement of human choline kinase alpha and beta in carcinogenesis: A different role in lipid metabolism and biological functions. *Adv. Enzyme Regul.* **51,** 183–194 (2011).

100. Trousil, S. *et al.* Alterations of choline phospholipid metabolism in endometrial cancer are caused by choline kinase alpha overexpression and a hyperactivated deacylation pathway. *Cancer Res.* **74,** 6867–6877 (2014).

101. Wang, L., Magdaleno, S., Tabas, I. & Jackowski, S. Early embryonic lethality in mice with targeted deletion of the CTP: phosphocholine cytidylyltransferase α gene (Pcyt1a). *Mol. Cell. Biol.* **25,** 3357–3363 (2005).

102. Ridsdale, R., Tseu, I., Wang, J. & Post, M. CTP:Phosphocholine Cytidylyltransferase alpha Is a Cytosolic Protein in Pulmonary Epithelial Cells and Tissues. *J. Biol. Chem.* **276,** 49148–49155 (2001).

103. Karim, M., Jackson, P. & Jackowski, S. Gene structure, expression and identification of a new CTP:phosphocholine cytidylyltransferase β isoform. *Biochim. Biophys. Acta - Mol. Cell Biol. Lipids* **1633,** 1–12 (2003).

104. Lykidis, A., Murti, K. G. & Jackowski, S. Cloning and characterization of a second human CTP:phosphocholine cytidylyltransferase. *J. Biol. Chem.* **273,** 14022–14029 (1998).

105. Lykidis, A., Baburina, I. & Jackowski, S. Distribution of CTP : Phosphocholine Cytidylyltransferase (CCT) Isoforms. *J. Biol. Chem.* **274,** 26992–27001 (1999).

106. Kalmar, G. B., Kay, R. J., Lachance, A., Aebersold, R. & Cornell, R. B. Cloning and expression of rat liver CTP: phosphocholine cytidylyltransferase: an amphipathic protein that controls phosphatidylcholine synthesis. *Proc. Natl. Acad. Sci.* **87,** 6029–6033 (1990).

107. Johnson, J. E., Aebersold, R. & Cornell, R. B. An amphipathic α-helix is the principle membrane-embedded region of CTP:Phosphocholine cytidylyltransferase. Identification of the 3-(trifluoromethy)-3-(m-[125I]iodophenyl) diazirine photolabeled domain. *Biochim. Biophys. Acta - Biomembr.* **1324,** 273–284 (1997).

108. Wang, Y., Macdonald, J. I. S. & Kent, C. Identification of the nuclear localization signal of rat liver CTP:phosphocholine cytidylyltransferase. *J. Biol. Chem.* **270,** 354–360 (1995).

109. Cornell, R. B. *et al.* Functions of the C-terminal domain of CTP: phosphocholine cytidylyltransferase. Effects of C-terminal deletions on enzyme activity, intracellular localization and phosphorylation potential. *Biochem. J.* **310 (Pt 2,** 699–708 (1995).

110. Taneva, S. G., Patty, P. J., Frisken, B. J. & Cornell, R. B. CTP:phosphocholine cytidylyltransferase binds anionic phospholipid vesicles in a cross-bridging mode. *Biochemistry* **44,** 9382–9393 (2005).

111. Johnson, J. E. *et al.* Comparison of the lipid regulation of yeast and rat CTP: phosphocholine cytidylyltransferase expressed in COS cells. *Biochem. J.* **285 (Pt 3,** 815–820 (1992).

112. Watkins, J. D. & Kent, C. Immunolocalization of membrane-associated CTP:phosphocholine cytidylyltransferase in phosphatidylcholine-deficient Chinese hamster ovary cells. *J. Biol. Chem.* **267,** 5686–5692 (1992).

113. Pelech, S. L., Pritchard, P. H., Brindleyg, D. N. & Vance, D. E. Fatty Acids Promote Translocation of CTP:PhosDhocholine Cytidylyltransferase to the Endoplasmic Reticulim and Stimulate Rat Hepatic Phosphatidylcholine Synthesis. *J. Biol. Chem.* **258,** 6782–6788 (1983).

114. Attard, G. S., Templer, R. H., Smith, W. S., Hunt, A. N. & Jackowski, S. Modulation of CTP:phosphocholine cytidylyltransferase by membrane curvature elastic stress. *Proc. Natl. Acad. Sci.* **97,** 9032–9036 (2000).

115. Yang, W., Boggs, K. P. & Jackowski, S. The association of lipid activators with the amphipathic helical domain of CTP:phosphocholine cytidylyltransferase accelerates catalysis by increasing the affinity of the enzyme for CTP. *J. Biol. Chem.* **270,** 23951–23957 (1995).

116. Friesen, J. A., Seo Park, Y. & Kent, C. Purification and kinetic characterization of CTP:phosphocholine cytidylyltransferase from saccharomyces cerevisiae. *Protein Expr. Purif.* **21,** 141–148 (2001).

117. Lee, J., Taneva, S. G., Holland, B. W., Tieleman, D. P. & Cornell, R. B. Structural basis for autoinhibition of CTP: Phosphocholine cytidylyltransferase (CCT), the regulatory enzyme in phosphatidylcholine synthesis, by its membrane-binding amphipathic helix. *J. Biol. Chem.* **289,** 1742–1755 (2014).

118. Ramezanpour, M., Lee, J., Taneva, S. G., Tieleman, D. P. & Cornell, R. B. An auto-inhibitory helix in CTP:phosphocholine cytidylyltransferase hijacks the catalytic residue and constrains a pliable, domain-bridging helix pair. *J. Biol. Chem.* **293,** 7070–7084 (2018).

119. MacDonald, J. I. S. & Kent, C. Identification of phosphorylation sites in rat liver CTP: Phosphocholine cytidylyltransferase. *J. Biol. Chem.* **269,** 10529–10537 (1994).

120. Wieprecht, M., Wieder, T., Paul, C., Geilen, C. C. & Orfanos, C. E. Evidence for phosphorylation of CTP:phosphocholine cytidylyltransferase by multiple proline-directed protein kinases. *J. Biol. Chem.* **271,** 9955–9961 (1996).

121. Wieprecht, M., Wieder, T., Geilen, C. C. & Orfanos, C. E. Growth factors stimulate phosphorylation of CTP: phosphocholine cytidylyltransferase in HeLa cells. *FEBS Lett.* **353,** 221–224 (1994).

122. Mallampalli, R. K., Ryan, A. J., Salome, R. G. & Jackowski, S. Tumor Necrosis Factor-alpha Inhibits Expression of CTP : Phosphocholine Cytidylyltransferase. **275,** 9699–9708 (2000).

123. Sanghera, J. S. & Vance, D. E. CTP:Phosphocholine cytidylyltransferase is a substrate for cAMP-dependent protein kinase in vitro. *J. Biol. Chem.* **264,** 1215–1223 (1989).

124. Pelech, S. L. & Vance, D. E. Regulation of rat liver cytosolic CTP: phosphocholine cytidylyltransferase by phosphorylation and dephosphorylation. *J. Biol. Chem.* **257,** 14198–202 (1982).

125. Ryan, A. J., Andrews, M., Zhou, J. & Mallampalli, R. K. C-Jun N-terminal kinase regulates CTP:phosphocholine cytidylyltransferase. *Arch. Biochem. Biophys.* **447,** 23–33 (2006).

126. Yang, W. & Jackowski, S. Lipid activation of CTP:phosphocholine cytidylyltransferase is regulated by the phosphorylated carboxyl-terminal domain. *Journal of Biological Chemistry* **270,** 16503–16506 (1995).

127. Wang, Y. & Kent, C. Effects of altered phosphorylation sites on the properties of CTP:phosphocholine cytidylyltransferase. *Journal of Biological Chemistry* **270,** 17843–17849 (1995).

128. Wang, Y. & Kent, C. Identification of an inhibitory domain of CTP:phosphocholine cytidylyltransferase. *Journal of Biological Chemistry* **270,** 18948–18952 (1995).

129. Houweling, M., Jamil, H., Hatch, G. M. & Vance, D. E. Dephosphorylation of CTP-phosphocholine cytidylyltransferase is not required for binding to membranes. *J. Biol. Chem.* **269,** 7544–7551 (1994).

130. Hatch, G. M., Jamil, H., Utal, A. K. & Vance, D. E. On the mechanism of the okadaic acid-induced inhibition of phosphatidylcholine biosynthesis in isolated rat hepatocytes. *J. Biol. Chem.* **267,** 15751–15758 (1992).

131. Arnold, R. S., DePaoli-Roach, A. A. & Cornell, R. B. Binding of CTP:Phosphocholine cytidylyltransferase to lipid vesicles: Diacylglycerol and enzyme dephosphorylation increase the affinity for negatively charged membranes. *Biochemistry* **36,** 6149–6156 (1997).

132. Sugimoto, H. *et al.* Identification of Ets-1 as an important transcriptional activator of CTP:Phosphocholine cytidylyltransferase alpha in COS-7 cells and co-activation with transcriptional enhancer factor-4. *J. Biol. Chem.* **278,** 19716–19722 (2003).

133. Sugimoto, H. *et al.* Sp1 is a co-activator with Ets-1, and net is an important repressor of the transcription of CTP:phosphocholine cytidylyltransferase ?? *J. Biol. Chem.* **280,** 40857–40866 (2005).

134. Sugimoto, H., Bakovic, M., Yamashita, S. & Vance, D. E. Identification of Transcriptional Enhancer Factor-4 as a Transcriptional Modulator of CTP:Phosphocholine Cytidylyltransferase α. *J. Biol. Chem.* **276,** 12338–12344 (2001).

135. Bakovic, M., Waite, K. & Vance, D. E. Oncogenic Ha-Ras transformation modulates the transcription of the CTP:phosphocholine cytidylyltransferase α gene via p42/44MAPK and transcription factor Sp3. *J. Biol. Chem.* **278,** 14753–14761 (2003).

136. Arsenault, D. J., Yoo, B. H., Rosen, K. V. & Ridgway, N. D. ras-induced up-regulation of CTP:phosphocholine cytidylyltransferase alpha contributes to malignant transformation of intestinal epithelial cells. *J. Biol. Chem.* **288,** 633–643 (2013).

137. Ridgway, N. D. & Lagace, T. A. Regulation of the CDP-choline pathway by sterol regulatory element binding proteins involves transcriptional and post-transcriptional mechanisms. *Biochem. J.* **372,** 811–819 (2003).

138. Brewer, J. W. & Jackowski, S. UPR-mediated membrane biogenesis in B cells. *Biochem. Res. Int.* **2012,** (2012).

139. Sriburi, R., Jackowski, S., Mori, K. & Brewer, J. W. XBP1: A link between the unfolded protein response, lipid biosynthesis, and biogenesis of the endoplasmic reticulum. *J. Cell Biol.* **167,** 35–41 (2004).

140. Bakovic, M., Waite, K., Tang, W., Tabas, I. & Vance, D. E. Transcriptional activation of the murine CTP:phosphocholine cytidylyltransferase gene (Ctpct): Combined action of upstream stimulatory and inhibitory cis-acting elements. *Biochim. Biophys. Acta - Mol. Cell Biol. Lipids* **1438,** 147–165 (1999).

141. Bakovic, M., Waite, K. a & Vance, D. E. Functional significance of Sp1, Sp2, and Sp3 transcription factors in regulation of the murine CTP:phosphocholine cytidylyltransferase alpha promoter. *J. Lipid Res.* **41,** 583–94 (2000).

142. Golfman, L. S., Bakovic, M. & Vance, D. E. Transcription of the CTP : Phosphocholine Cytidylyltransferase Gene Is Enhanced during the S Phase of the Cell Cycle *. **276,** 43688–43692 (2001).

143. Banchio, C., Schang, L. M. & Vance, D. E. Activation of CTP:phosphocholine cytidylyltransferase alpha expression during the S phase of the cell cycle is mediated by the transcription factor Sp1. *J. Biol. Chem.* **278,** 32457–32464 (2003).

144. Banchio, C., Schang, L. M. & Vance, D. E. Phosphorylation of Sp1 by cyclin-dependent kinase 2 modulates the role of Sp1 in CTP:phosphocholine cytidylyltransferase alpha regulation during the S phase of the cell cycle. *J. Biol. Chem.* **279,** 40220–40226 (2004).

145. McMaster, C. R. & Bell, R. M. Phosphatidylcholine biosynthesis in Saccharomyces cerevisiae: Regulatory insights from studies employing null and chimeric sn-1,2-diacylglycerol Choline- and ethanolaminephosphotransferases. *J. Biol. Chem.* **269,** 28010–28016 (1994).

146. Henneberry, Annette, L., Wright, M. M. & McMaster, C. R. The major sites of cellular phospholipid synthesis and the molecular determinants of fatty acids and lipid head group specificity. *Mol. Biol. Cell* **13,** 3149–3161 (2002).

147. Henneberry, A. L., Wistow, G. & McMaster, C. R. Cloning, genomic organization, and characterization of a human cholinephosphotransferase. *J. Biol. Chem.* **275,** 29808–29815 (2000).

148. Hanahan, D. & Weinberg, R. A. The hallmarks of cancer. *Cell* **100,** 57–70 (2000).

149. Taddei, M. L., Giannoni, E., Fiaschi, T. & Chiarugi, P. Anoikis: An emerging hallmark in health and diseases. *J. Pathol.* **226,** 380–393 (2012).

150. Ridgway, N. D. The role of phosphatidylcholine and choline metabolites to cell proliferation and survival. *Crit. Rev. Biochem. Mol. Biol.* **48,** 20–38 (2013).

151. Aboagye, E. O. & Bhujwalla, Z. M. Malignant transformation alters membrane choline phospholipid metabolism of human mammary epithelial cells. *Cancer Res.* **59,** 80–84 (1999).

152. Mori, N., Wildes, F., Takagi, T., Glunde, K. & Bhujwalla, Z. M. The Tumor Microenvironment Modulates Choline and Lipid Metabolism. *Front. Oncol.* **6,** (2016).

153. Lacal, J. C., Moscat, J. & Aaronson, S. A. Novel source of 1,2-diacylglyercol elevated in cells transformed by Ha-ras oncogene. *Nature* **330,** 269–272 (1987).

154. Ramírez de Molina, A. *et al.* Overexpression of choline kinase is a frequent feature in human tumor-derived cell lines and in lung, prostate, and colorectal human cancers. *Biochem. Biophys. Res. Commun.* **296,** 580–583 (2002).

155. Challapalli, A. *et al.* Exploiting altered patterns of choline kinase-Alpha expression on human prostate tissue to prognosticate prostate cancer. *J. Clin. Pathol.* **68,** 703–709 (2015).

156. Umemura, A. *et al.* p62, Upregulated during Preneoplasia, Induces Hepatocellular Carcinogenesis by Maintaining Survival of Stressed HCC-Initiating Cells. *Cancer Cell* **29,** 935–948 (2016).

157. Iorio, E. *et al.* Activation of phosphatidylcholine cycle enzymes in human epithelial ovarian cancer cells. *Cancer Res.* **70,** 2126–2135 (2010).

158. Xiong, J. *et al.* MYC is a positive regulator of choline metabolism and impedes mitophagy-dependent necroptosis in diffuse large B-cell lymphoma. *Blood Cancer J.* **7,** (2017).

159. Chen, J. L. *et al.* Autophagy Induction Results in Enhanced Anoikis Resistance in Models of Peritoneal Disease. *Mol. Cancer Res.* **15,** 26–34 (2017).

160. Yang, J. *et al.* Integration of autophagy and anoikis resistance in solid tumors. *Anat. Rec.* **296,** 1501–1508 (2013).

161. Klionsky, D. J. *et al.* Guidelines for the use and interpretation of assays for monitoring autophagy (3rd edition). **12,** 1–222 (2016).

162. Mizushima, N., Yoshimori, T. & Ohsumi, Y. The Role of Atg Proteins in Autophagosome Formation. *Annu. Rev. Cell Dev. Biol.* **27,** 107–132 (2011).

163. Kim, J., Kundu, M., Viollet, B. & Guan, K. L. AMPK and mTOR regulate autophagy through direct phosphorylation of Ulk1. *Nat. Cell Biol.* **13,** 132–141 (2011).

164. Russell, R. C., Yuan, H. X. & Guan, K. L. Autophagy regulation by nutrient signaling. *Cell Res.* **24,** 42–57 (2014).

165. Dall'Armi, C., Devereaux, K. A. & Di Paolo, G. The role of lipids in the control of autophagy. *Curr. Biol.* **23,** R33–R45 (2013).

166. Nakamura, S. & Yoshimori, T. New insights into autophagosome–lysosome fusion. *J. Cell Sci.* **130,** 1209–1216 (2017).

167. Axe, E. L. *et al.* Autophagosome formation from membrane compartments enriched in phosphatidylinositol 3-phosphate and dynamically connected to the endoplasmic reticulum. *J. Cell Biol.* **182,** 685–701 (2008).

168. Hayashi-Nishino, M. *et al.* A subdomain of the endoplasmic reticulum forms a cradle for autophagosome formation. *Nat. Cell Biol.* **11,** 1433–1437 (2009).

169. Ylä-Anttila, P., Vihinen, H., Jokitalo, E. & Eskelinen, E. L. 3D tomography reveals connections between the phagophore and endoplasmic reticulum. *Autophagy* **5,** 1180–1185 (2009).

170. Hamasaki, M. *et al.* Autophagosomes form at ER-mitochondria contact sites. *Nature* **495,** 389–393 (2013).

171. Ravikumar, B., Moreau, K., Jahreiss, L., Puri, C. & Rubinsztein, D. C. Plasma membrane contributes to the formation of pre-autophagosomal structures. *Nat. Cell Biol.* **12,** 747–757 (2010).

172. Girardi, J. P., Pereira, L. & Bakovic, M. De novo synthesis of phospholipids is coupled with autophagosome formation. *Med. Hypotheses* **77,** 1083–1087 (2011).

173. Levine, B., Kroemer, G. & Roussy, I. G. Review Autophagy in the Pathogenesis of Disease. 27–42 (2008). doi:10.1016/j.cell.2007.12.018

174. Zhong, Z., Sanchez-lopez, E. & Karin, M. Review Autophagy , Inflammation , and Immunity : A Troika Governing Cancer and Its Treatment. *Cell* **166,** 288–298 (2016).

175. White, E., Mehnert, J. M. & Chan, C. S. CCR FOCUS Autophagy , Metabolism , and Cancer. 5037–5047 (2015). doi:10.1158/1078-0432.CCR-15-0490

176. Lazova, R. *et al.* Punctate LC3B expression is a common feature of solid tumors and associated with proliferation, metastasis, and poor outcome. *Clin. Cancer Res.* **18,** 370–379 (2012).

177. Ma, X. H. *et al.* Measurements of tumor cell autophagy predict invasiveness, resistance to chemotherapy, and survival in melanoma. *Clin. Cancer Res.* **17,** 3478–3489 (2011).

178. Yang, S. *et al.* Pancreatic cancers require autophagy for tumor growth. *Genes Dev.* **25,** 717–729 (2011).

179. Sato, K. *et al.* Autophagy is activated in colorectal cancer cells and contributes to the tolerance to nutrient deprivation. *Cancer Res.* **67,** 9677–9684 (2007).

180. Yang, A. & Kimmelman, A. C. Inhibition of autophagy attenuates pancreatic cancer growth independent of TP53/TRP53 status. *Autophagy* **10,** 1683–1684 (2014).

181. Ohsumi, Y. Kamada 2000, Tor-mediated induction of autophagy via an Apg1 protein kinase complex. *J. Cell Biol.* **150,** 1507–1513 (2000).

182. Kim, J. *et al.* Differential regulation of distinct Vps34 complexes by AMPK in nutrient stress and autophagy. *Cell* **152,** 290–303 (2013).

183. Lee, J. W., Park, S., Takahashi, Y. & Wang, H. G. The association of AMPK with ULK1 regulates autophagy. *PLoS One* **5,** 1–9 (2010).

184. Vicinanza, M. *et al.* PI(5)P regulates autophagosome biogenesis. *Mol. Cell* **57,** 219–234 (2015).

185. Polson, H. E. J. *et al.* Mammalian Atg18 (WIPI2) localizes to omegasome-anchored phagophores and positively regulates LC3 lipidation. *Autophagy* **6,** 506–522 (2010).

186. Ichimura, Y. *et al.* A ubiquitin-like system mediates protein lipidation. *Nature* **408,** 488–492 (2000).

187. Kirisako, T. *et al.* Formation Process of Autophagosome Is Traced with Apg8 / Aut7p in Yeast. *Jcb* **147,** 435–446 (1999).

188. Kirisako, T. *et al.* The reversible modification regulates the membrane-binding state of Apg8/Aut7 essential for autophagy and the cytoplasm to vacuole targeting pathway. *J. Cell Biol.* **151,** 263–275 (2000).

189. Kabeya, Y. *et al.* LC3, a mammalian homolog of yeast Apg8p, is localized in autophagosome membranes after processing. *EMBO JournalEMBO J.* **19,** 5720–5728 (2000).

190. Fujita, N. *et al.* The Atg16L Complex Specifies the Site of LC3 Lipidation for Membrane Biogenesis in Autophagy. *Mol. Biol. Cell* **19,** 2092–2100 (2008).

191. Xie, Z., Nair, U. & Klionsky, D. J. Atg8 Controls Phagophore Expansion during Autophagosome Formation. *Mol. Biol. Cell* **19,** 3290–3298 (2008).

192. Mizushima, N. *et al.* A protein conjugation system essential for autophagy. **395,** 395–398 (1998).

193. Pankiv, S. *et al.* p62/SQSTM1 binds directly to Atg8/LC3 to facilitate degradation of ubiquitinated protein aggregates by autophagy*[S]. *J. Biol. Chem.* **282,** 24131–24145 (2007).

194. Wang, H. *et al.* GABARAPs regulate PI4P-dependent autophagosome:lysosome fusion. *Proc. Natl. Acad. Sci.* **112,** 7015–7020 (2015).

195. Hasegawa, J. *et al.* Autophagosome–lysosome fusion in neurons requires INPP5E, a protein associated with Joubert syndrome. *EMBO J.* **35,** 1853–1867 (2016).

196. Cai, M. *et al.* Phospholipase D1-regulated autophagy supplies free fatty acids to counter nutrient stress in cancer cells. *Cell Death Dis.* **7,** e2448 (2016).

197. Hur, J. H. *et al.* Phospholipase D1 deficiency in mice causes nonalcoholic fatty liver disease via an autophagy defect. *Sci. Rep.* **6,** 1–13 (2016).

198. Gardner, B. M., Pincus, D., Gotthardt, K., Gallagher, C. M. & Walter, P. Endoplasmic Reticulum Stress Sensing in the Unfolded Protein Response. *Cold Spring Harb. Perspect. Biol.* **5,** a013169–a013169 (2013).

199. Fu, S. *et al.* Aberrant lipid metabolism disrupts calcium homeostasis causing liver endoplasmic reticulum stress in obesity. *Nature* **473,** 528–531 (2011).

200. Volmer, R., van der Ploeg, K. & Ron, D. Membrane lipid saturation activates endoplasmic reticulum unfolded protein response transducers through their transmembrane domains. *Proc. Natl. Acad. Sci.* **110,** 4628–4633 (2013).

201. Promlek, T. *et al.* Membrane aberrancy and unfolded proteins activate the endoplasmic reticulum stress sensor Ire1 in different ways. *Mol. Biol. Cell* **22,** 3520–3532 (2011).

202. Halbleib, K. *et al.* Activation of the Unfolded Protein Response by Lipid Bilayer Stress. *Mol. Cell* **67,** 673–684.e8 (2017).

203. Liu, X. De *et al.* Transient aggregation of ubiquitinated proteins is a cytosolic unfolded protein response to inflammation and endoplasmic reticulum stress. *J. Biol. Chem.* **287,** 19687–19698 (2012).

204. Shi, Y. *et al.* Identification and characterization of pancreatic eukaryotic initiation factor 2 alpha-subunit kinase, PEK, involved in translational control. *Mol. Cell. Biol.* **18,** 7499–509 (1998).

205. Vattem, K. M. & Wek, R. C. Reinitiation involving upstream ORFs regulates ATF4 mRNA translation in mammalian cells. *Proc. Natl. Acad. Sci.* **101,** 11269–11274 (2004).

206. B'Chir, W. *et al.* The eIF2α/ATF4 pathway is essential for stress-induced autophagy gene expression. *Nucleic Acids Res.* **41,** 7683–7699 (2013).

207. Katsuragi, Y., Ichimura, Y. & Komatsu, M. p62 / SQSTM1 functions as a signaling hub and an autophagy adaptor. **282,** 4672–4678 (2015).

208. Zhang, D. D. & Hannink, M. Distinct cysteine residues in Keap1 are required for Keap1-dependent ubiquitination of Nrf2 and for stabilization of Nrf2 by chemopreventive agents and oxidative stress. *Mol. Cell. Biol.* **23,** 8137–51 (2003).

209. Jain, A. *et al.* p62/SQSTM1 is a target gene for transcription factor NRF2 and creates a positive feedback loop by inducing antioxidant response element-driven gene transcription. *J. Biol. Chem.* **285,** 22576–22591 (2010).

210. Komatsu, M. *et al.* The selective autophagy substrate p62 activates the stress responsive transcription factor Nrf2 through inactivation of Keap1. *Nat. Cell Biol.* **12,** 213–223 (2010).

211. Ichimura, Y. *et al.* Phosphorylation of p62 Activates the Keap1-Nrf2 Pathway during Selective Autophagy. *Mol. Cell* **51,** 618–631 (2013).

212. Wang, Y., Macdonald, J. I. S. & Kent, C. Regulation of CTP : Phosphocholine Cytidylyltransferase in HeLa Cells. *J. Biol. Chem* **268,** 5512–5518 (1993).

213. Lagace, T. A. & Ridgway, N. D. The rate-limiting enzyme in phosphatidylcholine synthesis regulates proliferation of the nucleoplasmic reticulum. *Mol. Biol. Cell* **16,** 1120–1130 (2005).

214. Sweitzer, T. D. & Kent, C. Expression of wild-type and mutant rat liver CTP:phosphocholine cytidylyltransferase in a cytidylyltransferase-deficient Chinese Hamster Ovary cell line. *Arch. Biochem. Biophys.* **311,** 107–116 (1994).

215. Jamil, H., Yao, Z. & Vance, D. E. Feedback regulation of CTP : phosphocholine cytidylyltransferase translocation between cytosol and endoplasmic reticulum by Feedback Regulation of CTP : Phosphocholine Cytidylyltransferase Translocation between Cytosol and Endoplasmic Reticulum by Phospha. *J. Biol. Chem.* **265,** 4332–4339 (1990).

216. Yao, Z., Jamil, H. & Dennis Vance. Choline Deficiency Cytidylyltransferase in Rat Liver Causes Translocation of CTP : Phosphocholine from Cytosol to Endoplasmic Reticulum. *J. Biol. Chem.* **265,** 4326–4331 (1990).

217. Moscat, J. & Diaz-meco, M. T. Minireview p62 at the Crossroads of Autophagy , Apoptosis , and Cancer. *Cell* **137,** 1001–1004 (2009).

218. Lykidis, a, Jackson, P. & Jackowski, S. Lipid activation of CTP: phosphocholine cytidylyltransferase alpha: characterization and identification of a second activation domain. *Biochemistry* **40,** 494–503 (2001).

219. Röhrig, F. & Schulze, A. The multifaceted roles of fatty acid synthesis in cancer. *Nat. Rev. Cancer* **16,** 732–749 (2016).

220. Hui, L. *et al.* mTOR-dependent suppression of protein phosphatase 2A is critical for phospholipase D survival signals in human breast cancer cells. *J. Biol. Chem.* **280,** 35829–35835 (2005).

221. Agassandian, M. *et al.* Oxysterols inhibit phosphatidylcholine synthesis via ERK docking and phosphorylation of CTP:phosphocholine cytidylyltransferase. *J. Biol. Chem.* **280,** 21577–21587 (2005).

222. Avivar-Valderas, A. *et al.* PERK Integrates Autophagy and Oxidative Stress Responses To Promote Survival during Extracellular Matrix Detachment. *Mol. Cell. Biol.* **31,** 3616–3629 (2011).

223. Howe, E. N., Cochrane, D. R. & Richer, J. K. Targets of miR-200c mediate suppression of cell motility and anoikis resistance. *Breast Cancer Res.* **13,** R45 (2011).